

**UCSF**

**UC San Francisco Electronic Theses and Dissertations**

**Title**

CARBOHYDRATE BINDING RECEPTORS IN LEUKOCYTE MIGRATION AND ACTIVATION

**Permalink**

<https://escholarship.org/uc/item/74h1k0cb>

**Author**

Patnode, Michael L.

**Publication Date**

2013

Peer reviewed|Thesis/dissertation

Carbohydrate Binding Receptors in  
Leukocyte Migration and Activation

by

Michael L. Patnode

DISSERTATION

Submitted in partial satisfaction of the requirements for the degree of

DOCTOR OF PHILOSOPHY

in

Biomedical Sciences

in the

GRADUATE DIVISION

of the

UNIVERSITY OF CALIFORNIA, SAN FRANCISCO



© Copyright 2013

By

Michael L. Patnode

*To Ray and Karen Patnode*

*with my love and gratitude*

## ACKNOWLEDGMENTS

This work would not have been possible without the guidance of my mentor Dr. Steven Rosen. Steve has exhibited a seemingly unlimited capacity to review my writing and presentations, and provide feedback on my ideas. He has been intimately involved in my experiments, down to the level of technical details. At the same time, he has allowed me the freedom to pursue questions that are outside of his area of expertise. This style of mentoring requires expertise on the part of the mentor, and I am incredibly grateful for the experience. Throughout my five and a half years in his lab, Steve has made it clear that his expectations for me are high, yet he has never expressed disappointment at those times when I failed to meet them. He has also been incredibly generous with his resources, and flexible with his own plans, as my timeline for graduation has evolved. The most effective means that any mentor has for influencing trainees is the example they provide. Steve's scientific integrity is absolute. The rigor with which he evaluates experiments is exceptional. He is masterful in organizing collaborations, and shares credit without hesitation. His dedication to his work is matched by a commitment to family. For providing such a strong and consistent example of how to be successful in science, and in life, I thank him.

The individuals that Steve has brought into his lab have also played a large part in my development. Mark Singer has served as a resource for all manner of experimental techniques and has never hesitated to provide me with valuable historical perspectives on science and politics. Mark has also helped shape my concepts of lab citizenship, safety, and ethics. I thank Dr. Hidenobu Kanda for his patient mentorship during my first few

months in the lab, Dr. Inna Maltseva for her sense of humor and kind words of encouragement, and Dr. Annette Bistrup introducing me to several excellent local music venues and giving me advise on choosing a graduate mentor that has proved to be pivotal. I owe thanks to two medical students from Linköping University, Lotten Tegesjö and Matilda Elin, who made impressive contributions, in just a few short months, to the experiments presented in this dissertation. Thanks are also due to other members of the Rosen lab who have given me advise and help over the years, Dr. Sheena Kerr, Dr. Hanayo Arata-Kawai, Dr. Renhong Tang, Dr. Hassan Lemjabbar-Alaoui, Yang-Qing Wang, and Qing Xue.

I have been privileged to interact with many world-class senior scientists at UCSF. Dr. Richard Locksley's enthusiasm and encouragement afforded me the confidence to pursue my ideas about helminth immunity. He and the researchers in his lab provided crucial intellectual and technical assistance in testing these ideas. Dr. Max Krummel has been a steadfast collaborator, offering his resources and expertise in biological imaging. Dr. Emily Thornton in the Krummel lab, spent many hours teaching me the basics of two-photon microscopy. Sebastian Peck in the Biological Imaging Development Center exhibited remarkable determination as we struggled to develop a system for imaging nematodes and granulocytes in live, anesthetized mice. Due to his efforts, this system eventually proved to be very successful. I thank Dr. John Fahy for impressing upon me the importance of combining model animal work with patient samples, despite the challenges that human research presents. I am indebted to Dr. Susan Fisher for her critical and perceptive assessment of my initial research proposal. It was this assessment that allowed me to avoid several pitfalls inherent to the problem of Siglec-F specificity. I

thank Dr. David Erle for the consistent optimism, creativity, and sense of humor he brought to our many meetings. I also thank Dr. Tony DeFranco, who served as my mentor during my first few months at UCSF. He has always been willing to take the time to discuss my results or help me prepare for a presentation. Dr. Neetu Gupta who supervised my work while I was in Tony's lab was inspirational to me, not only because of the discipline with which she approached research, but also because her example proved to me that one can balance family life with the demands of a career in science.

My work has benefitted from several involved collaborations, which were initiated by Steve. These contributions are detailed in the next section. I want to add here that it has been a pleasure to meet and work with Dr. Kenji Uchimura, Dr. Kay-Hooi Khoo, and Dr. Paul Crocker. They have expressed an interest in my ideas and career beyond that which is typical of a simple scientific collaboration.

Many thanks are due to Lisa Magargal and Monique Piazza, the administrators of the Biomedical Sciences Graduate Program. Their efforts have made the complicated rules and requirements involved in securing graduate funding all but invisible to me. They respond to student questions and concerns with astonishing speed, and are responsible for the comforting sense of community that exists in this graduate program.

I thank my classmates, particularly Dr. Jan Lui and Dr. Kristen Coakley for their invaluable friendship in tough times, as well as good times. Many other friends I have made at UCSF have supported me in important ways over the years, including Dr. Chris Allen, Dr. Brandon Sullivan, Dr. Lee Reinhardt, Dr. April Price, and Dr. Jesse Green. Friends in Washington State, Elliot Newlin, Emily Sershon, and Faizal Hadi, provided important moral support during my first few years in San Francisco. I also have to thank

Kinichi Bando, Haruyo Bando, Dr. Joanne Bando, and Dr. Kathy Bando for their warmth and friendship over the past four years.

I owe a debt of gratitude to my mother Karen Bunger and my father Lou Patnode. Their determination and sacrifice have made it possible for me to come this far. They radiate the honesty, passion, and creativity that I strive to make the basis of my personality. I also thank my younger brother David Patnode for his near-paranormal comprehension of my ideas and sense of humor. His commitment to originality inspires my own work.

To Kaoru, there is no way to communicate on paper the profound effect that you have had on everything I think and feel and do. Thank you for being my closest collaborator, my best friend, and part of me.



## CONTRIBUTIONS TO PRESENTED WORK

All of the work described in this dissertation was performed under the supervision and guidance of Dr. Steven D. Rosen.

Sections of Chapter 1, and all of Chapter 2, are reproduced from the publication, [Patnode, M.L., Yu, S.Y., Cheng, C.W., Ho, M.Y., Tegesjö, L., Sakuma, K., Uchimura, K., Khoo, K.H., Kannagi, R., and Rosen, S.D. (2013). KSGal6ST generates galactose-6-O-sulfate in high endothelial venules but does not contribute to L-selectin-dependent lymphocyte homing. *Glycobiology* 23, 381-394]. Dr. Kay-Hooi Khoo, Dr. Reiji Kannagi, and Dr. Kenji Uchimura assisted in revising the text for this publication. Keiichiro Sakuma in the laboratory of Dr. Kannagi performed the ELISA in Figure 5A. Dr. Uchimura performed the keratan sulfate analysis in Figure 2. Dr. Shin-Yi Yu, Dr. Ming-Yi Ho, and Chu-Wen Cheng in the laboratory of Dr. Khoo acquired and analyzed all of the mass spectrometry data in Figure 4. Lotten Tegesjö performed the homing experiments in Figure 7B.

Sections of Chapter 3, and all of Chapter 4, are reproduced from a manuscript in preparation by Patnode, M.L., Singer, M.S., Cheng, C.W., Elin, M., Crocker, P.R., Khoo, K.H., and Rosen, S.D. Dr. Paul Crocker assisted in revising the text for this manuscript. Mark Singer performed the BAL fluid fractionation in Figure 11 and Figure 14. Matilda Elin made the initial observations presented in Figure 5B, and assisted with various important aspects of the project. Dr. Chu-Wen Cheng in the laboratory of Dr. Khoo acquired and analyzed all of the mass spectrometry data in Figure 15.

Sections of Chapter 5, and all of Chapter 6, are reproduced from a manuscript in preparation by Patnode, M.L., Bando, J.K., Locksley R.M., and Rosen, S.D. Dr. Richard Locksley provided critical insights that guided the experiments. Jennifer Bando provided *N. brasiliensis* larvae for *in vitro* assays and performed *N. brasiliensis* infections. Other individuals who provided assistance and reagents are acknowledged at the ends of Chapters 2, 4, and 6.

# CARBOHYDRATE BINDING RECEPTORS IN LEUKOCYTE MIGRATION AND ACTIVATION

By Michael L. Patnode

## ABSTRACT

The addition of sulfate to glycan structures can regulate their ability to serve as ligands for glycan-binding proteins. While sulfate groups present on the monosaccharides glucosamine, uronate, N-acetylglucosamine, and N-acetylgalactosamine are recognized by defined receptors that mediate important functions, the functional significance of galactose-6-*O*-sulfate (Gal6S) is not known. However, *in vitro* studies using synthetic glycans and sulfotransferase overexpression suggest that Gal6S is a recognition determinant for the lymphocyte homing receptor, L-selectin. Additionally, glycan array studies have implicated Gal6S as a recognition determinant for the inhibitory sialic acid-binding receptor, Siglec-F. Only two sulfotransferases have been shown to generate Gal6S, namely keratan sulfate galactose 6-*O*-sulfotransferase (KSGal6ST) and chondroitin 6-*O*-sulfotransferase-1 (C6ST-1). I have used mice deficient in KSGal6ST and C6ST-1 to test whether Gal6S contributes to ligand recognition by L-selectin and Siglec-F *in vivo*.

First, I establish that KSGal6ST is selectively expressed in lymph node high endothelial venules (HEVs), and generates Gal6S-containing glycans in lymph nodes, including 6,6'-disulfo-3'sLN (Sia $\alpha$ 2 $\rightarrow$ 3[6S]Gal $\beta$ 1 $\rightarrow$ 4[6S]GlcNAc) in HEVs.

Nevertheless, short-term homing of lymphocytes to lymph nodes is normal in KSGal6ST-deficient mice, indicating that the Gal6S-containing structures I detected do not contribute to L-selectin ligand recognition in this setting.

Next, I characterize Siglec-F ligand expression on leukocyte populations and find that this expression is largely restricted to cell types also expressing Siglec-F, namely eosinophils, neutrophils, and alveolar macrophages. I also demonstrate the presence of Siglec-F ligand activity in bronchoalveolar lavage fluid fractions containing polymeric secreted mucins. Surprisingly, none of the ligands I describe are diminished in mice lacking KSGal6ST and C6ST-1, arguing against the prevailing view that Gal6S is a critical recognition determinant for this receptor. These results refine our understanding of the biological ligands for L-selectin and Siglec-F, and introduce a mouse model for investigating the functions of Gal6S in other contexts.

Lastly, I explore the mechanisms controlling eosinophil accumulation in response to parasitic nematodes *in vitro* and *in vivo*. My studies reveal that sensing and synthesis of leukotriene B<sub>4</sub> is required for normal eosinophil accumulation in response to *N. brasiliensis*. Thus, nematodes induce leukotriene production in eosinophils, and this mediator is subsequently required to amplify eosinophil accumulation.

# CONTENTS

## Chapter 1: Structure and Function of L-selectin Ligands

<i>The Selectin Family and Leukocyte Homing</i> .....	2
<i>Ligands for L-selectin</i> .....	5
<i>Evidence for Galactose-6-O-Sulfate as a Binding Determinant for L-selectin</i> .....	7

## Chapter 2: KSGal6ST Generates Galactose-6-O-Sulfate in High Endothelial Venules But Does Not Contribute to L-selectin Dependent Lymphocyte Homing

<i>Summary and Results</i> .....	12
<i>Figures</i> .....	21
<i>Discussion</i> .....	29
<i>Future Prospects</i> .....	35
<i>Materials and Methods</i> .....	38

## Chapter 3: Structure and Function of the CD33-Related Siglecs

<i>The Siglec Family and Inhibitory Receptor Signaling</i> .....	47
<i>Ligands for the CD33-Related Siglecs</i> .....	52
<i>Evidence for Galactose-6-O-Sulfate as a Binding Determinant for Siglec-F</i> .....	55

## Chapter 4: Galactose-6-O-Sulfatotransferases Are Not Required for the Generation of Siglec-F Ligands on Leukocytes or Lung Epithelial Cells

<i>Summary and Results</i> .....	59
<i>Figures</i> .....	66
<i>Discussion</i> .....	73
<i>Future Prospects</i> .....	77
<i>Materials and Methods</i> .....	79

## Chapter 5: Mechanisms of Eosinophil Accumulation during Parasite Infection

<i>Eosinophil-Parasite Interactions</i> .....	86
<i>Eosinophil Recruitment and Survival</i> .....	89
<i>Evidence for Leukotriene-Driven Amplification of Granulocyte Recruitment</i> .....	93
<i>Figures</i> .....	97

## Chapter 6: Leukotriene-Driven Amplification of Eosinophil Accumulation in Response to Diverse Nematode Species

<i>Summary and Results</i> .....	99
<i>Figures</i> .....	107
<i>Discussion</i> .....	114
<i>Materials and Methods</i> .....	120
<i>Conclusion</i> .....	125
<i>References</i> .....	127

## FIGURES

### Chapter 2: KSGal6ST Generates Galactose-6-O-Sulfate in High Endothelial Venules But

#### Does Not Contribute to L-selectin Dependent Lymphocyte Homing

Figure 1: <i>Generation of KSGal6ST KO mice</i> .....	21
Figure 2: <i>Keratan sulfate analysis in KSGal6ST KO mice</i> .....	22
Figure 3: <i>KSGal6ST expression in HEVs</i> .....	23
Figure 4: <i>MS analysis of O-glycans in lymph nodes of KSGal6ST KO mice</i> .....	24
Figure 5: <i>Sialylated 6,6'-disulfated glycans in HEVs</i> .....	25
Figure 6: <i>Sialylated 6,6'-disulfated glycans in KSGal6ST KO mice</i> .....	26
Figure 7: <i>L-selectin ligand expression and lymphocyte numbers in KSGal6ST KO mice</i> .....	27
Figure 8: <i>Lymphocyte homing in KSGal6ST KO mice</i> .....	28

### Chapter 4: Galactose-6-O-Sulfatotransferases Are Not Required for the Generation of

#### Siglec-F Ligands on Leukocytes or in Lung Tissue

Figure 9: <i>Siglec-F ligand expression in peripheral blood leukocytes</i> .....	66
Figure 10: <i>Siglec-F ligand expression in resident lung cells</i> .....	67
Figure 11: <i>Siglec-F ligand expression in bronchoalveolar lavage fluid</i> .....	68
Figure 12: <i>Siglec-F ligand expression during N. brasiliensis infection</i> .....	69
Figure 13: <i>Siglec-F ligand expression in leukocytes of KSGal6ST/C6ST-1 DKO mice</i> .....	70
Figure 14: <i>Siglec-F ligand expression in lungs of KSGal6ST/C6ST-1 DKO mice</i> .....	71
Figure 15: <i>MS analysis of sulfated glycans in eosinophils</i> .....	72

### Chapter 5: Mechanisms of Eosinophil Accumulation during Parasite Infection

Figure 16: <i>Leukotriene synthesis and leukotriene receptor expression</i> .....	97
---	----

### Chapter 6: Leukotriene-Driven Amplification of Eosinophil Accumulation in

#### Response to Diverse Nematode Species

Figure 17: <i>Eosinophil migration in response to nematodes</i> .....	107
Figure 18: <i>Evidence for paracrine signaling in eosinophil migration towards nematodes</i> ...	108
Figure 19: <i>Involvement of leukotrienes in eosinophil migration towards nematodes</i> .....	109
Figure 20: <i>Evidence for LTB<sub>4</sub>-mediated migration towards nematodes</i> .....	110
Figure 21: <i>Eosinophil accumulation in the lung in response to nematodes</i> .....	111
Figure 22: <i>Involvement of leukotrienes in eosinophil accumulation in the lung</i> .....	112
Figure 23: <i>A model for leukotriene-driven migration in response to nematodes</i> .....	113



# **CHAPTER 1**

## **Structure and Function of L-selectin Ligands**

## **The Selectin Family and Leukocyte Homing**

P-selectin, E-selectin, and L-selectin, constitute a three-member family of type-1 transmembrane carbohydrate-binding receptors. The genes encoding these receptors (*SELP*, *SELE*, and *SELL*) are found adjacent to one another on chromosome 1. These genes have a high degree of amino acid sequence homology, suggesting that they arose as a result of gene duplication events (Watson et al., 1990). The general structural features of selectins are well conserved across vertebrate species (Sun et al., 2010). These features consist of an N-terminal C-type lectin domain (Kogelberg and Feizi, 2001), an epidermal growth factor-like domain, and up to ten short consensus repeats, which have homology to complement-binding proteins (Kirkitaдзе and Barlow, 2001). Selectins also contain an extracellular, membrane-proximal cleavage region. In L-selectin, this is a site of activation-dependent proteolysis mediated by ADAM-17 and at least one other protease (Scheller et al., 2011). The relatively short cytoplasmic domains of these receptors suggest that they have limited interactions with proteins in the cytosol. However, there is evidence that L-selectin can transmit signals upon ligand binding, and the pathways involved are currently under investigation (Zarbock and Ley, 2009). P-selectin is expressed in platelets and is the primary component of Weibel-Palade bodies in endothelial cells (Lowenstein et al., 2005). Activation of endothelial cells by a number of diverse stimuli causes these granules to rapidly fuse with the plasma membrane, generating high densities of P-selectin on vessel walls. E-selectin expression is also induced in endothelial cells following activation, but in this case selectin expression is regulated at the level of transcription (Hartwell and Wagner, 1999). L-selectin, in contrast to E- and P- selectin, is constitutively expressed on nearly all circulating leukocytes, as

well as human cytotrophoblasts (Genbacev et al., 2003), and is not typically found in endothelial cells.

Leukocytes must exit the bloodstream and enter into tissues to perform a variety of functions important in homeostasis and immune responses (Butcher and Picker, 1996). This process is known as leukocyte recruitment and involves a multi-step cascade of molecular interactions (Ley et al., 2007). In inflamed vascular beds, P- and E-selectin bind the carbohydrate structure sLex (Sia  $\alpha 2 \rightarrow 3$  Gal  $\beta 1 \rightarrow 4$  [Fuc  $\alpha 1 \rightarrow 3$ ] GlcNAc), which is presented by the glycoprotein PSGL-1 located at the tips of leukocyte microvilli (Zarbock and Ley, 2009). The relatively weak affinity of this binding interaction, combined with the shear force of blood flow, causes leukocytes to roll along the walls of blood vessels. Leukocyte rolling enables the recognition of chemokines, such as IL-8, which are secreted by innate immune cells and subsequently presented on luminal endothelial heparan sulfate proteoglycans (HSPGs). Chemokines activate leukocytes through chemokine receptors, which are seven-pass transmembrane G-protein-coupled receptors (GPCRs). Inside-out chemokine signaling induces conformational changes in integrins, such as LFA-1 and VLA-4, and the binding of these activated integrins to immunoglobulin (Ig) superfamily receptors including ICAM-1 and VCAM-1 results in firm arrest on the vessel wall. Finally, events that are not yet fully understood mediate the passage of leukocytes between or directly through endothelial cells and into the tissue.

The process of lymphocyte homing to secondary lymphoid organs brings circulating naïve T- and B cells into contact with antigens to generate immune responses. In the presence of microbial products or other danger signals, dendritic cells in peripheral tissues cells exhibit increased expression of CCR7 and migrate into draining lymphatic

vessels, carrying associated antigens (Girard et al., 2012). The flow of lymph transports these cells, along with soluble antigens, to peripheral lymph nodes. In contrast, antigen delivery to Peyer's patches occurs through the transcytosis of luminal contents by M cells in the intestinal epithelium (Fujikuyama et al., 2012). Specialized compartments within secondary lymphoid organs accommodate the important cell-cell interactions responsible for antigen driven T cell activation, cytokine secretion, and proliferation, as well as B cell class switching and affinity maturation (Cyster, 2003). The entry of T and B cells into lymph nodes and Peyer's patches is critically dependent on their interactions with specialized post-capillary blood vessels known as high endothelial venules (HEVs) (Girard et al., 2012). HEVs are characterized by their plump endothelial cells, which contain extensive ER and golgi networks (Girard and Springer, 1995). The homing cascade is exemplified in lymph node HEVs, where tethering and rolling mediated by L-selectin reduces lymphocyte velocity by roughly 10 fold relative to the flow of blood. Lymphocyte rolling in Peyer's patches and mesenteric lymph nodes is also mediated by  $\alpha 4\beta 7$  integrin, expressed on lymphocytes. This receptor binds to MAdCAM-1 on HEVs and allows a fraction of lymphocytes (~50% in Peyer's patches and ~15% in mesenteric lymph nodes) to enter the tissue independent of L-selectin binding (Gorfu et al., 2009). The chemokine CCL21 is highly expressed in HEVs and presented by HSPGs on the luminal surface. Within seconds of tethering, signaling through CCR7 on leukocytes activates LFA-1, resulting in high affinity binding to ICAM-1 and ICAM-2 on the endothelium. Transendothelial migration in lymph nodes likely involves an extracellular lysophospholipase known as autotaxin, which is secreted into the vessel lumen by HEVs (Kanda et al., 2008; Zhang et al., 2012). This enzyme catalyzes the conversion of LPC

into LPA, enhancing lymphocyte motility through one or more LPA receptors that remain to be identified. Thus, the expression of a battery of adhesion molecules and secreted proteins by HEVs is critical for immune surveillance and the development of nascent immune responses.

### **Ligands for L-selectin**

Several mucin scaffolds expressed by HEVs have been identified as ligands for L-selectin, including GlyCAM-1, CD34, endomucin, podocalyxin, and nepmucin (Rosen, 2004). These ligands present terminal oligosaccharides that are bound by L-selectin. The best characterized of these glycans is 6-sulfo-sLex (Sia  $\alpha 2 \rightarrow 3$  Gal  $\beta 1 \rightarrow 4$  [Fuc  $\alpha 1 \rightarrow 3$ ][6S]GlcNAc) (Hemmerich et al., 1995; Mitsuoka et al., 1998). Antibodies recognizing this structure stain HEVs in human and mouse lymph nodes, and block L-selectin function (Arata-Kawai et al., 2011; Hirakawa et al., 2010; Mitsuoka et al., 1998). Accordingly, structures consistent with 6-sulfo-sLex have been detected on human CD34 by mass spectrometry (Hernandez Mir et al., 2009; Satomaa et al., 2002). The critical contributions of fucose and sialic acid to the 6-sulfo-sLex binding determinant have been demonstrated using mice deficient in  $\alpha 3$ -fucosyltransferases (FucT-IV and FucT-VII) (Homeister et al., 2001) or  $\alpha 3$ -sialyltransferases (ST3Gal-IV and ST3Gal-VI) (Yang et al., 2012). Similarly, mice lacking the core 2 (Core2GlcNAcT) and core 1 extension ( $\beta 3$ GlcNAcT-3) enzymes have established the importance of 6-sulfo-sLex capping groups on each of these O-glycan arms, and revealed that N-glycans capped with 6-sulfo-sLex also contribute to lymphocyte homing (Mitoma et al., 2007). Importantly, 6-sulfo-

sLex carries the sulfate modification N-acetylglucosamine-6-*O*-sulfate (GlcNAc6S), which is required for optimal binding by L-selectin (Rosen, 2004).

The attachment of sulfate esters to biomolecules is essential for development, survival, and reproduction in animals (Borghei et al., 2006; Bulow and Hobert, 2006). The diverse functions of carbohydrate sulfation reflect the diverse glycan substrates to which sulfate can be added (Khoo and Yu, 2010). Precise positioning of sulfate on these glycans can determine whether they serve as ligands for one or more glycan binding proteins. Heparan sulfate proteoglycans (HSPGs) provide a clear demonstration of these principles, since they carry long carbohydrate chains with variable sulfate modifications, including N-acetylglucosamine-6-*O*-sulfate, N-acetylglucosamine-3-*O*-sulfate, glucosamine-*N*-sulfate, and uronate-2-*O*-sulfate (Bishop et al., 2007). The creation of these sulfate modifications by distinct sulfotransferases dictates the binding of HSPGs to numerous growth factors, apolipoproteins and lipases, cell adhesion molecules, and extracellular matrix components (Bishop et al., 2007). Sulfate modifications on smaller glycans carried by glycoproteins and glycolipids also serve important functions. N-acetylgalactosamine-4-*O*-sulfate, which caps N-glycan chains on several glycoprotein hormones, is required for their recognition by the macrophage mannose receptor and efficient clearance from the circulation (Baenziger, 2003). Galactose-3-*O*-sulfate (Gal3S) is present on the glycolipids seminolipid and sulfatide, and is essential for spermatogenesis and normal myelin function (Honke et al., 2004). As mentioned above, GlcNAc-6-*O*-sulfate is an important component of the ligands recognized by L-selectin. In contrast, the functions of galactose-6-*O*-sulfate (Gal6S) have not been established. However, this modification has been implicated as a binding determinant for several



immunologically relevant receptors (Bochner et al., 2005; Campanero-Rhodes et al., 2006; Tateno et al., 2005; Tateno et al., 2010) including L-selectin.

Carbohydrate sulfation is dictated by the expression of sulfotransferases, enzymes that catalyze the transfer of sulfate from the universal donor 3'-phospho-adenosine-5'-phosphosulfate (PAPS) to specific hydroxyl or amino groups on nascent glycans in the Golgi network (Grunwell and Bertozzi, 2002). The galactose-/N-acetylgalactosamine-/N-acetylglucosamine-6-*O*-sulfotransferases constitute a highly related family of 7 enzymes, with diverse expression patterns and physiological functions (Fukuda et al., 2001). Two N-acetylglucosamine-6-*O*-sulfotransferases, GlcNAc6ST-1 (encoded by the gene *Chst2*) and GlcNAc6ST-2 (encoded by the gene *Chst4*), generate nearly all of the 6-sulfo-sLex in HEVs (Kawashima et al., 2005; Uchimura et al., 2005). Furthermore, GlcNAc6ST-1/GlcNAc6ST-2 double knockout (GlcNAc6ST1/2 DKO) mice exhibit a 75% decrease in lymphocyte homing to peripheral lymph nodes (Kawashima et al., 2005; Uchimura et al., 2005). Interestingly, the residual homing in these mice is L-selectin-dependent and, therefore, indicates the presence of alternative recognition determinants.

### **Evidence for Galactose-6-*O*-Sulfate as a Binding Determinant for L-selectin**

Several lines of evidence have suggested that Gal6S contributes to L-selectin-dependent lymphocyte homing. Firstly, Gal6S and GlcNAc6S were found in approximately equal abundance on mouse GlyCAM-1 and CD34 by anion exchange chromatography of monosaccharides released by mild acid hydrolysis (Bistrup et al., 1999; Hemmerich et al., 1994). Based on structural analysis of the O-glycans of GlyCAM-1, Hemmerich et al. proposed the existence of 6'-sulfo-sLex (Sia  $\alpha$ 2→3 [6S]Gal  $\beta$ 1→4 [Fuc

$\alpha 1 \rightarrow 3$ ]GlcNAc), as well as 6-sulfo sLex (Hemmerich et al., 1995). However, with respect to the former structure, it has subsequently been appreciated that the addition of sulfate to the 6-*O* position of galactose (Gal) and the addition of  $\alpha 3$  linked fucose on GlcNAc appear to be mutually exclusive within the same N-acetyllactosamine (LacNAc, Gal  $\beta 1 \rightarrow 4$  GlcNAc) unit *in vivo* (Hiraoka et al., 2007; Homeister et al., 2001; Torii et al., 2000). Indeed, 6'-sulfo-sLex was not found in GlyCAM-1 O-glycans analyzed by HPLC, although Gal6S was present at the termini of core 1 and core 2 arms (Hiraoka et al., 2007; Kawashima et al., 2005). The artificial addition of sulfate to the 6-*O* position of Gal within sLex only marginally enhances (Koenig et al., 1997), and can even inhibit, the binding of sLex to L-selectin-Fc fusion proteins (Galustian et al., 1997; Yoshino et al., 1997). However, Gal6S has been implicated as a binding determinant for L-selectin when present on structures other than sLex. When lactose (Gal  $\beta 1 \rightarrow 4$  Glc) neoglycolipids were synthesized with sulfate on the 6-*O* position of Gal, they exhibited binding to L-selectin-Fc and L-selectin-expressing Jurkat T cells (Bruehl et al., 2000). Furthermore, 6,6'-disulfo-lactose ([6S]Gal  $\beta 1 \rightarrow 4$  [6S]Glc) showed even more binding in these assays than either singly sulfated lactose, and also preferentially inhibited the binding of L-selectin-Fc to GlyCAM-1 (Bertozi et al., 1995). These observations raise the possibility that fucose and Gal6S in distinct LacNAc units can cooperate with GlcNAc6S for recognition by L-selectin.

Additional evidence implicating Gal6S as a binding determinant for L-selectin has come from studies of keratan sulfate galactose-6-*O*-sulfotransferase (KSGal6ST, encoded by the gene *Chst1*). Biochemical characterization of this sulfotransferase has established that it catalyzes 6-*O* sulfation of Gal in keratan sulfate (KS) chains (Fukuta et al., 1997),

which consist of repeating 6-sulfo-LacNAc (Gal  $\beta$ 1 $\rightarrow$ 4 [6S] GlcNAc) units intermittently modified with Gal6S (Bulow and Hobert, 2006). However, *in vitro* studies have shown that KSGal6ST is also capable of modifying Gal in small sialylated lactosamine oligosaccharides, such as 3'sLN (Sia  $\alpha$ 2 $\rightarrow$ 3 Gal  $\beta$ 1 $\rightarrow$ 4 GlcNAc) (Torii et al., 2000), which are present on the O-glycans of mucins expressed by HEVs. Indeed, it was previously demonstrated that KSGal6ST can add sulfate to GlyCAM-1 when both of these genes, along with FucT-VII and Core2GlcNAcT, are transiently overexpressed in COS-7 cells (Bistrup et al., 1999). Furthermore, this form of GlyCAM-1 was a superior substratum for lymphocyte rolling when compared to GlyCAM-1 produced without KSGal6ST overexpression (Tangemann et al., 1999). Similarly, transient overexpression of KSGal6ST, CD34, FucT-VII, and Core2GlcNAcT in CHO cells resulted in increased cell-surface binding of L-selectin-Fc relative to cells not overexpressing KSGal6ST (Bistrup et al., 1999). Intriguingly, KSGal6ST and GlcNAc6ST-2 had synergistic effects on L-selectin binding in this study, reminiscent of the synergy between Gal6S and GlcNAc6S within lactose neoglycolipids (Bruehl et al., 2000). Finally, stable overexpression of KSGal6ST, along with FucT-VII, in an endothelial cell monolayer increased its ability to support the rolling of L-selectin-expressing lymphoma cells (Li et al., 2001). All of these studies were performed with expression of FucT-VII, demonstrating that Gal6S can contribute to L-selectin ligand activity even in the presence of  $\alpha$ 3 linked fucose on GlcNAc. Additionally, KSGal6ST was at least as effective as either GlcNAc6ST-1 or GlcNAc6ST-2 in generating L-selectin ligand activity. However, the effects of Gal6S appear to depend on the exact experimental conditions, since another study found that transient overexpression of KSGal6ST in CHO cells stably expressing

CD34, FucT-VII, and GlcNAc6ST-1, actually reduced their ability to support lymphocyte rolling (Hiraoka et al., 2007).

Aside from KSGal6ST, only one other sulfotransferase has been shown to generate Gal6S, namely Chondroitin 6-*O*-sulfotransferase-1 (C6ST-1, encoded by the gene *Chst3*). This sulfotransferase is less likely to participate in generating L-selectin ligands for several reasons. C6ST-1 exhibits five-fold more GalNAc-6-*O*-sulfotransferase activity than Gal-6-*O*-sulfotransferase activity *in vitro* (Habuchi et al., 1996), and it has been shown to function in the synthesis of chondroitin sulfate, but not KS *in vivo* (Uchimura et al., 2002). Furthermore, C6ST-1 catalyzes 6-*O* sulfation of Gal on small sialylated oligosaccharides almost 100-fold slower than it does on extended KS chains, whereas KSGal6ST has the opposite preference (Habuchi et al., 1997). Most pertinently, C6ST-1-deficient mice do not exhibit defects in lymphocyte homing (Uchimura et al., 2002). KSGal6ST, in contrast to C6ST-1, has not been previously investigated with respect to its capacity to generate Gal6S *in vivo* or its functional contribution to lymphocyte homing.

In the following chapter I describe my efforts to determine whether Gal6S contributes to ligand recognition by L-selectin *in vivo*, taking advantage of mice deficient in KSGal6ST and C6ST-1.

## **CHAPTER 2**

### **KSGal6ST Generates Galactose-6-*O*-Sulfate in High Endothelial Venules But Does Not Contribute to L-selectin Dependent Lymphocyte Homing**

## SUMMARY

Here, we establish that KSGal6ST is selectively expressed in high endothelial venules (HEVs) in lymph nodes and Peyer's patches. We also determine by mass spectrometry, that KSGal6ST generates Gal6S on several classes of O-glycans in peripheral lymph nodes. Furthermore, KSGal6ST but not C6ST-1 is required for the generation of the Gal6S-containing glycan, 6,6'-disulfo-3'sLN (Sia  $\alpha$ 2 $\rightarrow$ 3 [6S] Gal  $\beta$ 1 $\rightarrow$ 4 [6S] GlcNAc) or a closely related structure in lymph node HEVs. Nevertheless, L-selectin-dependent short-term homing of lymphocytes is normal in KSGal6ST-deficient mice, indicating that the Gal6S-containing structures we detected do not contribute to L-selectin ligand recognition in this setting. These results refine our understanding of the biological ligands for L-selectin and introduce a mouse model for investigating the functions of Gal6S in other contexts.

## RESULTS

### Generation of KSGal6ST-deficient mice

In order to study the functions of KSGal6ST *in vivo*, we obtained heterozygous mice carrying a targeted allele of *Chst1* from the National Institutes of Health Knockout Mouse Project. The targeted allele contains the *E. coli* K-12 LacZ gene and a neomycin resistance cassette, which replace the single protein coding region of *Chst1* (Fig. 1A) (Valenzuela et al., 2003). We intercrossed mice heterozygous for this allele (*Chst1*<sup>+/-</sup> mice) to produce homozygous mice (*Chst1*<sup>-/-</sup> mice). Seven litters from *Chst1*<sup>+/-</sup> x *Chst1*<sup>+/-</sup> crosses yielded in total 12 *Chst1*<sup>+/+</sup>, 26 *Chst1*<sup>+/-</sup>, and 12 *Chst1*<sup>-/-</sup> pups, consistent with the expected Mendelian frequencies. We observed no gross physical or behavioral



abnormalities in *Chst1*<sup>-/-</sup> mice, except that male siblings housed together seemed particularly prone to fighting. Since *Chst1* is highly expressed in the cerebral cortex (www.biogps.org, GeneAtlas MOE430 probeset 1449147\_at, GeneAtlas U133A probeset 205567\_at) (Su et al., 2004), we performed reverse transcriptase PCR on total RNA from whole forebrain and verified the absence of *Chst1* transcripts in *Chst1*<sup>-/-</sup> animals (Fig. 1B).

*Chst1* is also expressed in the eye (Su et al., 2004), along with KS chains containing Gal6S (Bhavanandan and Meyer, 1967). Furthermore, KS is a known substrate for KSGal6ST (Fukuta et al., 1997), although this enzyme has not previously been shown to generate Gal6S *in vivo*. To determine whether KSGal6ST deficiency in *Chst1*<sup>-/-</sup> mice affects the sulfation pattern of KS, we isolated KS from whole eyes and performed HPLC analysis. We detected the Gal6S-containing oligosaccharides, (6S)GlcNAc  $\beta$ 1 $\rightarrow$ 3 (6S)Gal  $\beta$ 1 $\rightarrow$ 4 (6S)GlcNAc  $\beta$ 1 $\rightarrow$ 3 Gal and (6S)Gal  $\beta$ 1 $\rightarrow$ 4 (6S)GlcNAc, in KS from wild type mice (Fig. 2). However, these species were not detectable in KS from *Chst1*<sup>-/-</sup> mice, indicating the loss of KSGal6ST enzymatic activity in this tissue.

### **KSGal6ST is selectively expressed in HEVs**

Since *Chst1*<sup>-/-</sup> (hereafter, KSGal6ST KO) mice express the LacZ gene under the control of the *Chst1* promoter, we were able to use  $\beta$ -galactosidase activity as a surrogate for KSGal6ST expression. We performed whole mount X-Gal staining on organs from KSGal6ST KO mice and found expression in the brain, optic nerve and eye, lung, glomeruli of the kidney, and the thymus (Fig. 3A). KSGal6ST expression was also present in peripheral lymph nodes (PLN), mesenteric lymph nodes (MLN), and Peyer's

patches, most prominently in branched structures resembling blood vessels (Fig. 3B). Diffuse X-Gal staining was also seen in B cell follicles in Peyer's patches. Similar staining patterns were observed in *Chst1*<sup>+/-</sup> animals, whereas expression was not detectable in salivary gland, stomach, liver, heart, skeletal muscle, skin, ovary, or testes from either KSGal6ST KO or *Chst1*<sup>+/-</sup> mice (data not shown). As expected, we did not observe X-Gal staining in any tissue from wild type mice (Fig. 3A).

The branched X-Gal<sup>+</sup> structures in lymph nodes and Peyer's patches, coupled with the evidence that Gal6S can serve as a recognition determinant for L-selectin *in vitro*, prompted us to determine whether KSGal6ST was selectively expressed in HEVs. We performed immunofluorescence on tissue sections from X-Gal-stained KSGal6ST KO lymphoid organs using the endothelial cell marker CD31 and the HEV-specific antibody MECA-79, which has an absolute requirement for GlcNAc6S in the context of an extended core 1 O-glycan (Gal  $\beta$ 1 $\rightarrow$ 4 [6S]GlcNAc  $\beta$ 1 $\rightarrow$ 3 Gal  $\beta$ 1 $\rightarrow$ 3 GalNAc) (Yeh et al., 2001). We found strong KSGal6ST expression in MECA-79<sup>+</sup> HEVs from PLN and MLN, whereas other CD31<sup>+</sup> vessels in these tissues expressed KSGal6ST only weakly (Fig. 3C). In Peyer's patches, we also found selective expression of KSGal6ST in HEVs, as identified by CD31 expression and plump endothelial morphology.

### **KSGal6ST generates Gal6S on O-glycans in peripheral lymph nodes**

To determine whether KSGal6ST expression in lymph nodes is required to synthesize Gal6S, we performed a structural analysis of sulfated glycans in lymph nodes using mass spectrometry (MS). O-glycans were released from whole PLN extracts, permethylated, and the sulfated fractions were analyzed by MS as described previously (Khoo and Yu,

2010). In wild type PLN, direct MALDI-MS mapping in negative ion mode revealed the presence of both mono- and di-sulfated O-glycan structures, the three most abundant being the simple non-, mono- and di-Neu5Gc-sialylated Core 2 structures. NanoESI-MS analysis of di-sulfated structures from wild type mice showed that both sulfates were preserved to give doubly charged  $[M-2H]^{2-}$  molecular ions (Fig. 4A). As noted previously, the second sulfate was readily lost via MALDI in source fragmentation (Yu et al., 2009), which resulted in monosulfated species carrying an additional free OH group (Fig. 4C). Interestingly, structures that were extended with additional LacNAc units were mostly found in the di-sulfated fraction.

To validate the identity of these sulfated O-glycan structures and to define the precise location of sulfates, the same samples were further subjected to nanoLC-nanoESI-MS/MS analysis in negative ion mode, with each of the major components detected by MALDI-MS selected for nanoESI-HCD-MS/MS. Assignment of the sulfated residues was facilitated by diagnostic ions that were established using similar analyses of synthetic standards (Fig. 4B). In wild type mice, MS/MS on the mono-sulfated, mono-sialylated Core 2 structures clearly demonstrated that Gal3S, Gal6S, and GlcNAc6S were present, as indicated by their diagnostic ions (Fig. 4C). The ions for terminal Gal3S ( $m/z$  153, 181) were not observed in di-sialylated Core 2 structures, consistent with this modification being precluded by  $\alpha$ 3 linked sialic acid on both arms. In the mono-sulfated, di-sialylated structures, only the ions derived from GlcNAc6S were detected, whereas in the di-sulfated, di-sialylated structures, additional ions at  $m/z$  167 and 269 indicated that internal Gal6S was also present (data not shown). Likewise, in the di-sulfated mono-sialylated structures, ions indicative of internal Gal6S were found, along with the

additional presence of  $m/z$  253 and 283 derived from terminal Gal6S (Fig. 4C). The paucity of 6,6'-disulfated structures suggested that terminal sialylation of LacNAc units is favored over sulfation of Gal when GlcNAc6S is present. Thus, for the most abundant sulfated O-glycans, LacNAc units on the 6-arm were most often modified with GlcNAc6S and extended to 6-sulfo-3'sLN, while sialylated Gal6S was preferentially found on the 3-arm. LacNAc units modified with GlcNAc6S could be further fucosylated, and indeed we confirmed the presence of a structure consistent with 6-sulfo-sLex by MS/MS (data not shown).

Previous biochemical analysis of GlyCAM-1 O-glycans has demonstrated that the abundance of Gal6S-containing structures is substantially increased in GlcNAc6ST1/2 DKO mice (Kawashima et al., 2005). Therefore, we chose not to analyze KSGal6ST KO mice but instead to use the GlcNAc6ST1/2 DKO background to address whether KSGal6ST was required for the generation of Gal6S-containing O-glycans in lymph nodes. We intercrossed GlcNAc6ST1/2 DKO mice (hereafter, DKO mice) with KSGal6ST KO mice to produce GlcNAc6ST-1/GlcNAc6ST-2/KSGal6ST triple knockout mice (hereafter, TKO mice). These mice were born at the expected Mendelian ratio and were healthy and fertile with no gross physical or behavioral abnormalities. By MS and MS/MS analyses, as described above, we found that the MALDI MS profile and ion intensity for the simple Core 2 O-glycans was similar between wild type and DKO mice (Fig. 4C). However, the diagnostic fragment ions attributed to GlcNAc6S ( $m/z$  234, 195) were undetectable in DKO mice, while the  $^{3,5}A$  ion at  $m/z$  167 derived from Gal6S was the most abundant ion within the low mass region in each of the structures we examined. Thus, an increase in Gal6S in the PLN of DKO mice appears to have maintained the

overall amount of sulfated O-glycans, but prevented most additional LacNAc extension and fucosylation, giving rise to a much simpler MS profile. In agreement with previous biochemical analyses of GlyCAM-1 O-glycans (Hiraoka et al., 2007; Kawashima et al., 2005), 6'-sulfo-sLex was not found in wild type or DKO samples. From these data, we surmise that a considerable level of 6-sulfo-3'sLN is generated in wild type mice, which can then be converted to 6-sulfo-sLex, whereas additional sulfate on the 6-O position of Gal in 6-sulfo-LN or 6-sulfo-3'sLN is not favored. In DKO mice this competitive inhibition may be alleviated, leading to the observed increase in Gal6S concomitant with reduced LacNAc extension along with reduced  $\alpha$ 3 linked fucose. Importantly, in PLN from TKO mice, m/z 167 derived from Gal6S was not detected in any of the structures we analyzed (Fig. 4C). In fact, minimal levels of sulfated O-glycans were present, and MS/MS on the residual sulfated core 2 structures clearly showed that the remaining sulfate was a terminal Gal3S.

### **KSGal6ST generates sialylated, 6,6'-disulfated glycans in lymph node HEVs**

As reviewed above, 6,6'-disulfo-lactose neoglycolipids are recognized by L-selectin (Bruehl et al., 2000). In addition, a previous analysis of GlyCAM-1 O-glycans was consistent with the presence of 6,6'-disulfo-sLex (Sia  $\alpha$ 2 $\rightarrow$ 3 [6S]Gal  $\beta$ 1 $\rightarrow$ 4 [Fuc  $\alpha$ 1 $\rightarrow$ 3][6S]GlcNAc) and 6,6'-disulfo-3'sLN (Sia  $\alpha$ 2 $\rightarrow$ 3 [6S]Gal  $\beta$ 1 $\rightarrow$ 4 [6S]GlcNAc) in lymph nodes (Hemmerich et al., 1995). However, we were unable to detect 6,6'-disulfated structures in total lymph node O-glycans by MS. In order to determine whether these structures were expressed specifically in HEVs, we took advantage of monoclonal antibodies that were generated by immunizing mice with synthetic 6,6'-disulfo-sLex

glycolipids (Mitsuoka et al., 1998). We characterized the glycan specificity of these antibodies by ELISA using a series of synthetic glycolipids coated onto plastic wells and found that G270-2 (isotype IgM) bound the 6,6'-disulfo-sLex immunogen as well as 6,6'-disulfo-3'sLN (Fig. 5A). G270-2 binding exhibited an absolute requirement for Gal6S and was reduced by ~80% in the absence of either 6-O sulfation of GlcNAc or sialic acid.

Using G270-2, we then proceeded to determine whether 6,6'-disulfo-3'sLN, or a structural analogue, was present in lymphoid tissues. In PLN and MLN from wild type mice, G270-2 reacted with nearly all HEVs, although the staining was unevenly distributed among endothelial cells (Fig. 5B,C). In Peyer's patches, G270-2 reactivity was not observed in CD31<sup>+</sup> vessels (Fig. 6B). Instead, it was present in B cell follicles where it partially colocalized with the germinal center marker GL7 (Fig. 6C). We next investigated the structural requirements for G270-2 staining. Sialidase treatment of tissue sections reduced G270-2 staining of HEVs to background levels (Fig. 5B). Furthermore, G270-2 staining was completely absent in lymph nodes of GlcNAc6ST1/2 DKO mice (Fig. 5C). Staining was also reduced to control levels in lymph nodes from KSGal6ST KO mice (Fig. 6A). In contrast, we found no differences in G270-2 staining between C6ST-1 KO mice and wild type mice. As expected, MECA-79 staining in HEVs was not altered in the absence of either KSGal6ST or C6ST-1. In agreement with our findings in HEVs, G270-2 staining in germinal centers was reduced to control levels by sialidase treatment and absent in KSGal6ST KO as well as GlcNAc6ST1/2 DKO mice (Fig. 6B,C, data not shown).

## **KSGal6ST does not contribute to L-selectin ligand expression or lymphocyte homing**

We next addressed whether the Gal6S-containing structures we detected using MS and G270-2 contribute to L-selectin ligand activity *in vivo*. To directly detect L-selectin ligands, we first stained lymphoid organs with an L-selectin-Fc fusion protein. HEVs were identified by their CD31 expression and plump endothelial cells. L-selectin-Fc staining of HEVs was comparable in wild type and KSGal6ST KO mice (Fig. 7A). Consistent with previous findings (Kawashima et al., 2005; Uchimura et al., 2005), GlcNAc6ST1/2 DKO mice showed very weak, abluminal staining of HEVs (Fig. 7A). Mice deficient in L-selectin ligands exhibit a reduction in the number of lymphocytes and a decreased percentage of B cells in lymph nodes (Homeister et al., 2001; Kawashima et al., 2005; Mitoma et al., 2007; Uchimura et al., 2005; Yang et al., 2012). We observed no difference in the number of total lymphocytes in blood or lymphoid organs from KSGal6ST KO mice relative to wild type mice (Fig. 7B). There were small but significant decreases in B cells (3-10%) in PLN and MLN, as well as small increases in T cells (10%) in PLN, from KSGal6ST KO mice. However, these changes were also seen in peripheral blood, consistent with systemic effects on these populations.

Since L-selectin-Fc staining and lymphoid organ cellularity may not reveal subtle defects in L-selectin ligand activity, we evaluated short-term lymphocyte homing in KSGal6ST KO mice. We injected a 1:1 mixture of wild type and L-selectin KO donor splenocytes into the caudal vein of wild type and KSGal6ST KO recipient mice and measured the percentage of donor cells present in lymphoid organs after one hour. In agreement with previous findings (Arbones et al., 1994), L-selectin KO cells were 97%,

84%, and 30% inhibited in their ability to home to PLN, MLN, and Peyer's patches (p values between 0.01 and 0.0001) (Fig. 8A). We did not observe any defects in the homing of wild type splenocytes to lymph nodes in KSGal6ST KO mice. We did find a 33% increase in the percentage of wild type donor cells in Peyer's patches ( $p < 0.0005$ ) and a 24% increase in spleens ( $p < 0.05$ ) from KSGal6ST KO mice. However, similar increases in L-selectin KO donor cells were observed and thus this effect does not appear to reflect changes in L-selectin-dependent homing.

Previous work has demonstrated that GlcNAc6ST1/2 DKO mice exhibit residual L-selectin-dependent homing to PLN and MLN. To address whether KSGal6ST contributes to this ligand activity, we used TKO mice deficient in KSGal6ST, as well as GlcNAc6ST-1 and GlcNAc6ST-2. Although the absence of GlcNAc6ST-1 and GlcNAc6ST-2 reduced homing by 71% in PLN ( $p < 0.0001$ ) and 31% in MLN ( $p < 0.005$ ), consistent with previous findings (Kawashima et al., 2005; Uchimura et al., 2005), there was no further reduction in the absence of KSGal6ST (Fig. 8B). Instead, we found a 35% increase ( $p < 0.005$ ) in L-selectin-dependent homing to PLN in TKO mice. This increase was not observed in MLN.



# Figure I

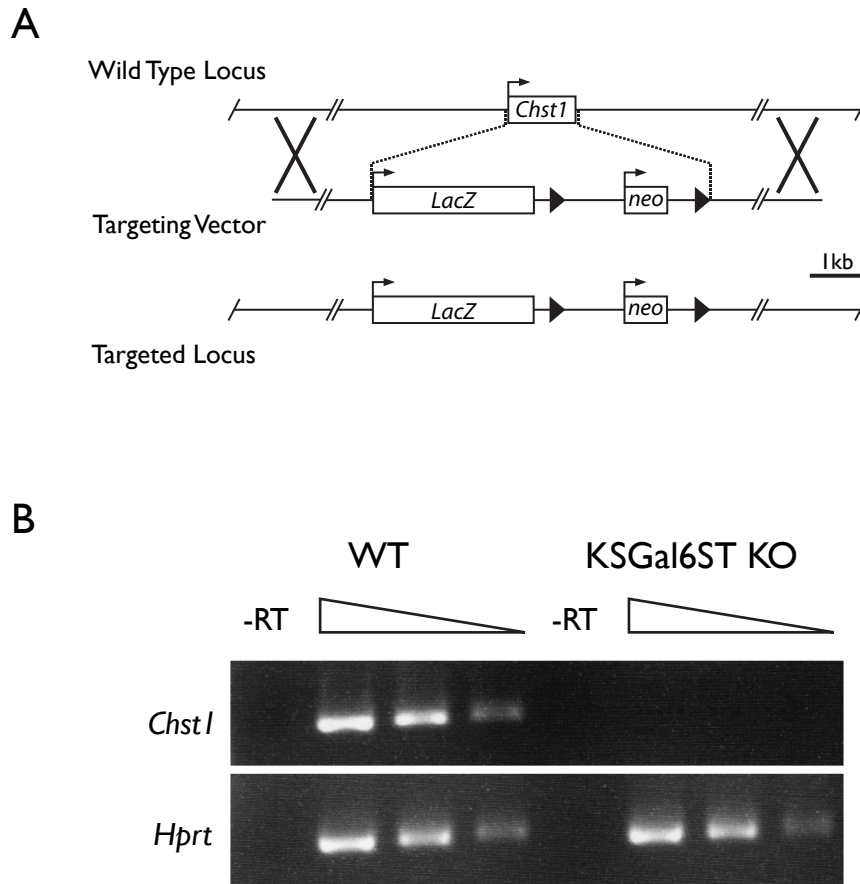


Figure I. Generation of KSGal6ST KO mice

(A) Schematic of the *Chst1* locus and the BAC targeting vector created by Regeneron Inc., which replaces the entire protein-coding region of *Chst1* with the *LacZ* and neomycin phosphotransferase (*neo*) genes. Boxes represent protein-coding regions of exons. Arrows represent transcriptional start sites. Arrowheads represent loxP sites. Xs denote regions of homologous recombination. Scale bar represents 1 kb (kilobase). (B) PCR products generated with primers specific for *Chst1* (206bp product) and *Hprt* (252bp product) using five-fold serial dilutions of cDNA from WT (wild type) or KSGal6ST KO mouse cortex as a template. No products were observed when RT (reverse transcriptase) was omitted from the cDNA synthesis reaction.

Figure 2

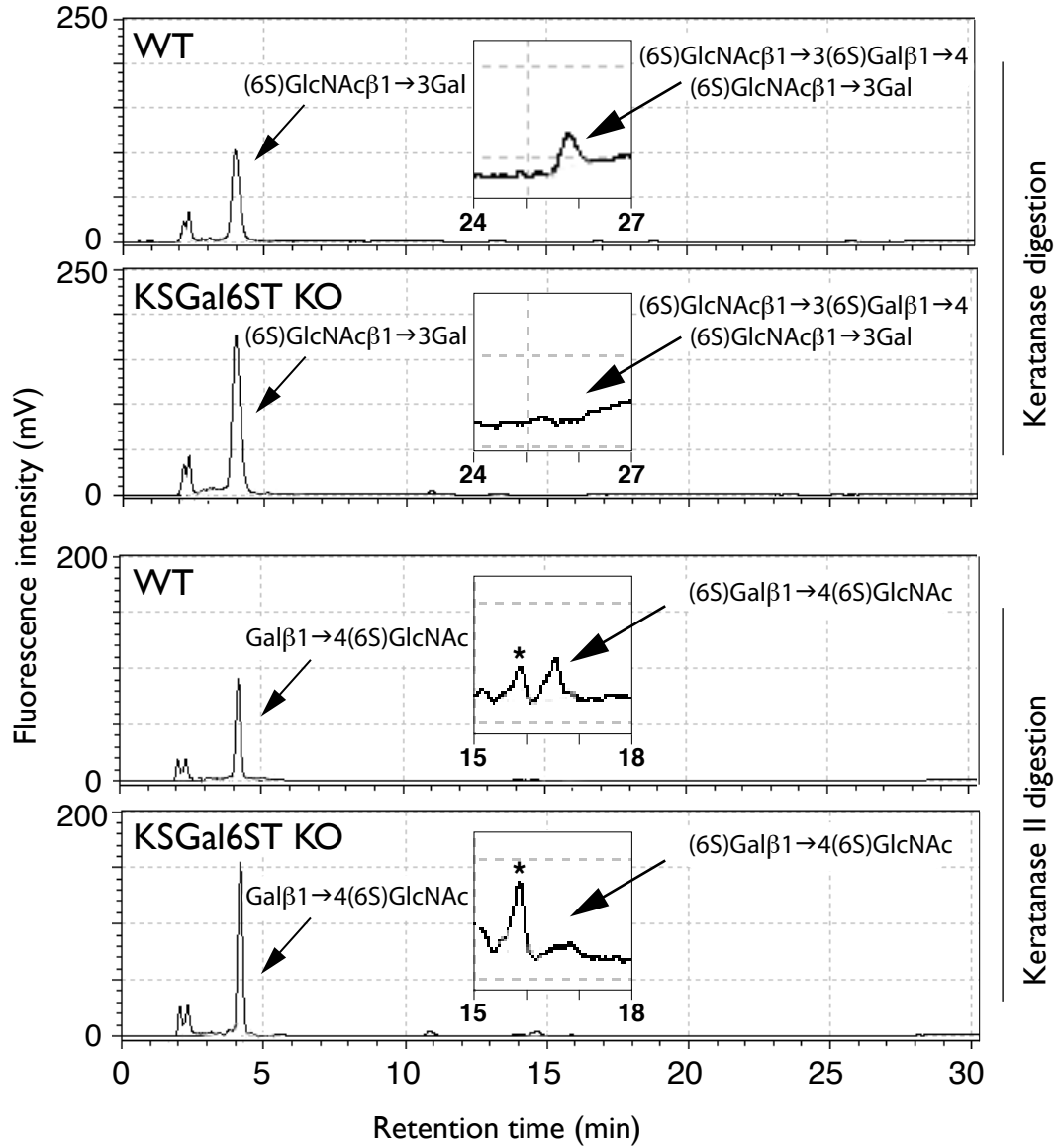


Figure 2. Keratan sulfate analysis in KSGal6ST KO mice  
 Reversed-phase ion-pair chromatography analysis of ocular KS from eyes of wild type (WT) and KSGal6ST KO mice. Standard substances were eluted at the peak positions indicated by arrows. Elution profiles around the peak positions of (6S)GlcNAc β1→3 (6S)Gal β1→4 (6S)GlcNAc β1→3 Gal and (6S)Gal β1→4 (6S)GlcNAc are magnified in insets. Peaks indicated by asterisks were not identified.

Figure 3

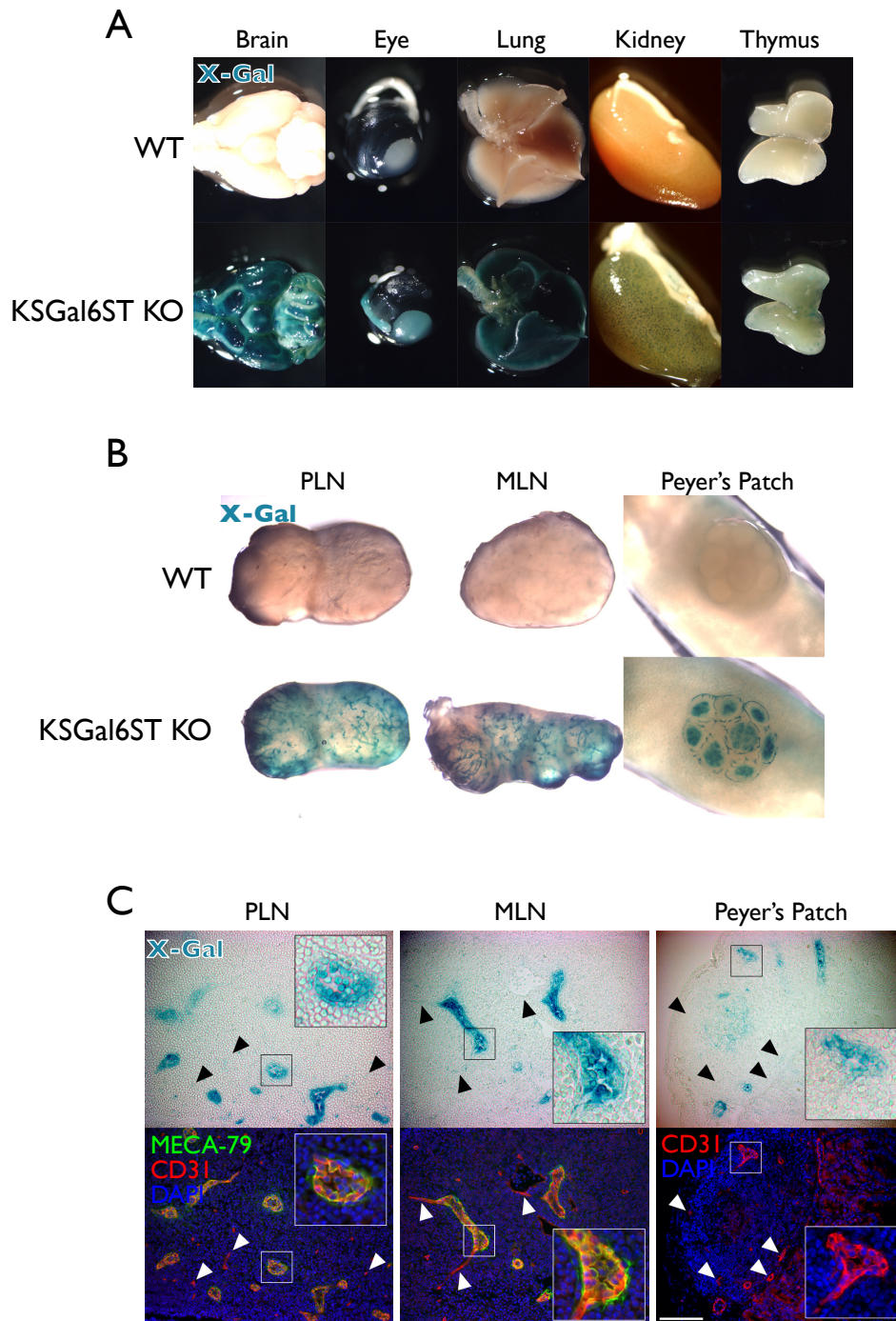


Figure 3. KSGal6ST expression in HEVs

(A), (B) Tissues from WT (wild type) or KSGal6ST KO mice analyzed for  $\beta$ -galactosidase activity using X-Gal (blue). (C) Bright field images (top) of cryostat-cut sections of lymphoid organs from KSGal6ST KO mice stained with X-Gal (blue). Fluorescent images (bottom) of the same sections stained with MECA-79 (green), anti-CD31 (red), and DAPI (blue). Insets show HEVs magnified 3x. Arrowheads highlight examples of vessels with weak X-Gal staining. Scale bar represents 100  $\mu$ m and applies to adjacent images. Isotype matched control antibodies were used to establish background fluorescence. PLN, peripheral lymph node; MLN, mesenteric lymph node.

Figure 4

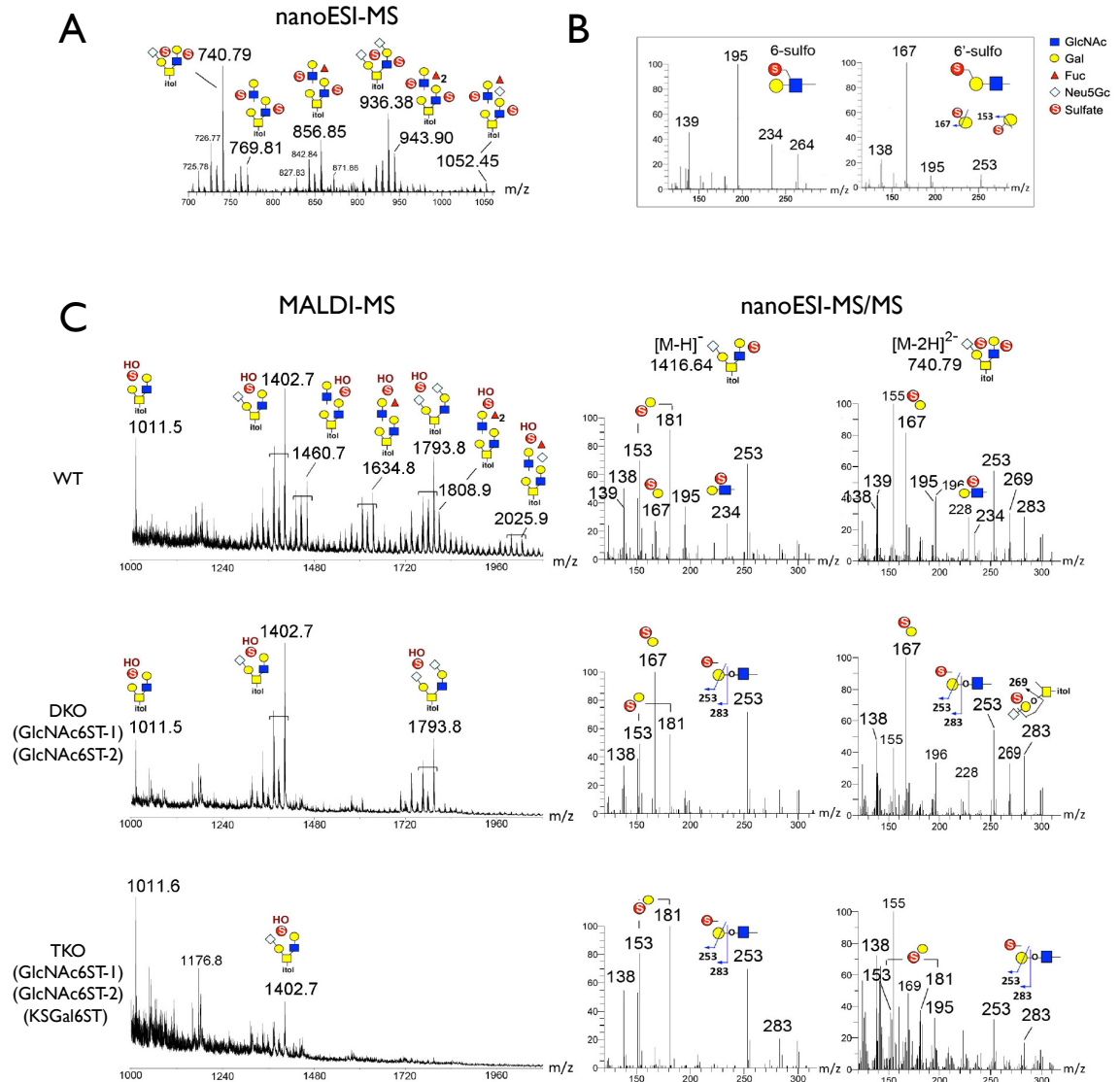


Figure 4. MS analyses of sulfated O-glycans in lymph nodes of KSGal6ST KO mice

(A) NanoLC-nanoESI-MS spectrum for WT di-sulfated permethylated O-glycan fractions (summed over a period of elution time for the major signals). Both sulfates were preserved under nanoESI-MS to give doubly charged  $[M-2H]^{2-}$  molecular ions. (B) Spectra for a panel of sulfated LacNAc standards analyzed to establish the diagnostic ions produced under nanoESI HCD MS/MS fragmentation. The singly charged low mass ions at  $m/z$  195 and 234 were reproducibly detected for all internal GlcNAc6S-containing glycans. In contrast, the  $^{3,5}A$  ion at  $m/z$  167 was detected for Gal6S-containing glycans, which could be distinguished from terminal Gal3S by the ions at  $m/z$  153 and 181 (not shown). (C) Spectra of the di-sulfated O-glycan fractions from WT, GlcNAc6ST-1/-2 DKO, and GlcNAc6ST-1/-2/KSGal6ST TKO lymph nodes analyzed in negative ion mode by MALDI-MS (left). The di-sulfated O-glycans were prone to losing a sulfite by in source fragmentation to produce  $[M-H]^{-}$  molecular ions carrying one sulfate and one free OH group. Low mass regions of the nanoESI HCD MS/MS spectra (right) of mono- and di-sulfated mono-sialylated core 2 structures from WT, DKO and TKO lymph nodes, annotated with diagnostic ions for sulfated structures (see B). Additional ions at  $m/z$  253 (E ion) and 283 (B ion) were indicative of terminal sulfated Gal whilst  $m/z$  269 (D ion) was derived from an internal sulfated Gal, as illustrated. The full spectra of each (data not shown) carried other neutral loss ions and non-reducing terminal fragment ions, which supported the assigned overall structures but did not allow differentiating the positions of sulfates. Assignment of the major peaks for all spectra is as annotated using the standard cartoon symbols. WT, wild type; DKO, double KO; TKO, triple KO.

## Figure 5

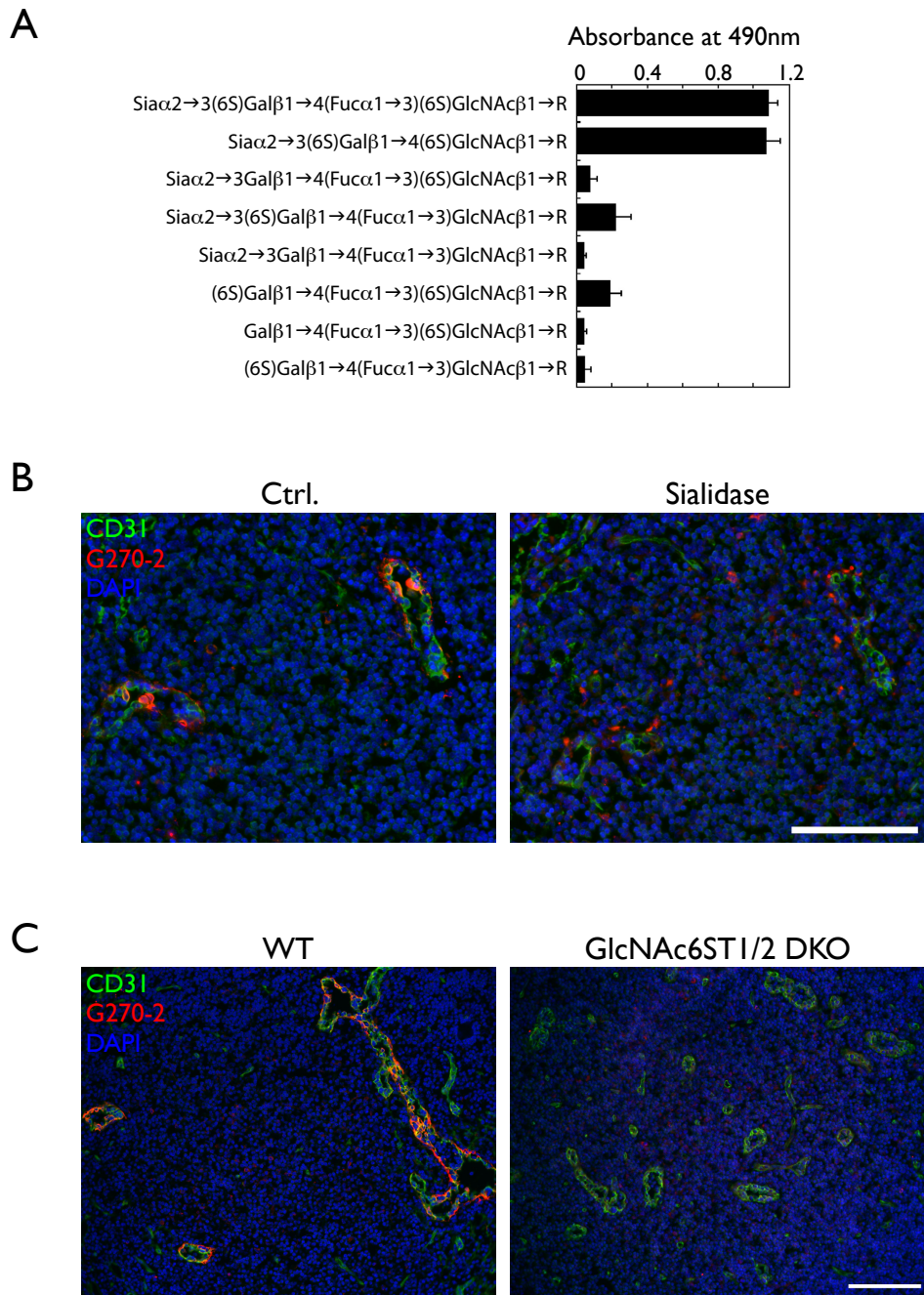


Figure 5. Sialylated 6,6'-disulfated glycans in HEVs

(A) Reactivity of G270-2 as determined by ELISA using 5 ng immobilized neoglycolipids per well. (B) Cryostat-cut serial sections of PLN from WT mice treated with sialidase or buffer alone (ctrl.), then stained with anti-CD31 (green), G270-2 (red), and DAPI (blue). (C) Cryostat-cut sections of PLN from WT and GlcNAc6ST-1/-2 DKO mice stained as in (B). All scale bars represent 100  $\mu$ m and apply to adjacent images. Isotype matched control antibodies were used to establish background fluorescence. PLN, peripheral lymph node; MLN, mesenteric lymph node; WT, wild type; DKO, double KO.



Figure 6

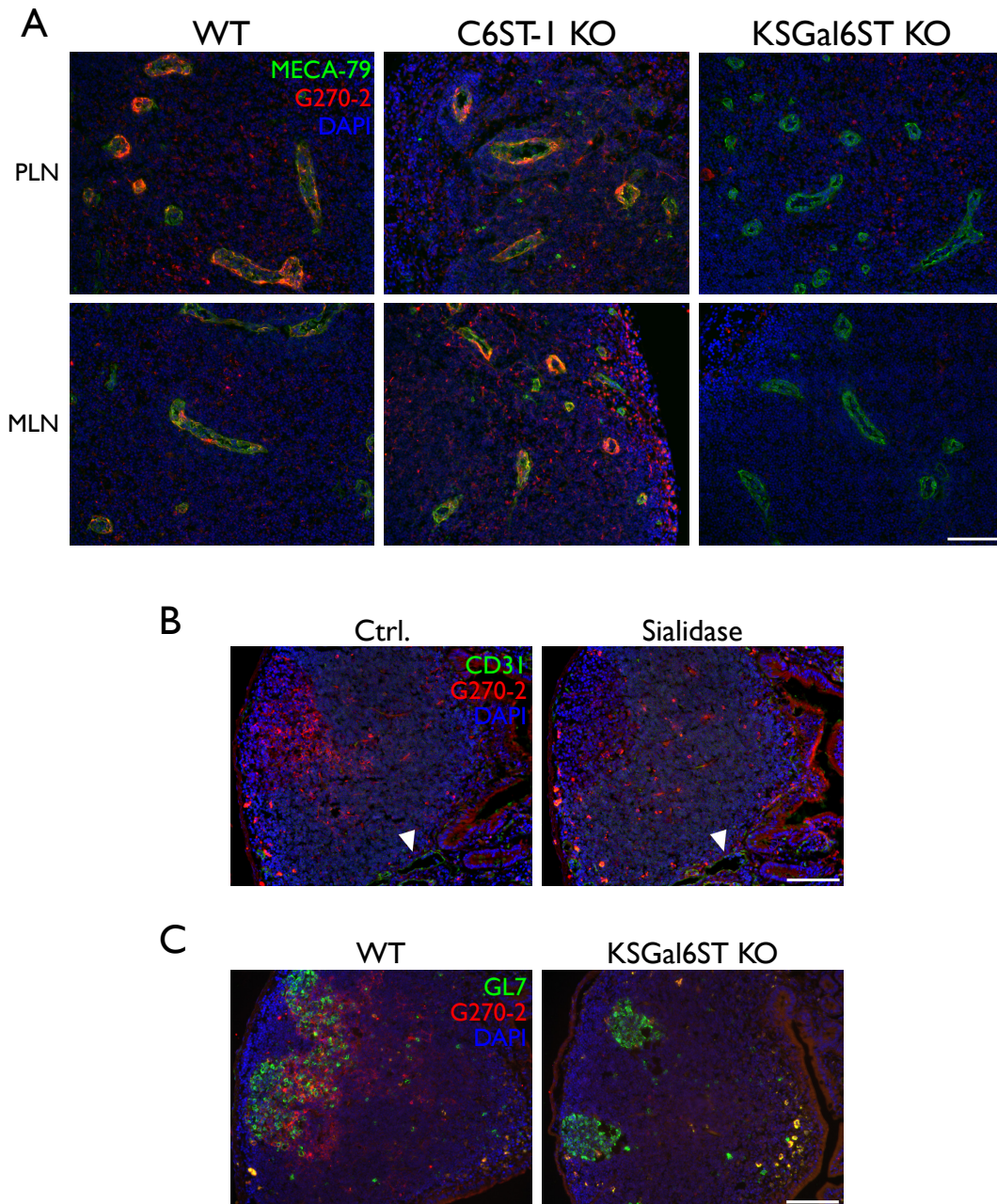


Figure 6. Sialylated 6,6'-disulfated glycans in KSGal6ST KO mice  
(A) Cryostat-cut sections of PLN and MLN from WT, C6ST-1 KO, and KSGal6ST KO mice stained with MECA-79 (green), G270-2 (red), and DAPI (blue). (B) Cryostat-cut serial sections of Peyer's patches from WT mice treated with neuraminidase or buffer alone (ctrl.), and then stained with anti-CD31 (green), G270-2 (red), and DAPI (blue). Arrowheads highlight examples of CD31<sup>+</sup> vessels. (C) Cryostat-cut sections of Peyer's patches from WT and KSGal6ST KO mice stained with GL7 (green), G270-2 (red), and DAPI (blue). All scale bars represent 100 μm and apply to adjacent images. Isotype matched control antibodies were used to establish background fluorescence. PLN, peripheral lymph node; MLN, mesenteric lymph node; WT, wild type; DKO, double KO.

Figure 7

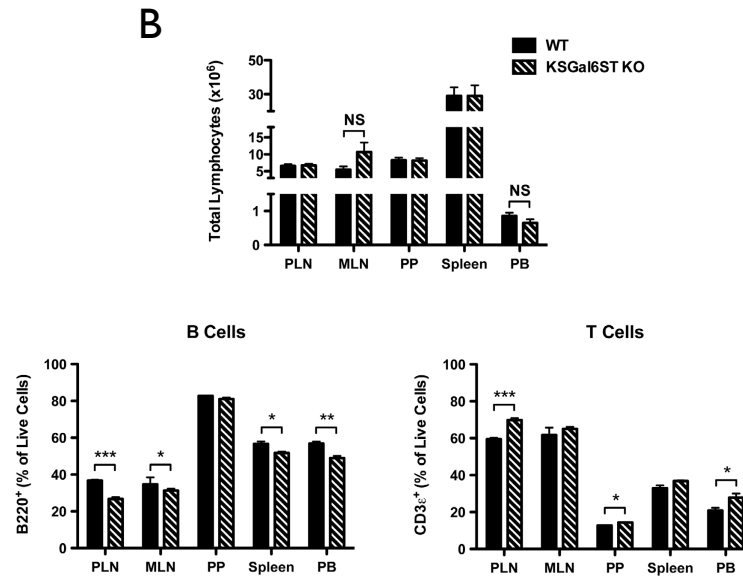
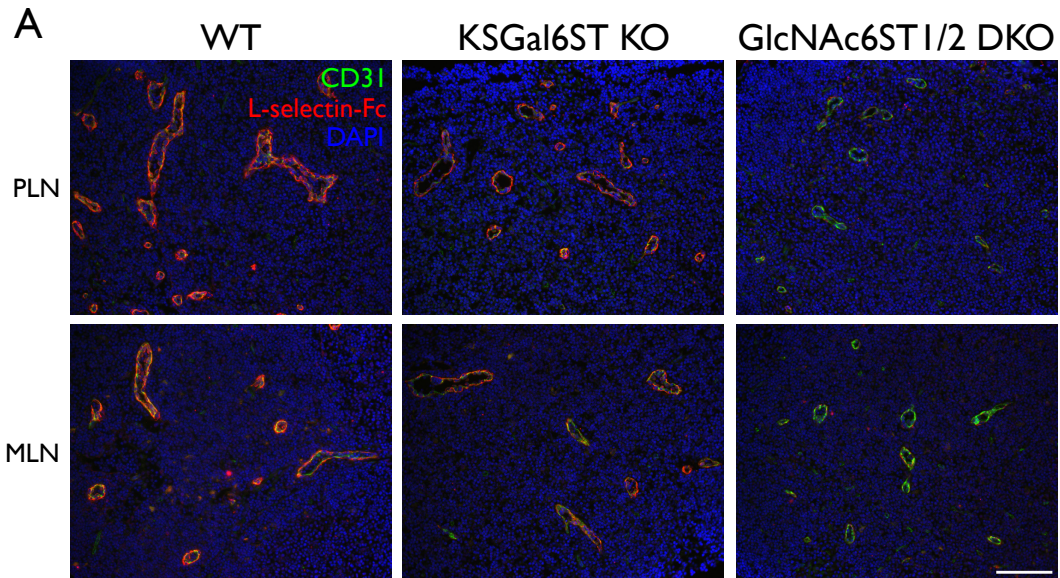
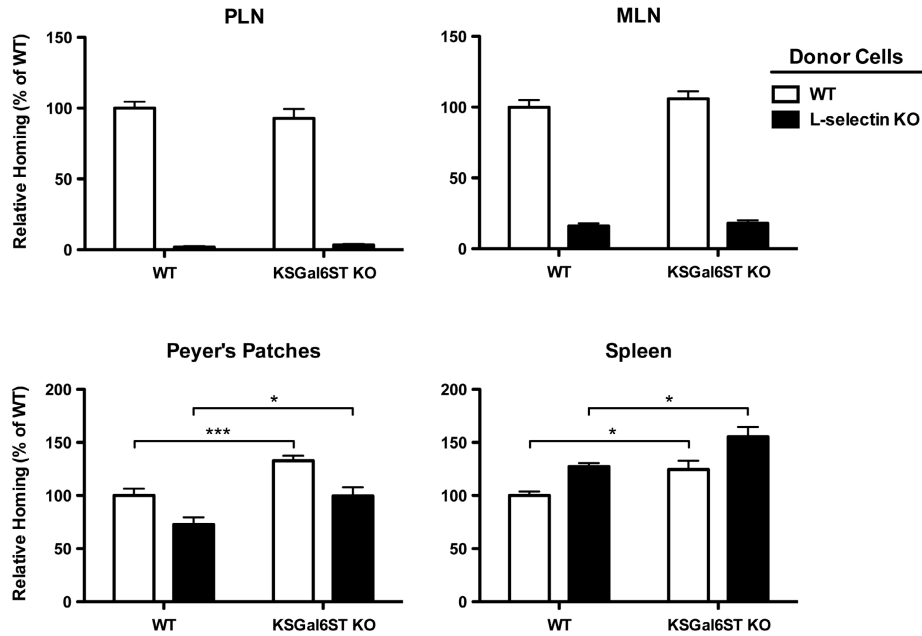


Figure 7. L-selectin ligand expression and lymphocyte numbers in KSGal6ST KO mice (A) Cryostat-cut sections of PLN and MLN from WT, KSGal6ST KO, and GlcNAc6ST1/-2 DKO mice stained with anti-CD31 (green), L-selectin-Fc (red), and DAPI (blue). Background fluorescence was established by staining separate sections with L-selectin-Fc in the presence of 10 mM EDTA. Scale bar represents 100  $\mu$ m and applies to adjacent images. (B) Total numbers (top) and percentages (bottom) of CD3 $\epsilon$ <sup>+</sup> T cells and B220<sup>+</sup> B cells in peripheral blood and lymphoid organs from WT (n = 4) and KSGal6ST KO (n = 3) mice. For MLN, n = 5 for WT, and n = 6 for KSGal6ST KO (p = 0.14). Differences between mouse genotypes are not significant unless otherwise noted. PLN, peripheral lymph node; MLN, mesenteric lymph node; PP, Peyer's patches; SPLN, spleen; PB, peripheral blood; WT, wild type; NS, not significant; \*, p<0.05; \*\*, p<0.005; \*\*\*, p<0.0005.

Figure 8

A



B

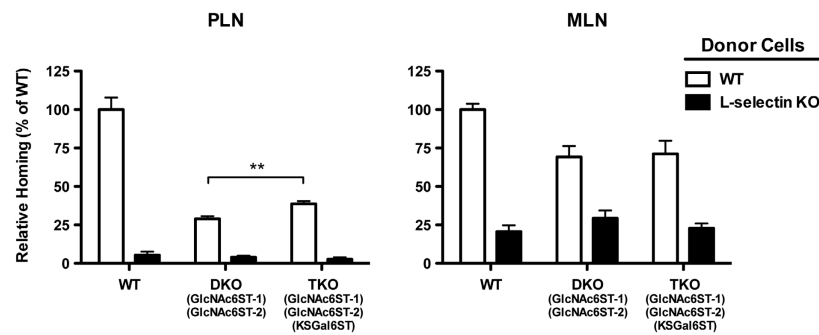


Figure 8. Lymphocyte homing in KSGal6ST KO mice

(A) Short-term lymphocyte homing to PLN, MLN, Peyer's Patches and Spleens of WT (n = 11) and KSGal6ST KO (n = 15) mice. Pooled results from three independent experiments are shown. (B) Short-term homing of splenocytes to PLN and MLN of WT (n = 6), GlcNAc6ST-1/-2 DKO (n = 7), and GlcNAc6ST-1/-2/KSGal6ST TKO (n = 8) mice. Pooled results from two independent experiments are shown. Differences between mouse genotypes are not significant unless otherwise noted. Homing of L-selectin KO splenocytes was significantly reduced relative to wild type splenocytes in all cases, except in homing to the spleen, where it was significantly enhanced (p values between 0.01 and 0.0001). Homing of WT splenocytes to PLN (p<0.0001) and MLN (p<0.005) was significantly reduced in DKO recipients relative to WT recipients. PLN, peripheral lymph node; MLN, mesenteric lymph node; PP, Peyer's patches; SPLN, spleen; PB, peripheral blood; WT, wild type; DKO, double KO; TKO, triple KO; NS, not significant; \*, p<0.05; \*\*, p<0.005; \*\*\*, p<0.0005.



## DISCUSSION

Our characterization of G270-2 staining points to the presence of 6,6'-disulfo-3'sLN, or a structural analogue, in lymph node HEVs. Indeed, our previous analysis of GlyCAM-1 O-glycans was consistent with the existence of this structure (Hemmerich et al., 1995). Studies using chemically synthesized glycans implicated 6,6'-disulfated structures in L-selectin recognition (Bertozzi et al., 1995; Bruehl et al., 2000). We found that G270-2 staining, though unchanged in C6ST-1 KO mice, was completely absent in KSGal6ST KO mice, providing *in vivo* confirmation of the Gal-6-*O*-sulfotransferase activity of KSGal6ST. Additionally, we established that KSGal6ST was required for the generation of all Gal6S-containing O-glycans that we detected by mass spectrometry in GlcNAc6ST1/2 DKO PLN. Nevertheless, KSGal6ST KO mice did not exhibit a detectable deficiency in short-term lymphocyte homing. Thus, we conclude that the G270-2 epitope and the broader class of glycans generated by KSGal6ST are dispensable for L-selectin function in this setting. We were unable to confirm the absence of Gal6S on N-glycans in KSGal6ST-deficient mice, because our N-glycan profiles were not of sufficient quality. Furthermore, recombinant C6ST-1 has Gal-6-*O*-sulfotransferase activity toward desulfated corneal KS chains and, to a much lesser extent, small sialylated lactosamine structures (Habuchi et al., 1997). Thus, it is possible that C6ST-1 generates Gal6S on KS proteoglycans, N-glycans, or other glycans not included in our mass spectrometry analysis. However, a previous characterization of C6ST-1 KO mice found that this enzyme does not contribute to short-term homing (Uchimura et al., 2002). In addition, we generated KSGal6ST/C6ST-1 DKO mice and found no changes in homing compared to wild type mice (data not shown), eliminating the possibility that

C6ST-1 makes compensatory contributions to lymphocyte homing in the absence of KSGal6ST. We consider the existence of an undescribed Gal-6-*O*-sulfotransferase unlikely, given the high degree of sequence similarity among the known members of the GlcNAc-, Gal-, GalNAc-6-*O*-sulfotransferase subfamily of sulfotransferases (Fukuda et al., 2001). Thus, we conclude that Gal6S does not contribute to L-selectin ligand activity during normal lymphocyte homing.

We also show that KSGal6ST does not contribute to the residual lymphocyte homing in GlcNAc6ST1/2 DKO mice. A previous analysis of GlyCAM-1 O-glycans revealed small amounts of GlcNAc6S on core 2 glycans in DKO mice (Kawashima et al., 2005), which could be responsible for the residual homing in both DKO and TKO mice. Our mass spectrometry analysis is consistent with this result, since we detected low levels of 6-sulfo-3'sLN on core 2 glycans in PLN of TKO mice. GlcNAc6ST-4 (*Chst7*) may be involved in generating these structures, since it is expressed in HEVs (Kawashima et al., 2005). However, we and others have recently shown that injection of an antibody that recognizes 6-sulfo-sLex on both O- and N-glycans fails to reduce residual homing to lymph nodes in DKO mice, indicating that the low level of 6-sulfo-sLex does not account for the residual ligand activity (Arata-Kawai et al., 2011; Hirakawa et al., 2010). The remaining ligands are likely to involve structures related to sLex, since injection of soluble E-selectin, which binds to sLex, blocks the residual lymphocyte homing to DKO PLN (Uchimura et al., 2005). Furthermore, sLex is sufficient for L-selectin-Fc binding (Foxall et al., 1992) and is surmised to be sufficient for L-selectin-dependent rolling on endothelial ligands *in vitro* (Li et al., 2001; Tangemann et al., 1999). Based on these observations, the simplest explanation for the residual lymphocyte homing to PLN in

DKO and TKO mice is that it involves suboptimal binding of L-selectin to structures that terminate in sLex lacking sulfation, as previously proposed (Kawashima et al., 2005).

Although the functions of Gal6S in HEVs are still unclear, we show that L-selectin-dependent homing to PLN is increased by 35% in TKO mice relative to DKO mice. These data are consistent with the possibility that this sulfate modification negatively regulates lymphocyte homing in some circumstances. Recombinant FucT-IV and FucT-VII cannot act on 6'-sulfo-3'sLN (Homeister et al., 2001), and recombinant KSGal6ST cannot act on sLex (Torii et al., 2000). Consistent with these findings, 6'-sulfo-sLex was not detected in HPLC analyses of GlyCAM-1 O-glycans (Hiraoka et al., 2007; Kawashima et al., 2005) or in the present MS analysis of total PLN O-glycans. Furthermore, CHO cell monolayers stably expressing CD34, FucT-VII, and GlcNAc6ST-1 have a reduced capacity to support lymphocyte rolling upon transient overexpression of KSGal6ST (Hiraoka et al., 2007). Thus, it has been proposed that the addition of sulfate to the 6-O position of Gal precludes the generation of L-selectin ligands by inhibiting the addition of  $\alpha$ 3 linked fucose on GlcNAc (Hiraoka et al., 2007). Since sLex is plausibly responsible for the residual homing in DKO mice, as discussed above, KSGal6ST deficiency may enhance this residual homing by allowing increased generation of sLex structures. Future studies examining the levels of sLex in TKO mice should address this hypothesis.

In contrast to our observations comparing DKO mice to TKO mice, we did not find that the absence of KSGal6ST alone enhances L-selectin-dependent homing. Multiple factors could account for this discrepancy. First, Gal6S appears to be less abundant in WT PLN than in DKO PLN, as suggested by a previous analysis of GlyCAM-1 O-

glycans (Kawashima et al., 2005) and our current MS analysis of PLN O-glycans. This effect is likely due to the increased availability of the sulfate donor PAPS in DKO mice, as previously proposed (Kawashima et al., 2005). The low abundance of Gal6S in wild type HEVs may result in a negligible increase in sLex structures in KSGal6ST KO mice and, hence, insignificant effects on homing. A second possibility is that 6-sulfo-sLex in wild type HEVs makes the predominant contribution to L-selectin ligand activity such that additional sLex generated in the absence of Gal6S does not appreciably increase homing. Regardless of the mechanisms underlying these differential effects of Gal6S on homing, it will be important to determine whether KSGal6ST influences leukocyte trafficking in other settings. For example, HEVs can develop during many chronic inflammatory diseases including rheumatoid arthritis, psoriasis, and ulcerative colitis (Drayton et al., 2006). Moreover, HEV-like vessels are induced in mouse models of chronic inflammation and tertiary lymphoid organ formation. The LacZ reporter allele and the monoclonal antibody G270-2 described in this report provide tools for determining whether KSGal6ST and 6,6'-disulfo-sLN are expressed in the HEV-like vessels at these ectopic lymphoid sites.

Our survey of KSGal6ST expression highlights several other tissues where Gal6S could have important functions. The intensity of X-Gal staining was strongest in the brain, which is in agreement with previously observed transcript levels in mice and humans. It has been shown that GlcNAc6ST-1 is required for 6-O sulfation of GlcNAc on KS in the mouse central nervous system (Zhang et al., 2006). Furthermore, these studies demonstrated that GlcNAc6ST-1 deficiency impairs glial scar formation and enhances neurite outgrowth after traumatic injury. Experiments using KSGal6ST KO

mice can address similar questions with respect to Gal6S in the brain. KS is also critical for normal corneal morphology and function, as evidenced by humans with mutations in the GlcNAc-6-*O*-sulfotransferase gene *CHST6* (c-GlcNAc6ST) (Akama et al., 2000), and mice with a targeted deletion in *Chst5* (i-GlcNAc6ST) (Hayashida et al., 2006). Furthermore, the monoclonal antibody 5D4, which recognizes a Gal6S-containing epitope within KS (Mehmet et al., 1986), stains the cornea (Hayashida et al., 2006) and retina (Ng and Streilein, 2001). Although we were unable to detect KSGal6ST expression in the cornea, we did detect strong expression in the retina and optic nerve. Our HPLC analysis establishes that KSGal6ST is required for generating Gal6S within ocular KS. Thus, KSGal6ST KO mice will be useful in determining whether this modification contributes to KS function in the eye.

We found KSGal6ST expression in the glomeruli of the kidney. The core protein of the KS proteoglycan lumican is expressed in the glomerular endothelial cell coat (Friden et al., 2011). Therefore, KSGal6ST may participate in sulfating KS chains on this proteoglycan scaffold. Additionally, the cell-surface mucin podocalyxin is expressed in foot processes of podocytes in the glomeruli (Nielsen and McNagny, 2009). Podocalyxin is required for the formation of the slit diaphragms through which blood plasma is filtered before entering the urinary space. The negative charge of podocalyxin, imparted by its sulfation and sialylation, is thought to be important for its function (Dekan et al., 1991). Accordingly, mice with a mutation in the sialic acid biosynthesis enzyme, GNE, do not form slit diaphragms and die from renal failure soon after birth (Galeano et al., 2007). Although we observed no gross morphological differences in glomeruli from KSGal6ST

KO mice, it remains to be determined whether KSGal6ST contributes to the sulfation of podocalyxin and affects its function in glomerular filtration.

We also found KSGal6ST expression as well as G270-2 reactivity in germinal centers of Peyer's patches and MLN. This staining has the same structural requirements as in HEVs and thus indicates the presence of 6,6'-disulfo-3'sLN, or a structural analogue. B cells express CD22, a member of the Siglec family that is known to negatively regulate B cell activation (Walker and Smith, 2008). Sialic acid on the 6-*O* position of Gal is required for CD22 binding (Paulson et al., 2012). Therefore, it is plausible that KSGal6ST impedes the generation of CD22 ligands by competing with  $\alpha 6$  sialyltransferases. It will be of interest to examine KSGal6ST KO mice in this context.

Sulfate serves as a recognition determinant for many immunological receptors. These include C-type lectins such as L-selectin, P-selectin, and the macrophage mannose receptor, as well as Siglecs such as Siglec-7, Siglec-9, and CD22 (Campanero-Rhodes et al., 2006; Kimura et al., 2007; Miyazaki et al., 2012). Screening of lectins using the Consortium for Functional Glycomics (CFG) glycan array has suggested the importance of Gal6S in ligands for several receptors on innate immune cells. Siglec-8, a sialic acid-binding lectin expressed on human eosinophils, binds 6'sulfo-sLex and 6'sulfo-3'sLN with remarkable specificity and shows an absolute requirement for sulfate on the 6-*O* position of Gal (Bochner et al., 2005). Similar experiments using Siglec-F have demonstrated that this Siglec also recognizes these structures (see chapters 3 and 4). Furthermore, ligands have been detected in the lung where we found strong expression of KSGal6ST. Human Siglec-7 and Siglec-5 and murine Siglec-E bind 6'sulfo-sLex, but these Siglecs also bind to glycans lacking Gal6S (Tateno et al., 2005). The C-type lectin,

langerin preferentially binds to 6'-sulfo-lactosamine on the glycan array, and also binds CHO cells transfected with KSGal6ST (Tateno et al., 2010). KSGal6ST expression in the lung could potentially generate structures recognized by resident dendritic cells, which express langerin. KSGal6ST KO mice provide a valuable tool for determining whether these receptors recognize Gal6S-containing structures *in vivo*.

## **FUTURE PROSPECTS**

Many important aspects of leukocyte entry into secondary lymphoid organs remain to be elucidated. Although Gal6S does not appear to contribute to L-selectin-dependent lymphocyte homing, this modification is expressed in HEVs and may function in aspects of lymphocyte entry that have not been as thoroughly investigated.

The direct visualization of lymphocytes in the process of transendothelial migration across HEVs was paramount in identifying these vessels as gateways to the lymph node stroma (Gowans and Knight, 1964). Yet, after more than a half-century of study, the molecules involved in this process are not completely understood (Ley et al., 2007). Once lymphocytes have firmly adhered to the surface of the HEVs, it seems likely that specific signals are necessary to a) guide them to a designated entrance, b) stimulate them to step inside, and c) to make sure they close the door behind them. In inflamed vasculature, neutrophils transmigrate rapidly, even traveling directly through the cytoplasm of endothelial cells. Excessive leukocyte recruitment in delicate tissues such as the lung is associated with vascular leakage, and can even be fatal (Bhattacharya and Matthay, 2013). Indeed, neutrophils are required for lung edema in mouse models of acute

respiratory distress syndrome. Transmigration of leukocytes across the blood-brain barrier in mouse models of multiple sclerosis has been associated with increased vascular permeability (Daneman, 2012). In contrast, staggering numbers of lymphocytes constitutively cross HEVs without evidence of vascular leakage. Advances in intra-vital imaging have revealed that lymphocytes often crawl along the vessel wall before inserting themselves between endothelial cells where other lymphocytes have recently entered (Bajenoff et al., 2006). It remains to be demonstrated whether this migration is induced by chemokines, or by LPA produced locally as a result of autotaxin bound to lymphocyte or endothelial surfaces (Kanda et al., 2008; Zhang et al., 2012). The subsequent events that mediate the opening and closing of the endothelial junctions are not well understood. Studies of inflamed endothelium suggest that homotypic binding of JAMs or CD99 could act as a zipper between leukocytes and endothelial cells (Ley et al., 2007). The strong expression of KSGal6ST in HEVs and kidney glomeruli may reflect specialized functions for Gal6S in regulating vascular permeability. Future studies exploring how HEV integrity is maintained in the face of sustained lymphocyte influx could provide new insights into the breakdown of endothelial barriers during disease.

Lymph nodes undergo dramatic expansions in size during immune responses (Liao and Ruddle, 2006). It has been demonstrated that the sphingosine-1-phosphate receptor S1P<sub>1</sub> binds to CD69 and is internalized in response to inflammatory cytokines. This inhibits egress and increases the number of lymphocytes in lymph nodes, directly contributing to an increase in size (Shiow et al., 2006). On the other hand, there are additional changes in lymph node architecture that do not appear to be the direct result of lymphocyte accumulation (Liao and Ruddle, 2006). Shortly after immunization or



infection, HEVs in lymph nodes regress to a rudimentary state. They lose their characteristic plumpness and cease to express several HEV-specific genes including GlcNAc6ST-2, FucT-VII, and GlyCAM-1. Following this HEV atrophy, blood and lymph vessels undergo extensive elaboration and remodeling, and HEV characteristics return. Activation of the lymphotoxin receptor  $LT\beta R$  on endothelial cells is required for these processes, and the additional signals involved are the subject of current research. As the immune response subsides, the lymph node returns to normal size. However, it is conceivable lymph node remodeling makes results in lasting changes to the vascular architecture, which could affect the entry of lymphocytes through HEVs, as well as that of dendritic cells and antigen through lymphatic vessels. Thus, a history of remodeling could increase the efficiency of lymphocyte interactions in lymph nodes draining certain tissues that are prone to infection or inflammation. Such a system would provide unique evolutionary advantages, as well as opportunities to manipulate immune responses. There appear to be very few LacNAc units carrying Gal6S in HEVs under homeostatic conditions, which may explain why this modification is dispensable for constitutive lymphocyte homing. However, the abundance of such structures might increase as a result of lymph node remodeling during infection or immunization. If these structures are elevated in lymph nodes with prior exposure to antigen, or if they are present in tertiary lymphoid organs, further studies of the ability of KSGal6ST to contribute to lymphocyte homing under these special circumstances would be warranted.

## MATERIALS AND METHODS

### Mice

*Chst1*<sup>-/-</sup> mice were generated by Regeneron Pharmaceuticals Inc. and the trans-NIH Knockout Mouse Project (KOMP) using published protocols (Valenzuela et al., 2003). Detailed information about the targeting construct is available on the Velocigene website (<http://www.velocigene.com/komp/detail/10172>). Briefly, upon recombination with the BAC targeting vector, a cassette containing the promoterless *E. coli* K12 LacZ gene and the neomycin phosphotransferase gene was introduced in place of the entire protein-coding region of *Chst1*. C57BL/6NTac embryonic stem (ES) cells were screened for the loss of one wild type copy of *Chst1* using Taqman quantitative PCR. Targeted ES cells were injected into BALB/c blastocysts, and the resulting chimeric offspring were bred until germline transmission was achieved. Mice deficient in GlcNAc6ST-1, GlcNAc6ST-2, and L-selectin have been described previously (Arbones et al., 1994; Uchimura et al., 2005). L-selectin KO mice were genotyped by FACS analysis of peripheral blood leukocytes stained with FITC-anti-mouse L-selectin (clone MEL-14, eBioscience). Sulfotransferase-deficient mice were genotyped by PCR as previously described (Uchimura et al., 2005). Primers specific for the genes *Chst1* (5'-CCTCTGCAACCACAACACTCTC-3', 5'-GCCTTCCAAGAACATTGCAT-3'), *Chst2* (5'-AAGCCTACAGGTGGTGCAGAA-3', 5'-CAGGACTGTAAACCCGCTCA-3'), *Chst3* (5'-ATGCATCTCTCTTGTCCCTGA-3', 5'-CACATACAGGTCGCATAGCAA-3'), *Chst4* (5'-GTAGCTCTCTTCATCCATATGTTTCG-3', 5'-CGTTTCCAAATGCTGCCCTAGCAC-3'), and LacZ (5'-GTCTGTCCTAGCTTCCTCACTG-3') were obtained from IDT. Alternate primers were

use to detect the *Chst2*<sup>-/-</sup> allele (5'-GCCAAAAGTGATCACCTCGT-3'), *Chst3*<sup>-/-</sup> allele (5'-AGGGCTATGTCTCACTGCCA-3') and *Chst4*<sup>-/-</sup> allele (5'-GGCTGTGCTGCTGGTGAAAGTCAT-3') in combination with a primer specific for the neomycin phosphotransferase gene (5'-AGCGTTGGCTACCCGTGATA-3'). C57BL/6J mice were obtained from Jackson Laboratories. All procedures involving animals were approved by the University California San Francisco Institutional Animal Care and Use Committee, and carried out in accordance with the guidelines established by the National Institutes of Health.

### **Reverse transcriptase PCR**

Mouse forebrain was homogenized by sonication in RLT buffer (Qiagen). Total RNA was extracted using RNeasy mini kit (Qiagen) according to manufacturer's instructions. cDNA was synthesized using superscript III reverse transcriptase (Invitrogen) according to manufacturer's instructions. PCR was performed as above using primers specific for *Chst1* (5'-TTGGCAGCCGAGGCTTGTCG-3', 5'-TGCCGTACCAAAGCCGCCAG-3') and *Hprt* (5'-TTGCTGGTGAAAAGGACCTCTCG-3', 5'-CCACAGGACTAGAACACCTGCTAA-3').

### **Preparation and structural analysis of ocular keratan sulfate**

Ocular KS was isolated and analyzed as described previously for heparan sulfate (Hosono-Fukao et al., 2011) with slight modifications. Adult mouse eyes (~50 mg) were suspended in 2 mL 0.2 N NaOH and incubated at room temperature overnight. The samples were neutralized with 4 N HCl and then treated with DNase I and RNase A (0.04

mg/ml each) (Roche) in 50 mM Tris-HCl, pH 8.0, 10 mM MgCl<sub>2</sub> for 3 hours at 37° C, followed by treatment with actinase E (0.08 mg/ml) (Kaken Pharmaceutical Co., Ltd., Tokyo, Japan) at 50° C overnight. Samples were heated to inactivate enzymes, centrifuged at 5,000 x g and 4° C for 10 minutes, and the supernatant was collected and mixed with an equal volume of 50 mM Tris-HCl, pH 7.2. The keratan sulfate was purified by DEAE-Sepharose column chromatography. The oligosaccharide compositions of the keratan sulfate after digestion with keratanase or keratanase II overnight were determined by reversed-phase ion-pair chromatography with post-column fluorescent labeling. Gal6S-containing oligosaccharide components were identified using authentic sulfated oligosaccharide markers and digestion products released from bovine corneal keratan sulfate by the action of endo-β-galactosidase or keratanase. Keratan sulfate from bovine cornea, endo-β-galactosidase (*Escherichia freundii*), keratanase (*Pseudomonas* sp.), and keratanase II (*Bacillus* sp. Ks 36) were purchased from Seikagaku, Tokyo, Japan.

### **X-Gal and immunofluorescence staining**

For X-Gal staining, tissues were fixed, washed, and stained with X-Gal staining solutions (Millipore) according to manufacturer's instructions, with incubation in X-Gal overnight. Tissues not stained with X-Gal were fixed in 4% PFA for 1 hour, then incubated in 30% sucrose overnight. All tissues were embedded in OCT compound (Sakura Finetek) and frozen by immersion in 2-methylbutane chilled in liquid nitrogen. Tissues were sectioned at 5 μm thickness in a cryostat and then fixed in -20° C acetone for 10 minutes. For sialidase experiments, sections were treated with 50 mU/mL *Arthrobacter ureafaciens*

sialidase (Roche Applied Sciences) in pH 5.0 acetate buffer at 37° C for 1 hour. Sections were blocked with 3% BSA and 5% normal sera from mouse, rat, goat, or donkey (Sigma), depending on the experiment. MECA-79 (BioLegend), biotin-MECA-79 (BioLegend), CD31 (Goat pAb, R&D Systems), biotin-CD31 (clone 390, eBioscience), human L-selectin-IgG (R&D Systems), and GL7 (eBioscience) were incubated with sections at 1 to 5 µg/mL for 1 hour. G270-2 was incubated with sections at 10 µg/mL for 6 hours. Nonspecific rat IgM (clone eBRM, eBioscience), biotin-rat IgM (clone eBRM, eBioscience), mouse IgM (clone 11E10, eBioscience), and goat IgG (Invitrogen) were used to establish background fluorescence. For L-selectin-Fc staining, background fluorescence was established using control sections stained in the presence of 10 mM EDTA. Secondary reagents, Cy3-goat anti-rat IgM, Cy2-goat anti-rat IgG, Cy2-streptavidin, and Cy3-streptavidin were obtained from Jackson ImmunoResearch and incubated with sections at 1 µg/mL for 30 minutes. All antibodies were diluted in Dulbecco's PBS (D-PBS) with 3% BSA. All sections were incubated with DAPI (Invitrogen) at 0.5 µg/mL in PBS for 5 minutes to label nuclei. Images were acquired using a Nikon Optiphot microscope equipped with an AxioCam HR at fixed exposure. Multi-channel images were created and processed in parallel using Photoshop software (Adobe).

### **Mass spectrometry analysis**

O-glycan samples were prepared from whole PLN lysates, permethylated and fractionated into non-, mono- and di-sulfated fractions for MALDI-MS analyses as described previously (Khoo and Yu, 2010; Yu et al., 2009). NanoLC-MS/MS analyses of

the permethylated, sulfated glycans were performed on a nanoACQUITY UPLC System (Waters) coupled to an LTQ-Orbitrap Velos hybrid mass spectrometer (Thermo Scientific) using the same nanoLC conditions and MS acquisition method as described previously (Shibata et al., 2012). NanoLC-MS/MS of the disulfated glycans was additionally carried out on a homemade nanoLC system comprised of a 50  $\mu\text{m}$  x 4 cm homemade polystyrene-divinylbenzene (PS-DVB) monolithic trap column and a 20  $\mu\text{m}$  x 4 m homemade PS-DVB grafted open tubular analytical column coupled to the same LTQ-Orbitrap Velos MS system. For this nanoLC system, sample was dissolved in 25% acetonitrile and separated at a constant flow rate of 150 nl/minute, with a linear gradient of 10–40% acetonitrile (with 1 mM ammonium bicarbonate) over 30 minutes, then increased to 80% acetonitrile over 5 minutes and held isocratically for another 10 minutes. The eluent was interfaced to the nanospray source based on the liquid junction configuration consisting of an uncoated emitter and a high voltage electrode. For each data-dependent acquisition cycle, the full scan MS spectrum ( $m/z$  500-2000) was acquired in the Orbitrap at 60,000 resolution (at  $m/z$  400) with automatic gain control (AGC) target value of  $5 \times 10^6$ . A target precursor inclusion list was applied to precede further selection of five most intense ions with intensity threshold of 300 counts for both collision induced dissociation (CID) and higher energy C-trap dissociation (HCD). The AGC target value and normalized collision energy applied for CID and HCD experiments were set as 20,000, 45% and 100,000, 100%, respectively. All MS/MS data were interpreted manually.

### **Generation of the monoclonal antibody G270-2**

G270-2 was generated as described previously (Mitsuoka et al., 1998). Briefly, 6,6'-disulfo-sLex glycolipids were adsorbed to *Salmonella minnesota* strain R595 and administered to Balb/c mice by repeated intraperitoneal injection. Splenocytes were harvested and fused with the mouse myeloma P3/X63-Ag8U1, and clones were screened for reactivity to the immunogen. The specificity of G270-2 was determined by ELISA using immobilized glycolipids as described previously (Mitsuoka et al., 1998).

### **Lymphocyte homing assay**

Short-term lymphocyte homing assays were carried out as described previously (Arbones et al., 1994) with slight modifications. Briefly, spleens from 10-12 week-old C57BL/6 wild type or L-selectin KO mice were mechanically dissociated with a syringe plunger and a 70  $\mu\text{m}$  cell strainer (BD Biosciences). Erythrocytes were lysed using ammonium chloride buffer (150 mM  $\text{NH}_4\text{Cl}$ , 10 mM  $\text{KHCO}_3$ , 100  $\mu\text{M}$  EDTA). Splenocytes of one genotype were incubated with 2 $\mu\text{M}$  CFDA-SE (Invitrogen), while splenocytes of the other genotype were incubated with 1 $\mu\text{M}$  CMTMR (Invitrogen), for 25 minutes in RPMI-1640 medium containing 0.2% FBS. Differentially labeled wild type and L-selectin KO splenocytes were washed with RPMI-1640 containing 2% FBS and combined in equal numbers. A 200  $\mu\text{L}$  aliquot containing  $20 \times 10^6$  total cells was injected into the lateral caudal vein of each age-matched (8-10 week old), sex-matched wild type, KSGal6ST KO, GlcNAc6ST1/2 DKO, or TKO mouse. After one hour, inguinal, axillary, and brachial lymph nodes, all mesenteric lymph nodes, all Peyer's patches, and spleens were collected. Lymph nodes were dispersed using ground glass microscope slides. Peyer's

patches and spleens were mechanically dispersed using cell strainers, as above. Splenic erythrocytes were lysed using ammonium chloride buffer. All cell suspensions were filtered through 100  $\mu\text{m}$  nylon mesh (ELKO Filtering Co.), and analyzed using a BD FACSort cytometer equipped with CellQuest software (BD). Further analysis was carried out using FlowJo software (Treestar Inc.). The frequencies of wild type and KO donor splenocytes relative to recipient cells in lymphoid organs were determined and normalized using the ratio of wild type to KO cells injected, as determined by FACS analysis.

### **Flow cytometry analysis of blood and lymphoid organs**

Blood (200  $\mu\text{L}$ ) was collected through the right ventricle into 5 mM EDTA, and then treated with ammonium chloride buffer to lyse erythrocytes. Lymphoid organs were collected and dissociated as described above. Cell numbers were determined using CountBright counting beads (Invitrogen) according to manufacturer's instructions. Separate aliquots of cells were incubated with 10  $\mu\text{g}/\text{mL}$  anti-mouse CD16/32 (clone 93, eBioscience) and then stained with 5  $\mu\text{g}/\text{mL}$  FITC-anti-mouse CD3 $\epsilon$  (clone 145-2C11, BioLegend) and APC-anti-mouse B220 (clone RA3-6B2, BioLegend). Viability was determined by adding 50  $\mu\text{L}/\text{mL}$  7AAD solution (BD Pharmingen). Cells were analyzed using the instrumentation and software described above.



### **Statistical analysis**

All graphical data were plotted as means plus the standard error mean using Prism 5 software (GraphPad Software, La Jolla, CA). Student's *t*-test was used to evaluate the statistical significance of differences between groups.

### **Funding**

This work was supported by the National Institutes of Health [GM-23547, GM-57411 to S.D.R., U01HG004085 to Velocigene at Regeneron, Inc., U01HG004080 to the CSD Consortium, U42RR024244 to the KOMP Repository at University of California, Davis]; the Academia Sinica and Taiwan National Science Council [grant number 99-2311-B-001-021-MY3 to K-H.K.]; the Ministry of Education, Culture, Sports, Science and Technology [Grant-in-Aid 24590364 to R.K.]; the Ministry of Health and Welfare [Grant-in-Aid for the Third-Term Comprehensive Ten-Year Strategy for Cancer Control to R.K.]; and the Taiwan National Core Facility Program for Biotechnology [NSC100-2325-B-001-029, NSC101-2319-B-001-003 to the Core Facilities for Protein Structural Analysis at Academia Sinica].

### **Acknowledgements**

We are grateful to Y.-Q. Wang, M. Elin, and M. Izawa for technical assistance. Additional technical support with nanoLC-MS/MS data acquisition was provided by C.C. Chou.

## **CHAPTER 3**

### **Structure and Function of the CD33-Related Siglecs**

## **The Siglec Family and Inhibitory Receptor Signaling**

Siglecs (sialic acid-binding immunoglobulin-like lectins) are a family of type-I transmembrane carbohydrate-binding receptors primarily expressed on circulating and tissue-resident leukocytes (Crocker et al., 2007; Varki and Angata, 2006). All Siglecs possess an extracellular N-terminal V-set Immunoglobulin (Ig) domain that recognizes sialic acid. However, each Siglec has a distinct binding profile with preferences for the linkage of sialic acid together with features of the underlying glycan. Siglecs also contain a variable number of extracellular C2-set Ig domains, which are important in determining whether the ligand-binding domain can interact with the glycocalyx of the Siglec-expressing cell (Crocker et al., 2007). The cytoplasmic domains of most Siglecs contain immunoreceptor tyrosine-based inhibition motifs (ITIMs) (with the consensus amino acid sequence I/V/L/S-X-Y-X-X-L/V), which can recruit inhibitory phosphatases to the signaling complexes generated by activating receptors. Many Siglecs also contain an ITIM-like region (with the consensus amino acid sequence D/E-Y-X-E-I/V-K/R), which can affect the recruitment of phosphatases in some circumstances (Crocker et al., 2007).

Five members of the Siglec family, sialoadhesin, CD22, MAG, Siglec-15, and CD33 are well conserved among mammals. In contrast, the CD33-related (CD33r) Siglecs are rapidly evolving, and there are no clear orthologs between mice and humans, with the exceptions of Siglec-G and Siglec-10. Thus, the CD33r Siglecs have been assigned the letters E through H in mice and the numbers 5 through 14 in humans. Most myeloid, NK, and B cells express at least one CD33r Siglec, but these receptors are absent from T cells in most cases. The strikingly restricted expression patterns of several Siglecs have led to their use as markers of specific cell populations. Sialoadhesin identifies subsets of

macrophages in the marginal zone of the spleen, marginal sinus of lymph nodes, bone marrow, liver, and lung (Klaas and Crocker, 2012). Siglec-H is a widely used marker for plasmacytoid dendritic cells (Blasius et al., 2006). Both Siglec-F in mice and Siglec-8 in humans are relatively specific markers for eosinophils (Zhang et al., 2004). Interestingly, Siglec-6 is found specifically on syncytiotrophoblasts and cytotrophoblasts in the placenta, providing a rare example of a non-hematopoietic Siglec (Winn et al., 2009). In most cases, the functional consequences of this highly selective Siglec expression are not understood.

A major mechanism of leukocyte activation involves the ligation of cell-surface receptors that contain or associate with cytoplasmic immunoreceptor tyrosine-based activation motifs (ITAMs). These receptors include the T cell receptor, B cell receptor, a subset of Ig Fc receptors, and C-type lectin receptors such as Dectin-1 and NKG2D on myeloid and NK cells, respectively (Humphrey et al., 2005; Kerrigan and Brown, 2011). Clustering or conformational changes in these receptors leads to phosphorylation of tyrosine residues in associated ITAMs by src-family kinases, which initiates subsequent downstream signaling events. ITAM signaling in lymphocytes is tightly controlled by ITIM-containing inhibitory receptors (Daeron et al., 2008). When ITIM-containing receptors enter the local membrane domains of activating signaling complexes, tyrosines in the ITIM become phosphorylated. This promotes the recruitment of the tyrosine phosphatases SHP-1 and SHP-2, or the inositol phosphatase SHIP, which offset the activity of kinases and limit activation. Inhibitory receptors including CTLA4, Fc $\gamma$ RIIB, PirB, CD22, and Ly49 family members, are critical for regulating lymphocyte activation

(Daeron et al., 2008). However, the importance of inhibitory receptors on macrophages, neutrophils, and eosinophils is not well established.

Eosinophils are circulating leukocytes that typically make up < 3% of leukocytes in blood (for a review of eosinophil functions see chapter 5). Eosinophil activation is mediated by cell surface receptors including cytokine receptors, Fc receptors, integrins, and C-type lectins (Hogan et al., 2008). These receptors trigger the release of a multitude of cytokines, eicosanoids, and granule proteins. Since these products can have detrimental effects on host physiology, eosinophil activation is likely to be restricted by inhibitory cell surface receptors similar to those that dampen lymphocyte activation (Ravetch and Lanier, 2000). Although no receptor has been conclusively demonstrated to serve this function *in vivo*, several candidate inhibitory receptors have been identified on eosinophils (Munitz et al., 2006; Munitz et al., 2008; Norris et al., 2007), including Siglec-F and Siglec-8.

Siglec-F is expressed by eosinophil precursors in mouse bone marrow and is constitutively present on mature eosinophils (Voehringer et al., 2007; Zhang et al., 2004). The level of Siglec-F on the eosinophil cell surface increases during allergic inflammation and upon migration into tissues (Voehringer et al., 2007; Zhang et al., 2007). Apart from eosinophils, only alveolar macrophages (Stevens et al., 2007) prominently express Siglec-F, although weak expression has been detected on peripheral blood neutrophils and on T cells during *in vitro* activation (Zhang et al., 2007). The consequences of ligand recognition by Siglec-F are still unclear. However, this receptor has been shown to promote apoptosis in eosinophils upon antibody cross-linking (Zhang et al., 2007; Zimmermann et al., 2008). Additionally, intravenous injection of either intact

antibodies or F(ab')<sub>2</sub> fragments directed against Siglec-F markedly depletes eosinophils from blood and tissues (Song et al., 2009a; Song et al., 2009b; Zimmermann et al., 2008). This effect is plausibly due to Siglec-F cross-linking and induction of apoptosis. In agreement with this interpretation, Siglec-F KO mice show systemic increases in eosinophil numbers during ovalbumin-induced lung inflammation, and a decrease in the number of apoptotic cells in the lung (Cho et al., 2010; Zhang et al., 2007). Thus, it has been proposed that ligands for Siglec-F may be important for dampening eosinophil accumulation during inflammation (Bochner, 2009).

Although the human genome does not contain an ortholog of Siglec-F, Siglec-8 is believed to represent a functional paralog based on several common features (Bochner, 2009). Siglec-8 is highly expressed on human eosinophils, although, unlike Siglec-F, it is found on basophils and mast cells but not on alveolar macrophages or neutrophils. In addition, antibody-mediated cross-linking of Siglec-8 induces eosinophil apoptosis (Nutku et al., 2003). This effect is accompanied by caspase cleavage, and is paradoxically potentiated by the eosinophil survival factors, IL-5 and GM-CSF. An inhibitor of reactive oxygen species production blunts eosinophil apoptosis, suggesting that mitochondrial-mediated apoptosis is also involved (Nutku et al., 2005). Siglec-9, present on human neutrophils, has also been shown to induce apoptosis with similar requirements for caspase activation and reactive oxygen species (von Gunten et al., 2005). The proximal signaling mechanisms by which these Siglecs activate apoptosis are not known. Various cell lines transfected with Siglec-7 or Siglec-9 do not exhibit apoptosis upon antibody-mediated cross-linking but, instead have reductions in activation-induced responses ranging from signaling through the TCR or FcεR, to the production of prostaglandins

(Avril et al., 2004; Ikehara et al., 2004; Miyazaki et al., 2012). In cord blood-derived mast cells, antibodies against Siglec-8 impair calcium signaling and prostaglandin release in response to FcεR cross-linking (Yokoi et al., 2008). These instances involving inhibition of ITAM-mediated activation suggest direct parallels to other ITIM-containing receptors (Turner and Kinet, 1999). However, recruitment of phosphatases by Siglec-8 has not been reported in any cell type.

Studies in mice have shed light on the functions of other CD33r Siglecs, including Siglec-G and Siglec-E. Siglec-G is expressed on peritoneal B1 cells, which are important for T cell-independent antibody responses, as well as the production of natural antibody (Fagarasan and Honjo, 2000). Siglec-G KO mice exhibit dramatic expansion of the B1 cell population and have higher titers of serum IgM (Hoffmann et al., 2007). Additionally, Siglec-G and Siglec-10 have been shown to interact with CD24 to repress inflammatory signaling in response to cellular damage signals such as heat shock proteins (Chen et al., 2009). It has been proposed that the abundant O-glycans on CD24 mediate Siglec-recognition in this system. However, the carbohydrate-dependence of this interaction remains to be tested (Varki, 2009). Siglec-G was also recently shown to inhibit cytosolic RNA sensing in B cells during vesicular stomatitis virus infection, acting through a novel mechanism that involves ubiquitin-mediated degradation of RIG-I (Chen et al., 2013). Siglec-E is expressed on several myeloid lineages including macrophages, neutrophils, eosinophils, and monocytes. Mice deficient in Siglec-E have exaggerated responses to LPS-induced lung inflammation (McMillan et al., 2013). The target of Siglec inhibition in this model is CD11b/β2 (Mac-1) integrin signaling, which is necessary for the recruitment of neutrophils to the lung. Despite these advances, the functions of Siglec-F

and many other CD33r Siglecs have remained elusive, in part, because endogenous ligands for these receptors have not been identified.

### **Ligands for the CD33-Related Siglecs**

Sialic acid is a 9-carbon  $\alpha$ -keto sugar widely expressed in animals of deuterostome lineage, including vertebrates and some invertebrates such as echinoderms. Sialic acid is the most heterogeneous of all of the monosaccharides and can be modified with hydroxyl, acetyl, methyl, sulfate, and phosphate groups to generate over 50 variations (Cohen and Varki, 2010). Most sialic acids begin as Neu5Ac, which is formed from N-acetylmannosamine-6-*O*-phosphate in the cytoplasm by the enzyme glucosamine (UDP-N-acetyl)-2-epimerase/N-acetylmannosamine kinase (GNE). Neu5Ac is then transported into the nucleus where it is converted into the nucleotide sugar, CMP-Neu5Ac. Sialic acid is typically transferred from CMP-Neu5Ac to the termini of N- and O-glycans and glycolipids. This is accomplished by a large family of sialyltransferases, comprised of 20 members in mammals (Takashima, 2008). Sialic acid is recognized by a wealth of eukaryotic and prokaryotic glycan-binding proteins, from C-type lectins to bacterial adhesins (Schauer, 2009). Although Siglecs are found on leukocytes, which are intimately involved in immune defense against microbes, it has been argued that host-derived ligands represent the major constraints on Siglec evolution (Klaas and Crocker, 2012). This is because sialic acid is rare outside the deuterostomes, with many bacterial and fungal species lacking the genes required for its biosynthesis (Cohen and Varki, 2010). In the case of several bacteria that synthesize sialic acid, it is plausible that this feature was acquired due to the advantage it provides in subverting host immunity (Varki



and Gagneux, 2012). For example, the sialylated capsular polysaccharide of group B *Streptococcus* engages Siglec-9 on human neutrophils and inhibits oxidative burst, granule protease release, and bacterial killing (Carlin et al., 2009). Since the majority of research on CD33r ligands has focused on endogenous ligands, the following discussion is restricted to this class.

A Siglec on a given cell can bind glycoproteins and glycolipids on the surface of that same cell (referred to as cis-ligands) or on another cell (referred to as trans-ligands). The clearest example of cis-ligand recognition is provided by CD22. This Siglec is restricted in its expression to mature B cells, and is not part of the rapidly evolving CD33r subfamily. Several cell surface molecules on B cells serve as ligands for CD22, including the BCR and CD45. Notably, CD22 itself is modified with glycans that can be recognized by adjacent CD22 molecules on the same cell (Han et al., 2005). Importantly, CD22 exhibits sialic acid-dependent redistribution to sites of B cell-B cell or B cell-T cell contact, indicating that homo- and heterotypic trans interactions can also take place (Collins et al., 2004). CD24 likely serves as a cis-ligand for Siglec-G and Siglec-10, although the glycans that mediate this interaction remain to be defined (Chen et al., 2009). Siglecs can bind secreted ligands including mucins (Belisle et al., 2010; Ishida et al., 2008; Ohta et al., 2010; Toda et al., 2008), and the acute phase protein  $\alpha$ 1-acid glycoprotein (Gunnarsson et al., 2007). Aside from these examples, endogenous ligands for Siglecs remain largely uncharacterized at the biochemical level (Varki, 2009).

Investigations of the glycan-binding specificities of CD33r Siglecs have been advanced in large part through the use of neoglycoconjugates. These molecules consist of chemically or enzymatically synthesized glycans attached to lipid, protein, or

polyacryllamide carriers. Currently, the most recent platforms for screening neoglycoconjugates are so-called glycan arrays (Blixt et al., 2004). In a typical glycan array experiment to probe the specificity of a Siglec, a Siglec-Fc fusion protein labeled with a fluorophore is reacted with a glass slide upon which hundreds of distinct glycan structures have been printed. The most recent version of the array produced by the Consortium for Functional Glycomics includes 610 structures, ranging from single monosaccharides to triantennary N-glycans made up of 36 units (<http://www.functionalglycomics.org/static/consortium/resources/resourcecoreh8.shtml>). The fluorescent intensity at each printed spot is used as a read-out of the binding interaction between a discrete glycan structure and the Siglec or other glycan-binding protein of interest. However, there are significant caveats associated with interpreting glycans array data. First, the number of structures represented, though large, does not approach the diversity of glycan determinants found in mammalian cells, which likely exceeds 3000 (Cummings, 2009). Second, the density and presentation of glycans on the array may be variably affected by properties of a given glycan structure, such as charge, and hydrophobicity (Blixt et al., 2004). Third, this approach represents a reduction to pure carbohydrate-protein interactions that does not take into account the potential contributions of the protein or lipid scaffolds that are present in endogenous ligands for glycan-binding proteins (Blixt et al., 2004). Despite these caveats, glycans arrays have been widely used to probe the binding specificity of mammalian lectins including the Siglecs.

CD22 provides a clear example of concordance between glycan array results and other experimental data. CD22-Fc binds with high selectivity to  $\alpha$ 2,6-sialylated LacNAc

structures on glycan arrays. This result is consistent with reported defects in the binding of CD22 to T and B cells in mice lacking  $\alpha$ 2,6-sialyltransferases (Walker and Smith, 2008). Furthermore,  $\alpha$ 2,6-sialyltransferase-deficient mice have a similar immunological phenotype when compared to mice expressing a mutated form of CD22 that cannot bind sialic acid. However, glycan array results obtained using other Siglecs have been more difficult to interpret. Siglec-9 was found to bind 6-sulfo-sLex using glycan arrays, whereas Siglec-7 bound this structure weakly (Campanero-Rhodes et al., 2006). However, an endothelial cell line transfected with the GlcNAc-6-*O*-sulfotransferase, GlcNAc6ST-1, bound more strongly to Siglec-7 than Siglec-9 (Miyazaki et al., 2012). This binding could be blocked using antibodies against 6-sulfo-sLex and 6-sulfo-LacNAc, demonstrating that it was highly specific. Moreover, Siglecs-E, -F, -8, -7, and -5 have all been shown to recognize Gal6S-containing structures on glycan arrays, raising the concern that some of these binding interactions may be artificial. As described below, the high selectivity of Siglec-8 and Siglec F for glycans modified with Gal6S has led to great interest in determining whether the endogenous ligands for these receptors require this structural feature.

### **Evidence for Galactose-6-*O*-Sulfate as a Binding-Determinant for Siglec-F**

Putative endogenous ligands for Siglec-F were first revealed indirectly through the use of sialylated glycans linked to polyacryllamide (PAA) scaffolds (Tateno et al., 2005). Eosinophils do not bind these glycans unless the eosinophils are first treated with sialidase, suggesting that the ligand-binding site of Siglec-F is occupied by cis-ligands, as is the case for CD22 and several other Siglecs (Varki and Angata, 2006). Direct detection

of Siglec-F ligands has since been achieved using a fusion protein consisting of the extracellular domain of Siglec-F fused to the Fc portion of human IgG (Siglec-F-Fc). Immunohistochemical staining of mouse lung sections with Siglec-F-Fc revealed sialic-acid dependent ligands on airway epithelial cells and luminal contents, as well as on mononuclear cells in alveolar spaces (Zhang et al., 2007). Furthermore, Siglec-F-Fc staining in these regions increases dramatically during allergic lung inflammation. However, the identities of the ligand-expressing cells and the basis for the increase in ligands during inflammation have not been determined.

Although endogenous ligands have yet to be biochemically defined, experiments using PAA-linked glycans have established that Siglec-F prefers  $\alpha$ 2,3-linked sialic acid residues (Angata et al., 2001). Consistent with this specificity, Siglec-F-Fc staining of airway epithelium and alveolar cells is blocked by the lectin MAA (which recognizes  $\alpha$ 2,3 linked sialic acids), and is absent in mice lacking the  $\alpha$ 2,3 sialyltransferase ST3Gal3 (Guo et al., 2011). Additionally, Siglec-F-Fc specificity has been probed using the CFG glycan array. These experiments revealed a striking preference for 6'-sulfo-sLex (Sia  $\alpha$ 2 $\rightarrow$ 3 [6S]Gal  $\beta$ 1 $\rightarrow$ 4 [Fuc  $\alpha$ 1 $\rightarrow$ 3][6S]GlcNAc) and 6'-sulfo-3'sLN (Sia  $\alpha$ 2 $\rightarrow$ 3 [6S]Gal  $\beta$ 1 $\rightarrow$ 4 GlcNAc) with no reactivity to the same structures lacking Gal6S (Tateno et al., 2005). Siglec-F-Fc also binds neoglycolipids containing 6'-sulfo-sLex, 6'-sulfo-3'sLN, and 6,6'-sulfo-sLex (Sia  $\alpha$ 2 $\rightarrow$ 3 [6S]Gal  $\beta$ 1 $\rightarrow$ 4 [Fuc  $\alpha$ 1 $\rightarrow$ 3][6S]GlcNAc), but not sLex (Sia  $\alpha$ 2 $\rightarrow$ 3 Gal  $\beta$ 1 $\rightarrow$ 4 [Fuc  $\alpha$ 1 $\rightarrow$ 3]GlcNAc) or 6-sulfo-sLex (Sia  $\alpha$ 2 $\rightarrow$ 3 Gal  $\beta$ 1 $\rightarrow$ 4 [Fuc  $\alpha$ 1 $\rightarrow$ 3][6S]GlcNAc) (Campanero-Rhodes et al., 2006) ([www.functionalglycomics.org](http://www.functionalglycomics.org), primscreen\_3253). Furthermore, eosinophils bind to 6'-sulfo-sLex and not 6-sulfo-sLex coupled to PAA, and this effect can be completely inhibited with an antibody to Siglec-F

(Tateno et al., 2005). An antibody that recognizes 6'-sulfo-sLex stains mouse airway epithelium (Kiwamoto et al., 2013), although this antibody also binds other glycans ([www.functionalglycomics.org](http://www.functionalglycomics.org), primscreen\_3255). Taken together, this evidence points to Gal6S as a recognition element for Siglec-F. As reviewed in chapter 2, we recently demonstrated that KGal6ST generates Gal6S *in vivo* on ocular KS, as well as on glycans in lymph nodes, including 6,6'-disulfo-3'sLN in high endothelial venules (Patnode et al., 2013). Furthermore, KSGal6ST transcripts are present in the lung (Tateno et al., 2010), and KSGal6ST protein has recently been detected in airway epithelium by immunohistochemistry (Guo et al., 2011). Thus, this enzyme is a strong candidate for controlling endogenous Siglec-F ligand synthesis in the lung.

The strongest case for convergent evolution of Siglec-F and Siglec-8 comes from analyses of Siglec-8 binding specificity. Siglec-8 recognizes glycans containing Gal6S, such as 6'-sulfo-sLex, 6,6'-disulfo-sLex, and 6'-sulfo-3'sLN, with even greater selectivity than Siglec-F (Bochner et al., 2005; Campanero-Rhodes et al., 2006; Rapoport et al., 2006) ([www.functionalglycomics.org](http://www.functionalglycomics.org), primscreen\_3249). Furthermore, polyvalent 6'-sulfo-sLex-PAA conjugates induce apoptosis when incubated with human eosinophils (Hudson et al., 2009). Although ligands for Siglec-8 and the cell types expressing them have not been identified, such studies could potentially be guided by the characterization of ligands for Siglec-F in mice.

In the following chapter, I describe my investigation of the expression pattern of these ligands, and address whether their synthesis requires the only known Gal-6-*O*-sulfotransferases KSGal6ST and C6ST-1.

## **CHAPTER 4**

### **Galactose-6-*O*-Sulfotransferases Are Not Required for the Generation of Siglec-F Ligands on Leukocytes or in Lung Tissue**

## SUMMARY

We have used mice deficient in both KSGal6ST and C6ST-1 to determine whether these sulfotransferases are required for the generation of Siglec-F ligands. First, we characterize ligand expression on leukocyte populations and find that this expression is largely restricted to cell types also expressing Siglec-F, namely eosinophils, neutrophils, and alveolar macrophages. We also detect Siglec-F ligand activity in bronchoalveolar lavage fluid fractions containing polymeric secreted mucins, including MUC5B.

Consistent with these observations, ligands in the lung increase dramatically during infection with the parasitic nematode, *N. brasiliensis*, which is known to induce eosinophil accumulation and mucus production. Surprisingly, none of the ligands we describe are diminished in mice lacking KSGal6ST and C6ST-1, indicating that neither of the known galactose-6-*O*-sulfotransferases is required for ligand synthesis.

Furthermore, Gal6S is undetectable in eosinophil and lung tissue O-glycans analyzed by mass spectroscopy. These results establish that ligands for Siglec-F are present on several cell types that are relevant during allergic lung inflammation and argue against the prevailing view that Gal6S is a critical recognition determinant for this receptor.

## RESULTS

### **Siglec-F ligands in blood are largely restricted to eosinophils and neutrophils**

To determine the expression pattern of Siglec-F ligands among leukocyte subsets in peripheral blood, we performed multi-parameter flow cytometry using a Siglec-F-Fc fusion protein with the Fc region derived from human IgG<sub>1</sub>. Siglec-E-Fc and CD22-Fc were used to assess the selectivity of Siglec-F-Fc staining. Human IgG did not stain any

of the leukocyte populations examined. We used IL4-GFP reporter mice to identify eosinophils and basophils, based on the selective expression of GFP in these cell populations (Mohrs et al., 2001; Voehringer et al., 2004). We simultaneously stained blood cells with antibodies specific for markers of the major leukocyte lineages; CD3 $\epsilon$  for T cells, CD19 for B cells, NK1.1 for NK cells, DX5 for basophils and NK cells, Ly-6G for neutrophils, and Ly-6C for classical monocytes.

Siglec-F-Fc stained > 99% of peripheral blood eosinophils (MFI, 2680) (Fig. 9A). This staining was completely dependent on sialic acid, since sialidase treatment of the cells reduced the signal to background. The percentage of neutrophils that stained with Siglec-F-Fc was variable, but was consistently between 60% and 90% (MFI, 2081). Up to 20% of neutrophils were resistant to sialidase treatment, perhaps indicating the expression of a resistant form of sialic acid (Corfield et al., 1992). Notably, neutrophils also express Siglec-F, albeit at lower levels than eosinophils (Zhang et al., 2007). We confirmed that this expression was specific, based on its absence in Siglec-F KO mice (Fig. 9B). Weaker and more variable Siglec-F-Fc staining was observed on < 5% of monocytes (MFI, 959) and < 40% of NK (MFI, 1004) cells, whereas staining was not detected on basophils, T cells, and B cells (Fig. 9A). In contrast to the highly restricted expression pattern of Siglec-F ligands, Siglec-E-Fc stained all leukocyte subsets examined, except B cells (Fig. 9A). CD22-Fc recognized B cells and T cells as previously reported (Torres et al., 1992), but did not detectably react with eosinophils, neutrophils, basophils, monocytes, or NK cells (Fig. 9A).



### **Alveolar macrophages and type II alveolar epithelial cells express Siglec-F ligands**

Since Siglec-F-Fc is reported to stain epithelial cells in the airways and mononuclear cells in alveoli (Zhang et al., 2007), we sought to determine the identities of the reactive cell types. We stained lung sections with Siglec-F-Fc, and simultaneously stained for sialoadhesin to mark macrophages (Ducreux et al., 2009) and pro-SP-C to mark type II alveolar epithelial cells (AEC) (Zhou et al., 1996) (Fig. 10A). Staining was detected in > 95% of alveolar macrophages. Thus, like eosinophils and neutrophils, these cells express both Siglec-F and Siglec-F ligands. In contrast, Siglec-F-Fc staining was not detected on sialoadhesin<sup>+</sup> peribronchiolar or perivascular macrophages (Fig. 10A), and these populations do not express Siglec-F as determined by immunostaining (data not shown). It was conceivable that the pattern of Siglec-F-Fc staining on leukocytes could be explained by the capture of soluble polyvalent ligands by Siglec-F, which would then be recognized by Siglec-F-Fc. However, Siglec-F-Fc staining of eosinophils, and alveolar macrophages was similar between Siglec-F KO and wild type mice, ruling out this possibility (Figure 10C). Neutrophil staining was also clearly present in Siglec-F KO mice, although the percentage of positive cells was variable between mice, as discussed above.

We also found that Siglec-F-Fc stained > 95% of type-II alveolar epithelial cells (Fig. 10A). At high magnification, the reactivity in these cells was punctate and often polarized toward the alveolar space, but it did not co-localize with granules containing pro-SP-C. We observed Siglec-F-Fc staining of the airway epithelium, as has been reported (Zhang et al., 2007), and we found that it was largely restricted to the luminal surface of the epithelial cells. Staining was not observed when Siglec-E-Fc or CD22-Fc was used,

although these reagents clearly stained cells in lymph node tissue sections (data not shown). Siglec-F-Fc staining in the lung was reduced to the level of background when sections were pretreated with sialidase. When we simultaneously stained for Siglec-F ligands, macrophages, and type II AEC, every Siglec-F-Fc<sup>+</sup> cell was either sialoadhesin<sup>+</sup>, pro-SP-C<sup>+</sup>, or exhibited a morphology consistent with airway epithelium (Figure 10B). Thus, alveolar macrophages, type II epithelial cells, and airway epithelial cells constitute the major classes of Siglec F ligand-expressing cells in normal lung.

### **Siglec-F ligands are present in mucin-containing fractions of bronchoalveolar lavage fluid**

Mucins are excellent candidates for Siglec ligands due to their abundant sialylated O-glycans (Thornton et al., 2008). Additionally, Siglec-F-Fc stains the apical surface of the airway epithelium as well as material in the lumen, where mucins are present (Zhang et al., 2007). To determine whether polymeric secreted mucins are recognized by Siglec-F, we followed methods to separate high molecular weight mucins from other proteins in airway secretions (Thornton et al., 2001). We concentrated mouse bronchoalveolar lavage (BAL) fluid by lyophilization and then solubilized this material in guanidine before fractionating the components by Sepharose CL-2B gel chromatography. The bulk of proteins, as monitored by OD 280, eluted in the internal volume of the column (fractions 8-12) (Fig. 11). We assayed fractions for Siglec ligands and MUC5B by ELISA. MUC5B, which forms complexes of 2 to 50 million Daltons, was enriched in the void volume and the adjacent fractions, consistent with previous findings (Thornton et al., 2001). Siglec-F ligand activity was also highly enriched in these fractions. Siglec-F-

Fc reactivity was completely eliminated by sialidase treatment. Neither CD22-Fc nor human IgG was reactive with any fraction.

### **Siglec-F ligand expression increases during parasitic worm infection**

Siglec-F ligand activity in airway epithelium and unidentified peribronchiolar mononuclear cells was found to increase during ova-induced inflammation in mice (Zhang et al., 2007). From our findings above, the accumulation of eosinophils and secreted mucins that accompany allergic lung inflammation could potentially account for this increase. To determine whether eosinophils express Siglec-F ligands in the lung during inflammation, we infected mice with the nematode, *N. brasiliensis*. This parasitic worm travels from the subcutaneous injection site through the vasculature to the lung (Camberis et al., 2003). It then migrates through the alveoli and ascends the airways before it enters the gastrointestinal tract. Mice were infected with *N. brasiliensis* larvae and, after nine days, the lungs were collected, sectioned, and stained.

During infection with this parasite, the airway epithelium thickens and there is increased mucus production and eosinophil accumulation (Coffman et al., 1989; Tomita et al., 2000). Compared to uninfected lung, the airway epithelium showed increased Siglec-F-Fc staining, which was present in the cytoplasm of epithelial cells as well as on the apical surface (Fig. 12A). To identify eosinophils, we used an antibody to eosinophil major basic protein (eMBP), a component of the primary granules in these cells (Hogan et al., 2008). As expected, many of the infiltrating cells were eMBP<sup>+</sup> eosinophils, and > 95% of these cells stained with Siglec-F-Fc (Fig. 12B).

### **Gal-6-O-sulfotransferases are not required for the generation of Siglec-F ligands**

As noted above, Siglec-F exhibits striking specificity for glycans containing Gal6S. Therefore, we wanted to determine whether the ligands described above required the action of the two known Gal6STs. We crossed KSGal6ST KO mice with C6ST-1 KO mice to generate KSGal6ST/C6ST-1 double knock out mice (hereafter, DKO mice). These mice exhibited no gross physical or behavior abnormalities.

We first performed Siglec-F-Fc staining in peripheral blood from wild type and DKO mice. We found that Siglec-F-Fc staining was unchanged in eosinophils and neutrophils from DKO mice compared to that of wild-type cells (Fig. 13A). There were reductions in the percentages of monocytes (< 30%) and NK cells (< 50%) that stained with Siglec-F-Fc, but this result likely reflects mouse-to-mouse variation in the percentages of cells in these populations (see Fig. 9A). Next, we found that increased epithelial and eosinophil Siglec-F-Fc staining during *N. brasiliensis* infection was unchanged in Siglec-F-Fc DKO mice (Fig. 13B). Furthermore, lung tissue sections and found that staining was unchanged in alveolar macrophages, type II cells, and airway epithelial cells in the absence of Gal6STs (Fig. 14A). When we titrated the concentration of Siglec-F-Fc to the limit of detection, there was still no difference in staining between wild type and DKO mice (data not shown). Finally, we determined whether Siglec-F ligands in BAL fluid required Gal6STs. Fractionated BAL fluid from wild type and DKO mice contained similar amounts of MUC5B in the void volume (Fig. 14B). Consistent with the epithelial staining we observed in tissue sections from DKO mice, Siglec-F-Fc reactivity in these fractions was independent of both KSGal6ST and C6ST-1.

### **Mass spectrometry analysis of sulfated glycans in eosinophils**

The presence of Siglec-F-Fc staining in mice deficient in the only known Gal6STs suggested that binding determinants other than Gal6S were responsible for the highly specific pattern of Siglec-F ligand expression. To determine whether Gal6S was present on cells that express Siglec-F ligands, we carried out structural analyses of sulfated glycans by mass spectrometry (MS). To collect large numbers of peripheral blood eosinophils, we used mice constitutively expressing the eosinophil growth factor IL-5 under the control of the mouse CD3 $\delta$  regulatory regions (Lee et al., 1997). We verified that eosinophils from these mice expressed Siglec-F ligands, comparable to those of wild-type eosinophils (Fig. 15A). We then isolated  $120 \times 10^6$  peripheral blood leukocytes, which contained 83% eosinophils, with the remaining cells being predominantly lymphocytes. N- and O-glycans were released from this sample, permethylated, and fractionated using liquid chromatography, as described previously (Patnode et al., 2013). Sulfated fractions were analyzed by MALDI-MS with major components selected for ESI-MS/MS. The only sulfated glycans that we detected were simple core 2 O-glycans capped with  $\alpha$ 2,3 linked Neu5Ac (Fig. 15B). Importantly, when we selected these structures for MS/MS analysis, Gal6S was not present. However, we did detect an ion indicative of sulfated N-acetylneuraminic acid ( $m/z$  269) with the sulfate present on the glycerol side-chain.

## Figure 9

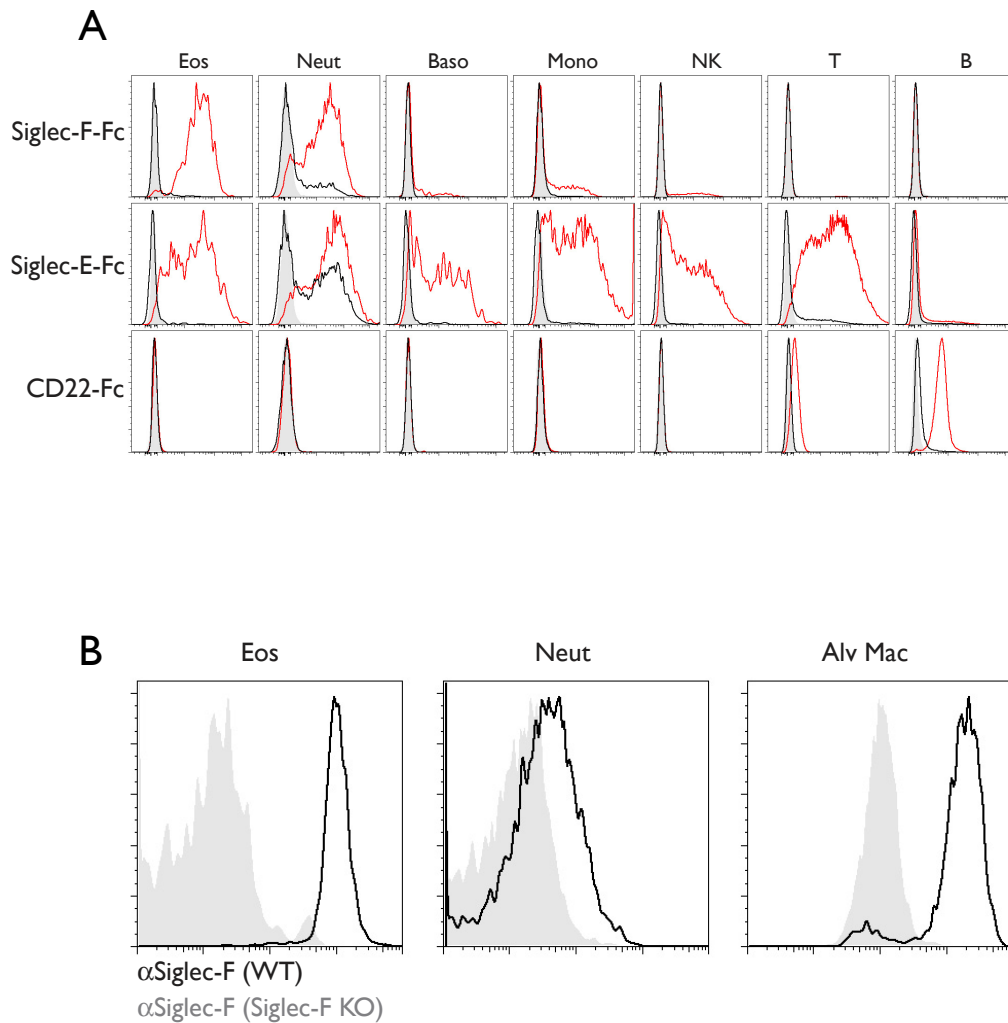
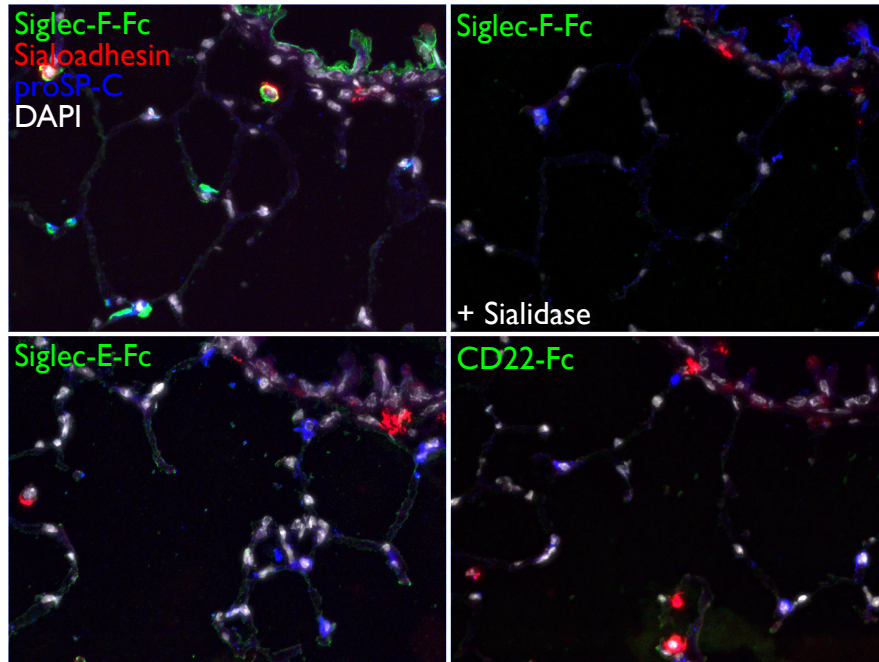


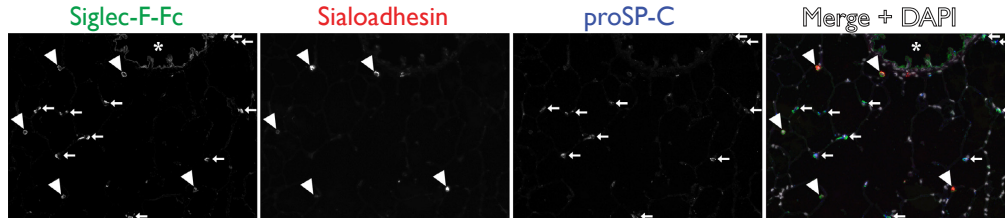
Figure 9. Siglec-F ligand expression in peripheral blood leukocytes  
 (A) Flow cytometry analysis of leukocyte subsets stained with Siglec-F-Fc, Siglec-E-Fc, and CD22-Fc (red histograms). Staining after sialidase treatment (black histograms) and staining with human IgG (grey histograms) are shown. (B) Flow cytometry analysis of Siglec-F expression on leukocytes from wild type (black histograms) or Siglec-F KO mice (grey histograms). Eos, eosinophils; Neut, neutrophils; Baso, basophils; Mono, classical monocytes; NK, natural killer cells; T, T cells; B, B cells; Alv Mac, alveolar macrophages.

## Figure 10

A



B



C

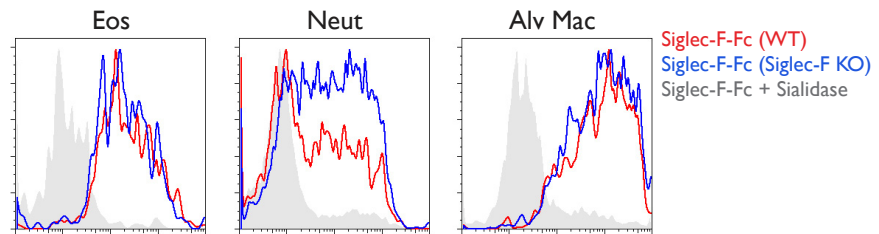


Figure 10. Siglec-F ligand expression in resident lung cells

(A) Cryostat-cut serial sections of lungs from WT mice stained with Siglec-F-Fc, Siglec-E-Fc, or CD22-Fc (green); anti-sialoadhesin (red); anti-proSP-C (blue); and DAPI (white). Siglec-F-Fc staining after neuraminidase treatment is also shown. (B) A low power view of the same section in (A). Arrows mark type II alveolar epithelial cells. Arrowheads mark alveolar macrophages. The asterisk marks airway epithelium. (C) Flow cytometry analysis of Siglec-F ligand staining of leukocytes from wild type (red histograms) or Siglec-F KO (blue histograms) mice. Sialidase treatment eliminated staining on cells from both Siglec-F KO (grey histograms) and wild type mice (not shown).

Figure 11

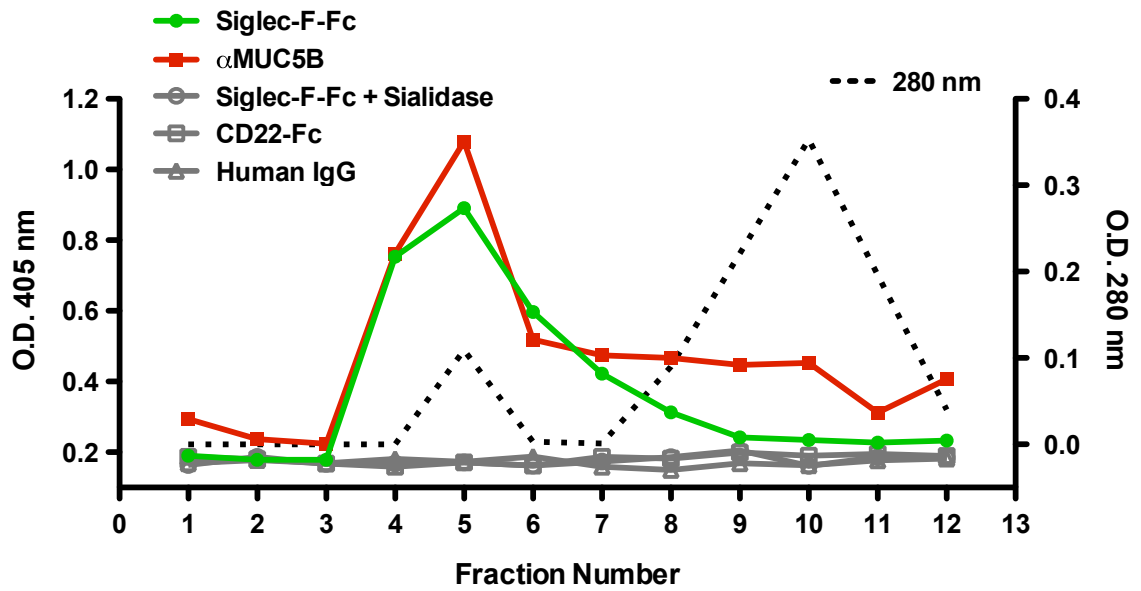


Figure 11. Siglec-F ligands in bronchoalveolar lavage fluid  
(A) Fractions of bronchoalveolar lavage fluid assayed by ELISA using Siglec-F-Fc (green filled circles), or anti-MUC5B (red filled squares). Total protein was determined by measuring absorbance at 280 nm (black dotted line). No signal was observed when wells were reacted with CD22-Fc (grey open squares), human IgG (grey open triangles), or treated with neuraminidase before incubation with Siglec-F-Fc (grey open circles).



## Figure 12

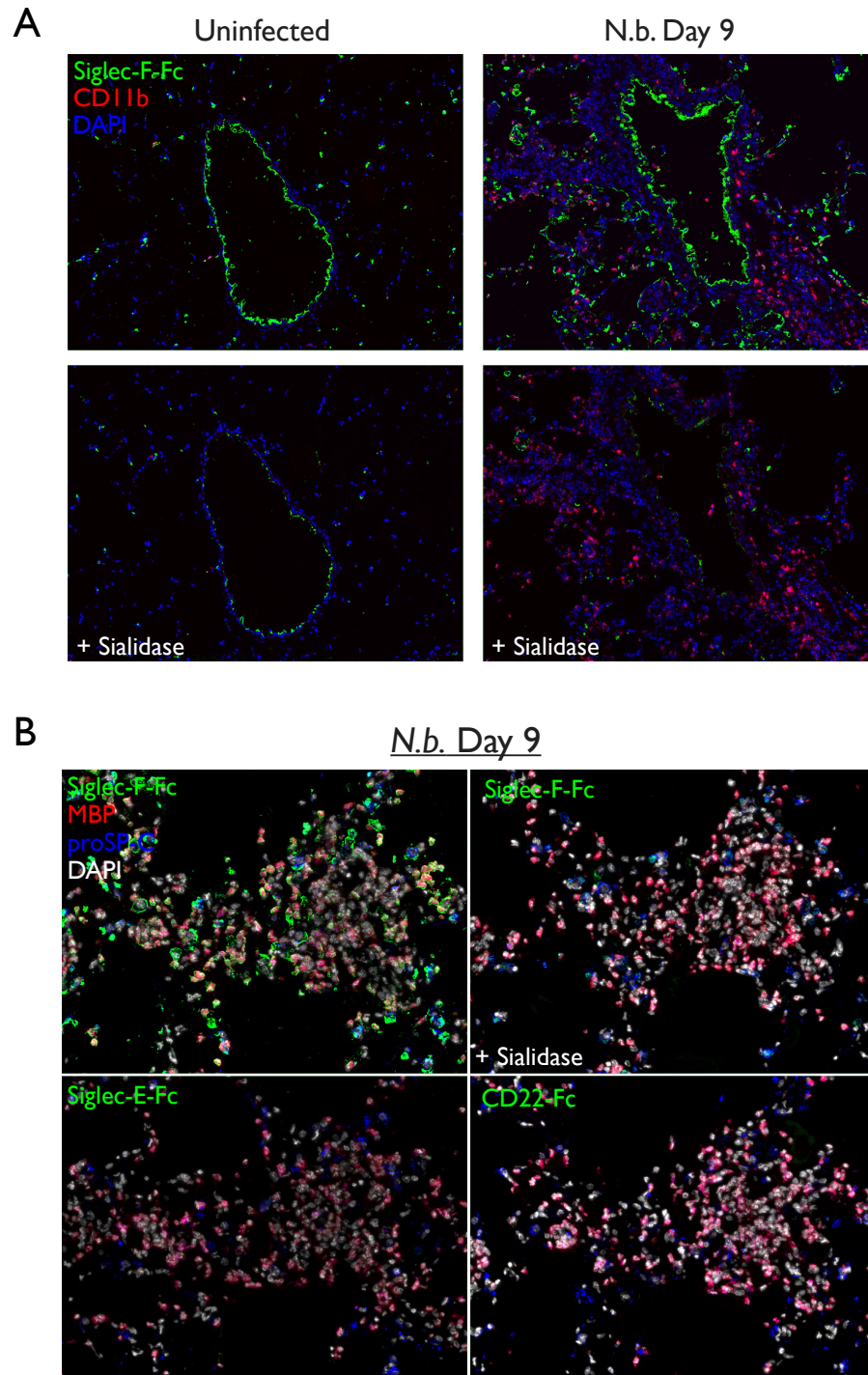


Figure 12. Siglec-F ligand expression during *N. brasiliensis* infection  
 (A) Cryostat-cut serial sections of lungs from *N. brasiliensis* infected or uninfected mice. Sections were treated with neuraminidase or buffer alone, then stained with Siglec-F-Fc (green), anti-CD11b (red), and DAPI (blue). (B) Separate images of the same lung sections from (A), treated with neuraminidase or buffer alone, then stained with Siglec-F-Fc, Siglec-E-Fc, or CD22-Fc (green); anti-eMBP (red); anti-proSP-C (blue); and DAPI (white).

## Figure 13

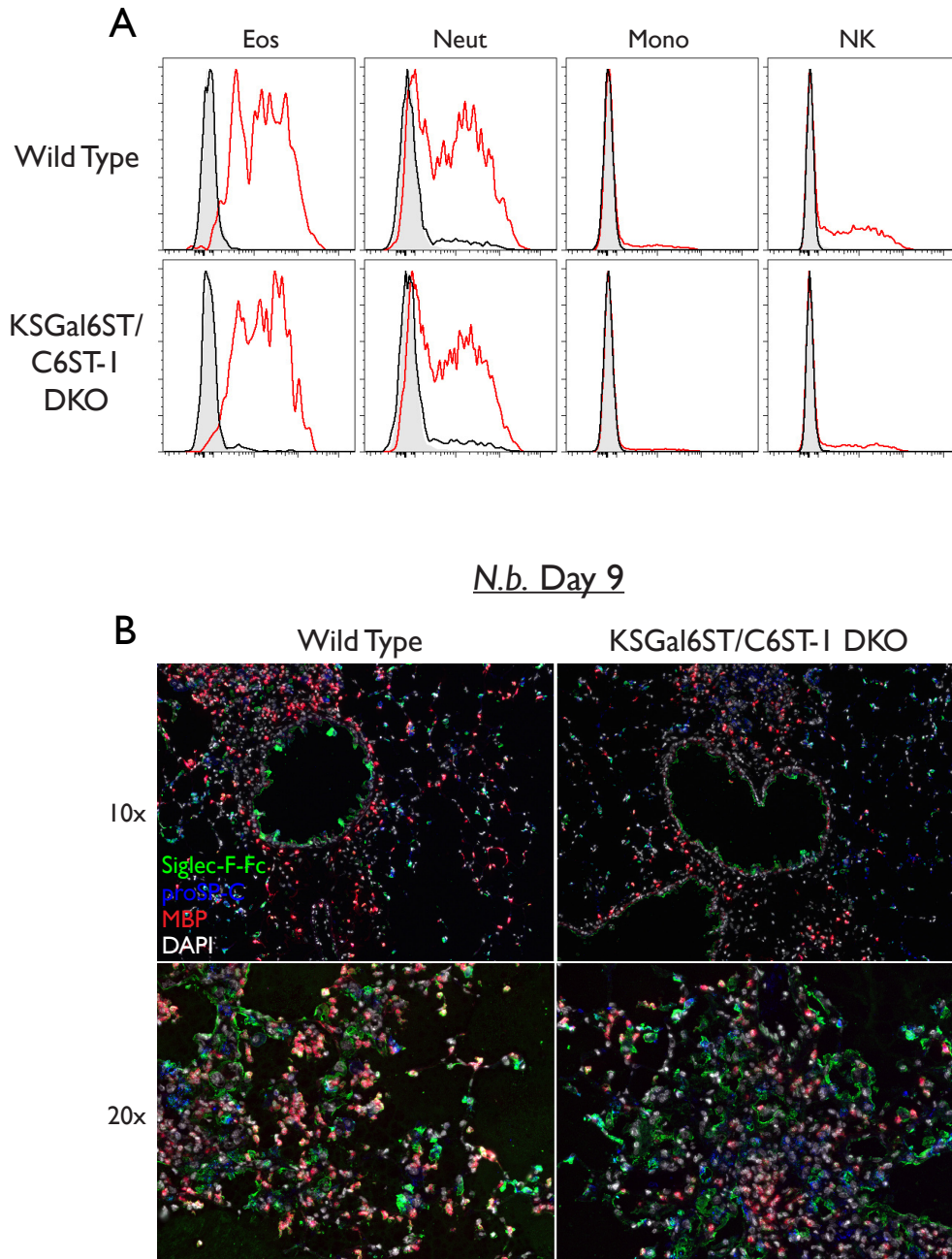


Figure 13. Siglec-F ligand expression in leukocytes from KSGal6ST/C6ST-I DKO mice

(A) Flow cytometry analysis of leukocyte subsets stained with Siglec-F-Fc (red histograms). Staining after neuraminidase treatment (black histograms) and staining with human IgG (grey histograms) are shown. (B) Cryostat-cut sections of lungs from *N. brasiliensis* infected mice. Sections were stained with Siglec-F-Fc (green), anti-eMBP (red), anti-proSP-C (blue), and DAPI (white). Low power (top) and high power (bottom) fields are shown. WT, wild type; DKO, KSGal6ST/C6ST-I double knock out; Eos, eosinophils; Neut, neutrophils; Mono, classical monocytes; NK, natural killer cells.

Figure 14

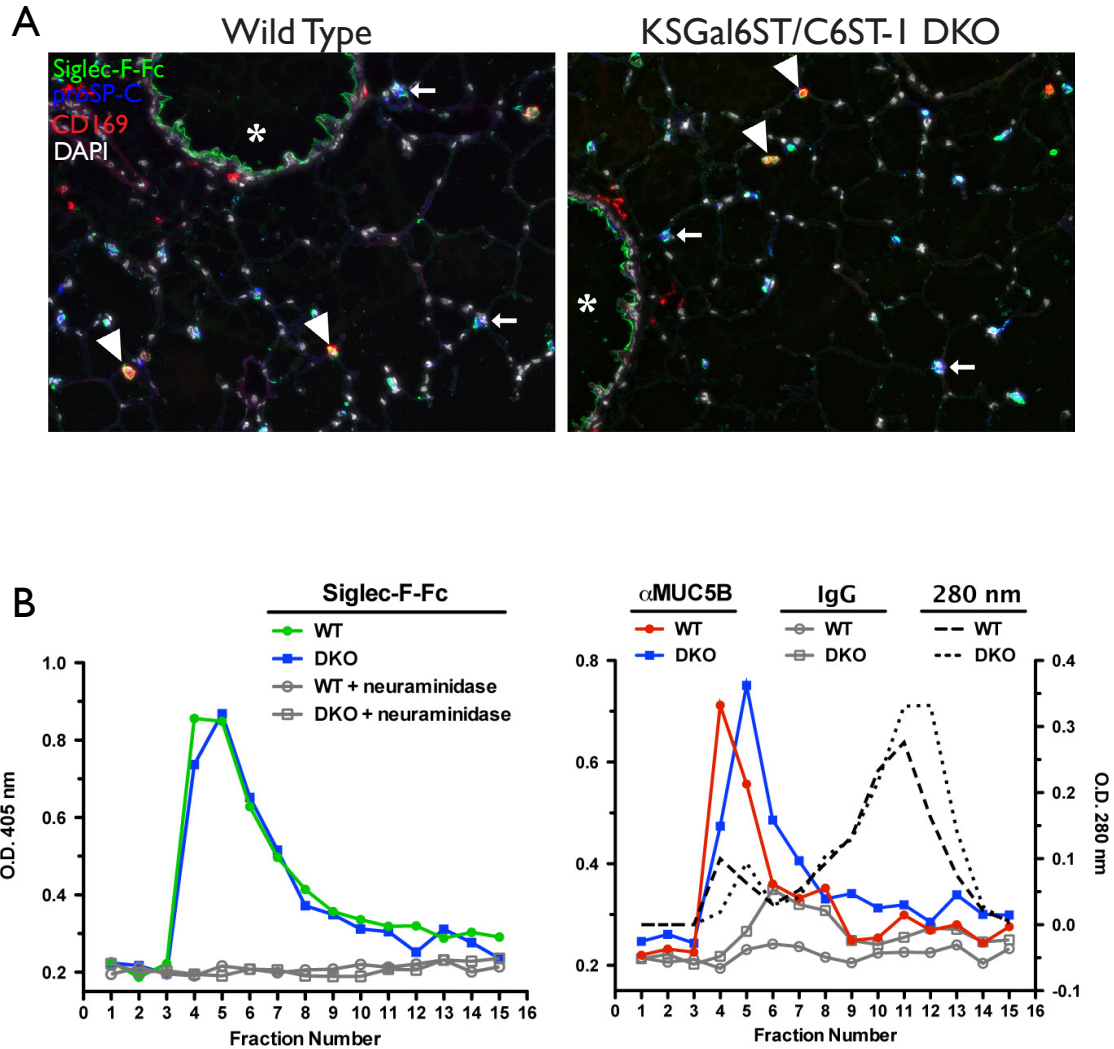


Figure 14. Siglec-F ligand expression lungs of KSGal6ST/C6ST-I DKO mice  
 (A) Cryostat-cut serial sections of lungs from WT or DKO mice stained with Siglec-F-Fc (green), anti-sialoadhesin (red), anti-proSP-C (blue), and DAPI (white). (B) Siglec-F-Fc reactivity (left) in bronchoalveolar lavage fluid fractions from WT (green filled circles) and DKO mice (blue filled squares), assayed by ELISA. Signal was eliminated by neuraminidase treatment (grey open circles, grey open squares). Anti-MUC5B reactivity (right) in bronchoalveolar lavage fluid fractions from WT (red filled circles) and DKO mice (blue filled squares), assayed by ELISA. Isotype control signal was minimal (grey open circles, grey open squares). Total protein was determined by measuring absorbance at 280 nm for wild type (black dotted line) and DKO mice (black dashed line).

Figure 15

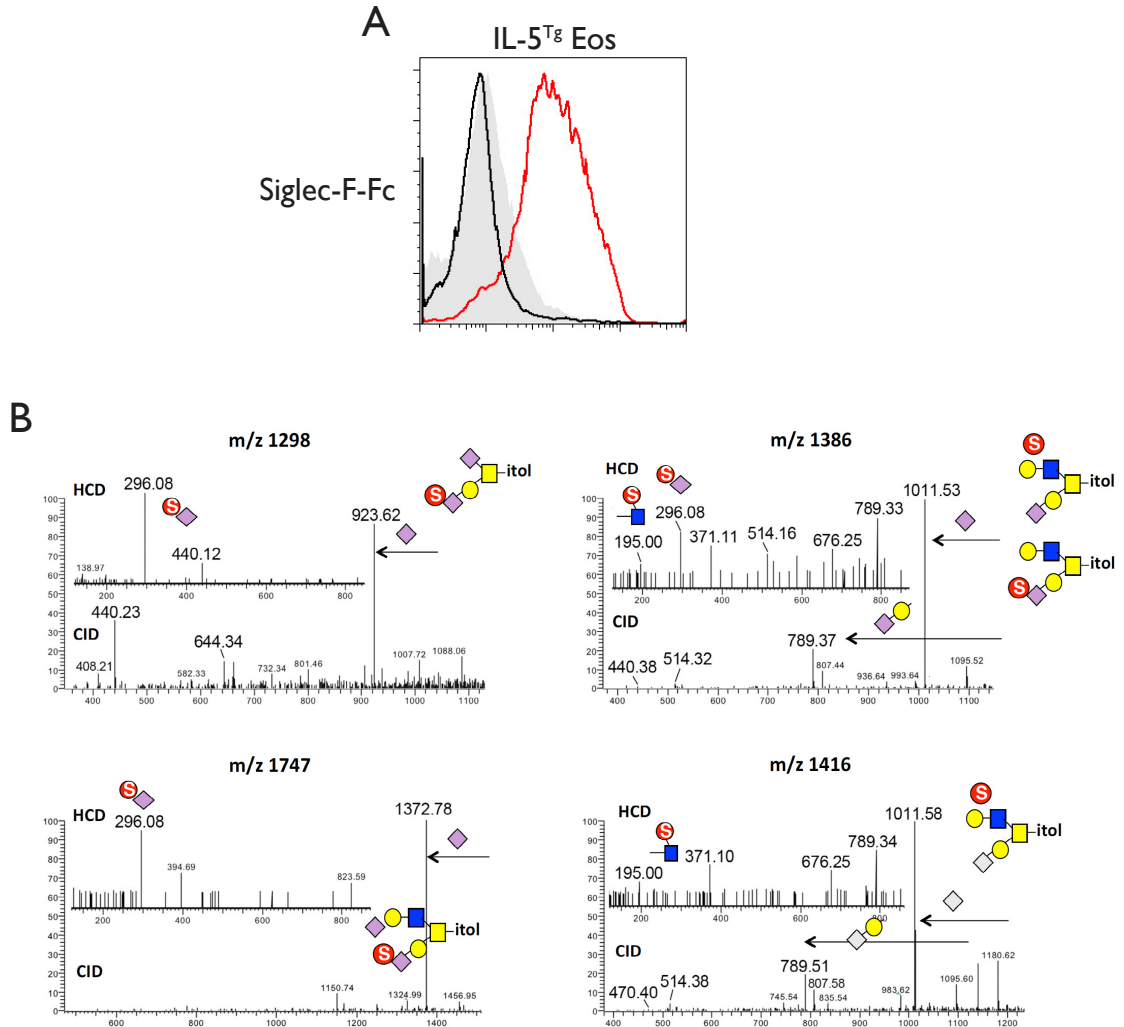


Figure 15. MS analysis of sulfated O-glycans in eosinophils

(A) Flow cytometry analysis of Siglec-F-Fc staining of IL-5 transgenic eosinophils (red histogram). Staining after neuraminidase treatment (black histogram) and staining with human IgG (grey histogram) are shown. (B) Low mass regions of the nanoESI HCD and CID MS/MS spectra of mono-sulfated di-sialylated (left) and mono-sulfated mono-sialylated (right) structures from IL-5 transgenic eosinophils. Assignment of the major peaks for all spectra is as annotated using the standard cartoon symbols.

## DISCUSSION

Here, we demonstrate that the cell types known to express Siglec-F, namely eosinophils, neutrophils, and alveolar macrophages, correspondingly express ligands for this receptor on their surface. This selective expression pattern cannot be explained by presentation of a soluble polyvalent ligand via Siglec-F or by Siglec-F itself functioning as a ligand, since we did not detect changes in ligand expression in Siglec-F KO mice. 6'-sulfo-sLex coupled to PAA has been shown to bind mouse eosinophils only after sialidase treatment, suggesting that the ligand-binding site of Siglec-F is occupied by cis-ligands (Tateno et al., 2005). Our findings represent the first direct demonstration of Siglec F ligands on mouse eosinophils. It remains to be seen whether the ligands we detected on neutrophils and alveolar macrophages also serve as cis-ligands for Siglec-F. As has been shown for CD22, cis-ligands can also act in trans when cells come into contact with one another, and these contacts appear to have functional significance in T cell-B cell interactions (Walker and Smith, 2008). Thus, ligand expression on eosinophils, neutrophils, and alveolar macrophages may indicate that important bi-directional trans-interactions occur between these cell types.

We have also demonstrated that Siglec-F ligands are present in high-molecular weight fractions of mouse BAL fluid. These fractions contain polymeric secreted mucins in humans (Thornton et al., 2001), and we verified that MUC5B was present. Mucins are highly sialylated glycoproteins with numerous O-glycans, and they have been shown to serve as ligands for carbohydrate-binding proteins. For example, mucins constitute functional ligands for L-selectin (Rosen, 2004; Thomas et al., 2009), CLEC-2 (Suzuki-Inoue et al., 2011), and galectins (Guzman-Aranguez and Argueso, 2010; Rhodes et al.,

2008; Sakuishi et al., 2011). Additionally, mucins have also been implicated as ligands for a number of Siglecs, including sialoadhesin, CD22, CD33, MAG, and Siglec-9 (Belisle et al., 2010; Ishida et al., 2008; Nath et al., 1999; Ohta et al., 2010; Swanson et al., 2007; Toda et al., 2008). We detected Siglec-F ligands on the apical membranes of airway epithelial cells but rarely in the cytoplasm, which is consistent with the localization of MUC5B in healthy mouse airways (Roy et al., 2011). Additionally, there was a marked increase in ligands during worm infection, and a portion of these was associated with the apical cytoplasm and cell surface of epithelial cells where secreted mucins are abundant (Tomita et al., 2000). However, we have not ruled out the possibility that membrane-bound ligands (mucins or otherwise) are also present on airway epithelial cells. Further studies with mice deficient in specific mucin genes should allow definitive identification of the high MW ligands we have observed in BAL fluid. We also found punctate Siglec-F-Fc staining in Type-II AECs. Like mucin-producing cells, Type-II AECs are highly secretory, releasing surfactant from lamellar granules into the alveoli (Whitsett et al., 2010). It is possible that these cells secrete ligands into the air spaces, which could account for the activity we detected in low molecular weight fractions of BAL fluid.

Dramatic increases in Siglec-F ligand expression are observed during ovalbumin-induced allergic lung inflammation (Zhang et al., 2007). We have extended this observation to inflammation that develops in response to the parasitic nematode, *N. brasiliensis*. Eosinophil accumulation and increased mucus production are features of both of these models (Carvalho et al., 2006). Given that we detected ligands on eosinophils and in mucin-containing fractions of BAL fluid, these sources likely



contribute to the increased Siglec-F-Fc staining. Eosinophils and neutrophils are known to migrate across the airway and alveolar epithelium during inflammation (Tam et al., 2011), and alveolar macrophages reside in the alveolar lumen. Siglec-F is thought to function as an inhibitory that dampens activation or promotes apoptosis upon ligand binding (see Chapter 3). Thus, ligands secreted by airway epithelial cells, and potentially by type-II AECs, could function to regulate the activation or survival of all three of these cell types in the luminal spaces of the lung.

There is also potential for Siglec-F-mediated interactions, both homotypic and heterotypic, between eosinophils, neutrophils, and alveolar macrophages during inflammation. We observed many examples of apparent cell-cell contact between these cell types in the inflamed lung. Alveolar macrophages are known to phagocytose granulocytes (Vandivier et al., 2006). An intriguing possibility is that Siglec-F ligation by cell surface ligands limits activation of both the granulocyte and the alveolar macrophage during this process. Siglec-F is also an endocytic receptor (Tateno et al., 2007) and may be directly involved in the uptake of these cells. Siglec-F-deficient mice exhibit general signs of enhanced allergic lung inflammation, such as increased airway smooth muscle thickness and systemic increases in eosinophil numbers (Cho et al., 2010; Zhang et al., 2007). Investigation of this phenotype has focused on effects intrinsic to eosinophils; however future studies should include the potential functions of Siglec-F on alveolar macrophages and neutrophils as well.

Screening with glycan arrays has implicated Gal6S as a recognition determinant for Siglec-F (Tateno et al., 2005). However, we found that the two known Gal6STs are not required for the generation of Siglec-F ligands. Although we cannot rule out the

possibility that another Gal6ST exists, we consider this unlikely due to the high degree of sequence similarity among the known GlcNAc-, Gal-, and GalNAc-6-O-sulfotransferases (Fukuda et al., 2001). Additionally, we have recently shown that KSGal6ST is required for generating a variety of Gal6S-containing glycans in the eye and lymph node (Patnode et al., 2013). Finally, we did not detect Gal6S in our analysis of eosinophil O-glycans, although we did detect sulfo-Neu5Ac. Therefore, we conclude that Gal6S is not required to generate any of the classes of Siglec-F ligands that we detected by histology and flow cytometry. Glycan array studies have revealed that several other Siglecs and C-type lectins bind to glycans containing Gal6S, including Siglec-E, Siglec-8, Siglec-7, Siglec-5, and Langerin (Campanero-Rhodes et al., 2006; Redelinghuys et al., 2011; Tateno et al., 2010) ([www.functionalglycomics.org](http://www.functionalglycomics.org), primscreen\_3891). In view of the present findings with Siglec-F, caution is advised in drawing conclusions about the involvement of Gal6S in the biological ligands for these receptors.

The selectivity of Siglec-F-Fc staining among leukocytes is likely based on the presence of a highly specific terminal glycan. The structural definition of this sialylated glycan remains an important area for future work. Interestingly, sulfo-Neu5Ac with the sulfate moiety on the C-7, C-8, or C-9 position of the glycerol side chain was the only sulfated monosaccharide we detected in glycans isolated from a sample containing large numbers of mouse eosinophils. Sialic acid is the most heterogeneous monosaccharide with over 50 variants, including the sulfated forms (variki cold spring harbor). Sulfo-sialic acid has been detected in sea urchin, mouse, rat, and human tissues (Bulai et al., 2003; Kitazume et al., 1996; Morimoto et al., 2001; Yamakawa et al., 2007). However, the functions of this modification and the enzymes responsible for its synthesis are not



known. Although our eosinophil preparation contained contaminating lymphocytes, we did not detect sulfo-sialic acids in a parallel analysis of total lymph node glycans, suggesting that this structure is not present on B cells or T cells (Patnode et al., 2013). Interestingly, we also detected sulfo-Neu5Ac in whole lung glycans. It will be of great interest to examine alveolar macrophages and neutrophils to determine whether the presence of sulfo-sialic acid correlates with Siglec-F ligand expression.

## **FUTURE PROSPECTS**

Important questions remain unanswered with respect to the basic functions of many CD33r Siglecs. Siglec-F is an attractive prototype for future studies due to the selective expression of this receptor and its ligands.

It has yet to be determined whether Siglec-F can regulate activation signals received by eosinophils. Studies using synthetic bifunctional ligands that simultaneously engage the BCR and CD22 or Siglec-G have demonstrated that co-ligation is important for inhibiting cellular activation (Courtney et al., 2009; Duong et al., 2010). In these studies, a polyvalent acrylamide carrier was modified with both nitrophenol (NP) groups (serving as BCR ligands) and  $\alpha$ 2,6-linked sialyl-LacNAc glycans (serving as ligands for CD22 and Siglec-G) (Duong et al., 2010). The presence of sialic acid on the carrier resulted in increased CD22 phosphorylation and association with SHP-1. This correlated with reduced phosphorylation of the BCR co-receptor CD19 and the membrane-associated activating kinase Akt, as well as reduced calcium flux. Strikingly, injection of the bifunctional acrylamide carrier into mice resulted in impaired antibody production compared to a carrier modified with NP alone, and this effect was dependent on CD22

and Siglec-G expression. Similar experiments using  $\alpha$ 2,3-linked sialyl-LacNAc glycans together with NP also demonstrated inhibitory effects of Siglec-ligands on B cell activation, though the inhibitory receptor that mediates these effects was not determined (Courtney et al., 2009).

These data raise the possibility that co-ligation of Siglec-F and activating receptors on eosinophils could be important for dampening eosinophil activation. Although eosinophils express few ITAM-containing receptors, Fc $\gamma$ RII and Fc $\alpha$ R1 are present on this cell type and mediate the recognition of IgG and IgA coated targets (Hogan et al., 2008). Simultaneous cross-linking of these receptors and Siglec-F could be the basis of a control mechanism to limit activation. Eosinophils from IL-5<sup>Tg</sup> mice provide a ready source of primary cells to perform biochemical assays to determine the conditions required for Siglec-F ITIM phosphorylation and the identities of the phosphatases that may associate with these sequences.. With detailed knowledge of Siglec-F signaling outcomes, efforts could then be directed at assessing which classes of leukocyte- and lung epithelial-derived ligands are biologically relevant. Finally, purification of the actual biological ligands using a Siglec-F-Fc affinity matrix, followed by glycan profiling of these ligands by mass spectrometry, could generate a list of candidate binding determinants for this receptor.

Investigations of Siglec-F function have focused on immune responses against helminths and allergens. However, eosinophil accumulation is also a feature of infections with some respiratory RNA viruses, such as respiratory syncytial virus (RSV) (Rosenberg et al., 2009). Eosinophils express several RNases, including eosinophil-derived neurotoxin and eosinophil cationic protein, which has led to speculation that this cell type

contributes to host defense against RNA viruses. Siglec-G has been shown to negatively regulate the cytoplasmic viral RNA sensor RIG-I during infection with vesicular stomatitis virus (VSV) and sendai virus (Chen et al., 2013). This results in significantly enhanced IFN- $\alpha$  and - $\beta$  production and resistance to infection in *Siglecg*<sup>-/-</sup> mice. One possible explanation for this effect is that VSV has co-opted Siglec-G signaling to inhibit viral detection. It has been proposed that glycans on the viral envelope could serve as ligands for Siglec-G to inhibit the production of anti-viral cytokines, but this possibility has not yet been tested. Eosinophils are permissive hosts for several RNA viruses including RSV, and lentiviruses (Rosenberg et al., 2009). The RSV attachment glycoprotein (G) is highly O-glycosylated and sialylated, therefore, it could also be modified with inhibitory Siglec ligands (Barretto et al., 2003). Eosinophils express receptors involved in viral detection, including toll-like receptors 7, 8, and 9 (Shamri et al., 2011). It will be important to investigate whether Siglec-F mediates inhibitory effects on interferon production in eosinophils, and whether RNA viruses have co-opted this pathway.

## **MATERIALS AND METHODS**

### **Mice**

Mice deficient in KSGal6ST (Patnode et al., 2013), C6ST-1 (Uchimura et al., 2002), and Siglec-F (Zhang et al., 2007), as well as 4get mice (Mohrs et al., 2001) and IL5 transgenic mice (Lee et al., 1997) have been described previously. KSGal6ST and C6ST-1 mice were genotyped by PCR as described previously and Siglec-F, 4get, and IL5 transgenic mice were genotyped by FACS of peripheral blood leukocytes stained with 1

µg/mL PE rat anti-mouse Siglec-F (BD Pharmingen). C57BL/6J mice were obtained from Jackson Laboratories. All procedures involving animals were approved by the University California San Francisco Institutional Animal Care and Use Committee, and carried out in accordance with the guidelines established by the National Institutes of Health.

### **Flow cytometry**

Blood (500 µL) from wild type or IL-5 transgenic mice was collected through the right ventricle into 5 mM EDTA in PBS, and then treated with ammonium chloride buffer (150 mM NH<sub>4</sub>Cl, 10 mM KHCO<sub>3</sub>, 100 µM EDTA) to lyse erythrocytes. Alveolar macrophages were collected by bronchoalveolar lavage with PBS. Cells were then treated with 50 mU/mL *Arthrobacter ureafaciens* sialidase (Roche Applied Sciences) in HBSS at 37° C for 1 h. *Vibrio cholerae* sialidase at 50 mU/mL in HBSS also eliminated Siglec-F-Fc and Siglec-E-Fc staining, but not CD22-Fc staining. Sialidase treatment did not affect the viability of the cells, or the binding of the antibodies we used. Cells were incubated with 10 µg/mL anti-mouse CD16/32 (clone 93, eBioscience) to block Fc receptors. To measure Siglec-F expression, cells were incubated with 1 µg/mL PE rat anti-mouse Siglec-F. Siglec-F-Fc, Siglec-E-Fc, and CD22-Fc were generated previously (Redelinghuys et al., 2011). Individual Siglec-Fc proteins or human IgG (Invitrogen) was incubated at 1.5 µg/mL with biotin goat-anti-human IgG at 0.75 µg/mL and APC streptavidin at 0.375 µg/mL for 1 h, then added to cells on ice for 1 h. Cells from 4get mice were then stained with an antibody cocktail containing 1 µg/mL PE anti-mouse Ly-6G, PerCP-Cy5.5 anti-mouse Ly6C, PE-Cy7 anti-mouse CD3ε, APC-Cy7 anti-mouse

CD11b, or a separate antibody cocktail containing 1 µg/mL PE anti-mouse NK1.1, PerCP-Cy5.5 anti-mouse CD19, PE-Cy7 anti-mouse DX5, APC-Cy7 anti-mouse CD3ε for 30 min. For experiments with WT and C6ST-1/KSGal6ST DKO blood, cells were stained with an antibody cocktail containing 1 µg/mL FITC anti-mouse Ly-6G, PE anti-mouse NK1.1, PerCP-Cy5.5 anti-mouse Ly6C, PE-Cy7 anti-mouse F4/80, and APC-Cy7 anti-mouse CD11b with eosinophils identified as CD11b<sup>+</sup>, NK1.1<sup>-</sup>, Ly-6C<sup>+</sup>, Ly-6G<sup>low</sup>, F4/80<sup>+</sup>, SSC<sup>high</sup>. All antibodies were from Biolegend unless otherwise stated. Viability was determined by adding 50 µL/mL 7AAD solution (BD Pharmingen) or 0.5 µg/mL DAPI. Cells were analyzed using a FACSort cytometer equipped with CellQuest software or an LSRII equipped with FACSDiva software. All cytometers and acquisition software were manufactured by BD. Further analysis was carried out using FlowJo software (Treestar Inc.). Mean fluorescence intensity (MFI) values represent the geometric mean after subtraction of the MFI for an identical population stained with isotype control antibody.

### **Immunofluorescence**

The left lobe of the lung was perfused with PBS, collected, and fixed in 2% PFA in PBS for 1 h, then incubated in 30% sucrose overnight at 4° C. Lungs were inflated with 50% OCT compound (Sakura Finetek) in PBS and embedded in OCT compound then frozen by immersion in 2-methylbutane chilled in liquid nitrogen. Tissues were sectioned at 5 µm thickness in a cryostat and then fixed in -20° C acetone for 10 min. For sialidase experiments, sections were treated with 50 mU/mL *Arthrobacter ureafaciens* sialidase (Roche Applied Sciences) in HBSS buffer at 37° C for 1 h. Sections were blocked for 1h

with 5% normal sera from mouse and goat (Sigma-Aldrich) diluted in 0.5% casein solution (Perkin Elmer) according to manufacturer's instructions. Antibodies against sialoadhesin (clone SER4, BioLegend), proSP-C (Millipore), eMBP (Denzler et al., 2000), CD11b (clone 390, eBioscience), 1  $\mu\text{g}/\text{mL}$  for 1 h. Nonspecific rat IgG1 (eBioscience) was used to establish background fluorescence. Siglec-F-Fc, Siglec-E-Fc, CD22-Fc, and human IgG were incubated with sections at 1  $\mu\text{g}/\text{mL}$  for 24 hrs. Secondary reagents, biotin goat anti-rat light chain, Cy3 goat anti-rabbit IgG, biotin goat anti-human IgG, and APC streptavidin were obtained from Jackson ImmunoResearch and incubated with sections at 1  $\mu\text{g}/\text{mL}$  for 30 min. For sialoadhesin and eMBP staining, HRP streptavidin and FITC tyramide (Perkin Elmer) were used according to manufacturer's instructions. All antibodies were diluted in 0.5% casein solution. All sections were incubated with DAPI (Invitrogen) at 0.5  $\mu\text{g}/\text{mL}$  in PBS for 5 min to label nuclei. Images were acquired using a Nikon Optiphot microscope equipped with an AxioCam HR at fixed exposure. Multi-channel images were created and processed in parallel using Photoshop software (Adobe).

### **Parasitic worm infection**

Parasite infections were carried out as previously described (Camberis et al., 2003). Briefly, mice were anesthetized using isofluorane and injected subcutaneously at the base of the tail with 500 *N. brasiliensis* L3 larvae. Mice were maintained on water containing 2 g/L neomycin sulfate, 100 mg/L polymixin B for 5 days, and sacrificed after 9 days.

### **BAL fluid fractionation and ELISA**

BAL fluid fractionation was carried out as described previously (Thornton et al., 2001) with minor modifications. Briefly, BAL was performed using water, and BAL fluid from 5 mice was pooled and lyophilized. Samples were resuspended in 0.5 mL 4M guanidine chloride and spun at 20,000 x g for 30 min to remove debris. A 18 cm x 1 cm column of Sepharose CL-2B (Sigma-Aldrich) was equilibrated with 4M guanidine chloride and calibrated using blue dextran. BAL fluid samples were applied to the column and a model 2110 fraction collector (BioRad) was calibrated to collect 1 mL fractions. The absorbance of each fraction was measured at 280 nm using a SmartSpec 3000 (BioRad). For ELISAs, 12  $\mu$ L aliquots of fractions were coated onto Immulon-2HB plates over night, incubated in 50 mM acetate buffer, pH 5.5 at 37° C for 1 h with or without 50 mU/mL *Arthrobacter ureafaciens* sialidase, then blocked with 3% BSA 1h. Siglec-F-Fc, Siglec-E-Fc, CD22-Fc, or human IgG was incubated at 2  $\mu$ g/mL with biotin goat-anti-human IgG at 1  $\mu$ g/mL and AP-streptavidin at 0.5  $\mu$ g/mL for 1 h, then added to wells for 1 h. Plates were washed and developed with PNPP in 10% diethanolamine pH 9.8 with 0.5 mM MgCl<sub>2</sub>. Optical density at 405 nm was measured using a model 680 microplate reader (BioRad).

### **Mass Spectrometry**

O-glycan samples were prepared from 120x10<sup>6</sup> peripheral blood leukocytes (83% eosinophils) from IL-5 transgenic mice. Samples were lyophilized then processed as described previously (Patnode et al., 2013). Briefly, glycans were isolated, permethylated, and fractionated into non-, mono- and di-sulfated fractions for MALDI-MS. NanoLC-MS/MS analyses of the permethylated sulfated glycans were performed on

a nanoACQUITY UPLC System (Waters) coupled to an LTQ-Orbitrap Velos hybrid mass spectrometer (Thermo Scientific). Additionally, the eluent from a nanoLC system was interfaced to the nanospray source and the full scan MS spectrum ( $m/z$  500-2000) was acquired in the Orbitrap. All MS/MS data were interpreted manually.

### **Acknowledgments**

We are grateful to J.K. Bando for assistance with *N. brasiliensis* infections, R.M. Locksley for 4get mice and helpful discussion, J.J. Lee for IL-5 transgenic mice and eMBP antibody, and A. Varki for Siglec-F KO mice.

### **Funding**

This work was supported by the National Institutes of Health [GM-23547, GM-57411 to S.D.R.]; the Academia Sinica and Taiwan National Science Council [grant number 99-2311-B-001-021-MY3 to K-H.K.]; and the Taiwan National Core Facility Program for Biotechnology [NSC100-2325-B-001-029, NSC101-2319-B-001-003 to the Core Facilities for Protein Structural Analysis at Academia Sinica] and a Wellcome Trust Senior Fellowship [WT081882 to P.R.C.].



## **CHAPTER 5**

### **Mechanisms of Eosinophil Accumulation during Parasite Infection**

## **Eosinophil-Parasite Interactions**

It has long been appreciated that eosinophil accumulation is a defining feature of the stereotyped immune response that takes place during infection with multicellular endoparasites (Klion and Nutman, 2004). Although eosinophils normally make up only 1-2% of granulocytes in peripheral blood, they can increase ~10 fold when hosts carry large helminth burdens. Furthermore, in peripheral tissues such as the lung, eosinophils can increase by ~1000 fold during worm infection (Voehringer et al., 2004). The localization of eosinophils around worms in tissues, such as the liver and intestine, suggests some level of interaction with parasites. Indeed, electron micrographs show eosinophil membranes closely juxtaposed to helminth cuticle or tegument (Klion and Nutman, 2004). Eosinophilia also correlates with resistance to reinfection with *Shistosoma* species following anti-helminth treatment. Thus, it was proposed as early as the 1930's that eosinophils contribute to host defense against helminths. Data supporting this hypothesis are provided by *in vitro* experiments in which eosinophils are incubated with parasitic nematodes or trematodes in the presence of anti-parasite antibody (Butterworth et al., 1975; Kazura and Grove, 1978). In these assays, eosinophil Fc-receptors stimulate irreversible adhesion to antibody-coated worms. Adhesion can also take place via complement receptors if active complement components are present in the culture (Ramalho-Pinto et al., 1978). Neutrophils participate in similar interactions with antibody- or complement-coated worms, consistent with their expression of receptors for Fc and complement (Dean et al., 1974). These assays provide striking images that suggest a clear function for eosinophils and neutrophils in attacking invading parasites (Glauert et al., 1978).

The most abundant proteins stored in eosinophil primary granules are eosinophil major basic protein, eosinophil peroxidase, eosinophil derived neurotoxin, and eosinophil cationic protein (Hogan et al., 2008). As their names suggest, these proteins are largely restricted to eosinophils and highly charged, due to their many arginine residues. Purified eosinophil granule products have been shown to decrease helminth survival when added to various larval stages in culture (Butterworth et al., 1979). Importantly, the adhesion of eosinophils to worms via Fc receptors or complement receptors results in the release of eosinophil granule products onto the nematode surface, and visible malformations in the cuticle or tegument (Glauert et al., 1978). However, at the time these studies were carried out, there were no available tools for determining whether adhesion to worms is strictly required for killing. Indeed, the addition of the calcium ionophore A23187 to eosinophil-helminth cultures resulted in larval killing in the absence of adhesion (David et al., 1980). Thus, the Ig-stimulated release of eosinophil products into the culture medium could contribute to larval death in these assays. Similar experiments using related free-living nematodes have not been reported, although these worms would presumably be more susceptible to killing due to the lack of mechanisms for evading eosinophil adhesion and toxicity.

The availability of eosinophil-deficient mice has allowed direct assessments of the contributions of eosinophils to helminth clearance (Klion and Nutman, 2004). The most widely used of these strains contains a targeted deletion in a palindromic, high-affinity binding site for the transcription factor GATA-1, which sits 500bp upstream of the *Gata1* start site (Yu et al., 2002). Although mice deficient in *Gata1* die *in utero* due to a block in erythropoiesis (Fujiwara et al., 1996), mice without the double GATA-1 binding site

(*AdblGatal* mice) exhibit a selective loss of the eosinophil lineage. Surprisingly, parasite burden in *AdblGatal* mice is increased in only a few models of helminth infection (Klion and Nutman, 2004), and in most of these models the effects are modest. There are divergent findings as to whether eosinophils exert these effects during primary or secondary challenges. Furthermore, there have been reports of reduced parasite numbers in the absence of eosinophils, which suggests that these cells are actually important for the success of certain pathogens (Fabre et al., 2009; Gebreselassie et al., 2012).

The limited evidence that eosinophils eliminate broad classes of helminths during infection has spurred investigations into other potential functions of this leukocyte. Eosinophils are found in adipose tissue, where they skew tissue macrophages toward an alternatively activated phenotype (Wu et al., 2011). Furthermore, the loss of eosinophils alters energy balance during infection with the nematode parasite, *N. brasiliensis*. Eosinophil-deficient mice have defects in plasma cell survival (Chu et al., 2011). This is thought to be due to the production of the plasma cell survival factors APRIL and IL-6 by eosinophils in the bone marrow. Asthma and allergy are inflammatory diseases that have many features in common with immune responses that take place during helminth infection (Allen and Maizels, 2011). Allergens and helminth antigens both give rise to T helper 2 cells, which orchestrate the immune response by producing a number of important cytokines. These include IL-4, which is responsible for inducing IgE class switching; IL-13, which contributes to tissue remodeling; and IL-5, which promotes the generation and survival of eosinophils. Although there is controversy about the contributions of eosinophils to disease processes in asthma and allergy (Lee and Lee, 2005), eosinophils have been shown to promote collagen deposition and mucus

production in multiple models of allergic lung inflammation (Fulkerson et al., 2006). In addition, eosinophil-deficient mice have reduced skin fibrosis in a model of atopic dermatitis (Oyoshi et al., 2012a). Investigations into the diverse functions of eosinophils in parasitic infections and allergic diseases are ongoing. Since eosinophil function appears to vary depending on the tissue environment, future studies would benefit greatly from a more complete understanding of the factors responsible for eosinophil recruitment and accumulation.

### **Eosinophil Recruitment and Survival**

Eosinophil survival is profoundly influenced by IL-5, a member of the type-I family of cytokines (Kouro and Takatsu, 2009). The *IL5* gene is highly conserved in mammals and resides in a gene cluster containing the functionally-related cytokines *IL4* and *IL13*. IL5 signals as a homodimer, binding to and assembling the multi-subunit IL5 receptor (IL5R), expressed on the surfaces of eosinophils and peritoneal B1 cells (Dyer et al., 2011). This receptor is comprised of the IL5R $\alpha$  chain and a common  $\beta$  chain ( $\beta_c$ ) that is shared with the IL3R and GMCSFR (Broughton et al., 2012). Recognition of IL-5 causes trans-phosphorylation of receptor-associated JAK1 and JAK2, leading to phosphorylation and nuclear translocation of STAT proteins, principally STAT5. IL-5 is produced by Th2 cells as well as subsets of innate lymphoid cells during helminth infection and allergen challenge. Through experiments using neutralizing IL-5 antibodies and mice with deletions in *IL5* or *IL5Ra*, it is clear that this cytokine is critical for eosinophil accumulation during inflammation. In addition, ectopic expression of IL-5 under the control of the CD3 $\delta$  gene in mice (*IL5<sup>Tg</sup>* mice) results in massive accumulation of

eosinophils in the blood, spleen, liver, and other tissues (Lee et al., 1997). Eosinophils develop normally in the absence of IL-5, most likely due to compensation by other cytokines that signal through the  $\beta_c$  chain (Kopf et al., 1996). Although IL-5 can stimulate eosinophil migration *in vitro* (Yamaguchi et al., 1988), the administration of this cytokine alone is not sufficient to induce eosinophil accumulation in lung (Yang et al., 2003). Thus, there has been interest in determining what signals attract eosinophils into tissues during immune responses.

Eotaxin-1 and eotaxin-2 are CC chemokines encoded by the genes *CCL11* and *CCL24*, respectively (Hogan et al., 2008). These molecules signal through CCR3, a GPCR that is expressed on most eosinophils, but is also found on Th2 cells and mast cells (Dyer et al., 2011; Pease, 2006). A third chemokine, CCL26, can also signal through CCR3, but is 10-fold less potent than eotaxin-1, and does not appear to contribute to eosinophil recruitment (Fulkerson et al., 2006; Kitaura et al., 1999; Shinkai et al., 1999). Mice deficient in CCR3 have defective eosinophil accumulation in models of chronic allergic inflammation induced by sensitization and challenge with *Aspigoillus fumigatus* extract (Fulkerson et al., 2006). *CCL11*<sup>-/-</sup> mice exhibit defects in eosinophil accumulation after injection of the filarial nematode *Brugia malayi*, and this effect is associated with increased worm survival (Simons et al., 2005). Eosinophil accumulation in the small intestine is ~50% reduced in the absence of eotaxin-1 during *Trichuris muris* or *Trichinella spiralis* infection (Dixon et al., 2006). However, CCR3 is also important in regulating basal numbers of eosinophils in the skin and intestine, which could confound studies using mice genetically deficient in the eotaxins or CCR3 from birth (Ma et al., 2002; Matthews et al., 1998). Eosinophil recruitment is intact in *CCR3*<sup>-/-</sup> mice during *N.*

*brasiliensis* infection (Knott et al., 2009), and in *CCL11*<sup>-/-</sup> mice after peritoneal injection of Sephadex beads or thioglycolate (Yang et al., 1998). Thus, there must be additional factors that contribute to eosinophil recruitment in certain settings.

Leukotrienes are eicosanoid lipid mediators produced primarily by myeloid leukocytes during inflammation (Haeggstrom and Wetterholm, 2002). Leukotriene synthesis is initiated by cellular activation, which results in recruitment of phospholipase A<sub>2</sub> to the plasma membrane. This enzyme generates arachadonic acid (AA) by cleaving polyunsaturated fatty acids from the polar headgroups of membrane phospholipids including phosphatidyl choline, phosphatidyl ethanolamine, and phosphatidylinositides (Fig. 16A). As a second consequence of leukocyte activation, 5-lipoxygenase (5-LO, encoded by the gene *Alox5*) translocates to the nuclear membrane and associates with 5-LO Associating Protein (FLAP) and AA to generate the unstable epoxide intermediate leukotriene A<sub>4</sub> (LTA<sub>4</sub>). Cells genetically deficient in *Alox5*, or treated with inhibitors of FLAP (such as the compound MK886) or 5-LO (such as the compound zileuton), do not produce detectable leukotrienes (Bell et al., 1992; Chen et al., 1994; Rouzer et al., 1990). Two classes of leukotrienes are synthesized from LTA<sub>4</sub>, namely LTB<sub>4</sub> and the cysteinyl leukotrienes (cysLTs) LTC<sub>4</sub>, LTD<sub>4</sub> and LTE<sub>4</sub>. Both classes of leukotrienes share a 20-carbon backbone containing three conjugated double bonds and a carboxylate group at the C1 position (Fig 1B). LTB<sub>4</sub> is generated by LTA<sub>4</sub> hydrolase (LTA<sub>4</sub>H), which opens the epoxide ring and creates a unique hydroxyl group at position C12. The CysLT LTC<sub>4</sub> is produced when LTA<sub>4</sub> is covalently modified with glutathione on C6 by the enzyme LTC<sub>4</sub> synthase (LTC<sub>4</sub>S). The glutathione peptide can then be hydrolyzed to a cys-gly dipeptide to produce LTD<sub>4</sub>, or a single cysteine residue to produce LTE<sub>4</sub>. Although many

cell types express LTA4H and LTC4S, leukotriene production is largely restricted to myeloid cells by virtue of the myeloid cell-specific expression pattern of 5-LO.

Four GPCRs that selectively recognize leukotrienes have been described in humans (Fig. 16B) (Kanaoka and Boyce, 2004; Tager and Luster, 2003). All of these receptors are seven-pass transmembrane proteins that require  $G\alpha_{i/0}$  to signal in leukocytes, however they can also signal through  $G_q$  when transfected into cell lines. CysLTR1 and CysLTR2 are expressed on many stromal and hematopoietic cell types in mice and humans. CysLTs are abundantly produced by human and mouse mast cells, eosinophils, and alveolar macrophages (Kanaoka and Boyce, 2004). Eosinophil-derived cysLTs were shown to be important for collagen deposition in the skin in a mouse model of atopic dermatitis (Oyoshi et al., 2012a). An inhibitor of CysLTR1, known as montelukast (trade name, Singulair) is widely used as an oral anti-inflammatory treatment for asthma and allergic rhinitis (Horwitz et al., 1998). In asthma, montelukast directly inhibits contraction in airway smooth muscle cells, which express CysLTR1. There are also effects on eosinophil recruitment in asthma patients that may be due to eosinophil expression of CysLTR1.

LTB4R1 is highly expressed on human and mouse neutrophils and eosinophils, and provokes robust chemotaxis (Tager and Luster, 2003). In contrast, LTB4R2 is widely expressed in humans, whereas it is not highly expressed in most mouse tissues. In mice deficient in LTB4R1, thioglycolate-induced eosinophil accumulation into the peritoneum is reduced by 60% (Tager et al., 2000). In a model of chitin induced lung inflammation, eosinophil accumulation in the lung is reduced by 85% in *LTB4R1*<sup>-/-</sup> mice (Reese et al., 2007). In both of these models, it is not yet clear whether this receptor is required on



eosinophils or on an accessory cell type. However, it is established that lung macrophages attract eosinophils through the production of LTB<sub>4</sub> (Reese et al., 2007). During *Strongyloides stercoralis* infection, treatment of mice with MK886 results in fewer eosinophils in the BAL fluid, peritoneum, and blood (Machado et al., 2005). A concomitant decrease in IL-5 production is also observed, making interpretation of this result difficult. Human eosinophils express LTA4H and have been shown to produce LTB<sub>4</sub> in response to the calcium ionophore A23187 (Condliffe et al., 1998; Haeggstrom and Wetterholm, 2002; Henderson et al., 1984). Importantly, the concomitant expression of leukotriene receptors and enzymes involved in leukotriene synthesis in a single cell type raises the possibility of homotypic cell-cell communication.

### **Evidence for Leukotriene-Driven Amplification of Granulocyte Recruitment**

LTB<sub>4</sub> makes major contributions to leukocyte accumulation in many inflammatory diseases, including rheumatoid arthritis, asthma, pancreatitis, and inflammatory bowel disease (Peters-Golden and Henderson, 2007). Mouse neutrophils can release LTB<sub>4</sub> after triggering of cell surface receptors for Ig, C5a, TNF $\alpha$ , LPS, or formyl-Met-Leu-Phe (fMLF) peptides (Condliffe et al., 1998; Sadik et al., 2012). In contrast, signals such as IL-8, CCL3, CXCL2, IL1 $\beta$ , and PAF do not induce detectable leukotriene production by this leukocyte (Afonso et al., 2012). Recent studies have demonstrated that fMLF induces neutrophils to produce LTB<sub>4</sub> in quantities sufficient to attract neighboring neutrophils (Afonso et al., 2012). In these experiments, neutrophils deficient in formyl peptide receptor 1 (Fpr1) were mixed with wild type cells, and the population was stimulated with fMLF. Strikingly, *Fpr1*<sup>-/-</sup> cells migrated toward the source of fMLF, and this effect

was dependent on leukotriene production in wild type cells. Thus, a leukotriene gradient created by wild type cells can compensate for the inability of neighboring cells to detect a primary chemoattractant. Furthermore, the migration of leukotriene-deficient neutrophils toward fMLF is defective compared to wild type cells, which could indicate that cell-cell communication is involved. However, cell polarization assays carried out at low neutrophil densities suggested that autocrine leukotriene signaling takes place in response to fMLF, whereby each neutrophil releases leukotrienes that bind to receptors on that same cell to enhance polarization. Therefore, it is possible that leukotrienes act primarily as autocrine factors for wild type neutrophils that are migrating toward fMLF. At higher cell density, increased leukotriene-dependent and leukotriene-independent cell polarization was observed. Thus, paracrine signaling between neutrophils likely contributes to polarization in this case, but the identity of the leukotriene-independent signal is not clear. It is difficult to perform under-agarose migration assays at limiting cell densities to dissect out the contributions of paracrine signaling. Additionally, since these migration assays are performed with the chemotactic source at a fixed distance from the target cells, they do not establish whether LTB<sub>4</sub> amplification increases the recruitment range of fMLF. Despite these caveats, this system provides clear evidence that leukotrienes can enhance chemotaxis in response to an existing gradient of chemoattractant. Although there are many non-chemotactic receptors that trigger leukotriene production, stimuli that induce migration in a strictly leukotriene-dependent fashion have not been reported.

Amplification by leukotriene synthesis predicts accelerating leukocyte accumulation over time. Observations in living mice using two-photon microscopy are consistent with

this type of behavior (Chtanova et al., 2008). When *Toxoplasma gondii* is introduced into the skin of mice, parasites are found in subcapsular sinus macrophages in draining lymph nodes after 4 hours. Neutrophils also accumulate in the lymph node subcapsular sinus, and these cells periodically undergo coordinated mass migration over distances  $> 50 \mu\text{m}$  and speeds of up to  $10 \mu\text{m}/\text{min}$  toward *T. gondii*. Neither the initiating events nor the factors that attract neutrophils have been determined for this system. However, it has been proposed that there is communication between migrating neutrophils in this setting. Additionally, neutrophils migrate  $> 200 \mu\text{m}$  at speeds of up to  $6 \mu\text{m}/\text{min}$  toward sterile, heat-induced necrotic foci in the liver (McDonald et al., 2010). This phenomenon has been shown to involve fMLF receptor, presumably due to the recognition of mitochondrial fMLF peptides. Although the evidence suggests that fMLF induces leukotriene production, the possibility that leukotrienes contribute to cell migration in this context was not addressed.

Neutrophils are required for the development of disease in the K/BxN serum transfer model of arthritis (Sadik et al., 2011). In this model, antibodies against glucose-6-phosphate isomerase are transferred into mice, resulting in immune complex deposition in the joint synovium and inflammatory cell activation and recruitment. The trafficking of neutrophils into the joints in this model does not take place in the absence of LTB<sub>4</sub>R1 (Kim et al., 2006). Transfer experiments demonstrated that LTB<sub>4</sub>R1 is required on neutrophils, but only for initiation of inflammation, after which LTB<sub>4</sub>R1-deficient neutrophils rely on CCR1 and CXCR2 for their recruitment (Sadik et al., 2011). Intriguingly, neutrophil expression of 5-LO is also required for neutrophil recruitment into the joint, and for disease progression (Chen et al., 2006). Both 5-LO and the

complement component 5a receptor 1 (C5aR1) must be co-expressed in neutrophils to initiate recruitment. Co-expression of Fc $\gamma$ RIII and the pro-inflammatory cytokine IL-1b is required in neutrophils at later stages of the response (Sadik et al., 2012). Thus, a multi-step cascade of lipids, cytokines, and chemokines controls neutrophil accumulation in the joint in this model of arthritis. It is proposed that complement deposition and release of C5a initially stimulates production of LTB<sub>4</sub> in rare tissue neutrophils. Leukotriene production draws in more neutrophils, which produce IL-1b after binding to Ig deposited in the joint. This cytokine induces the secretion of chemokine ligands for CCR1 by synovial stromal cells, as well as CXCR2 ligands by neutrophils themselves. Chemokine expression results in recruitment of more neutrophils expressing these receptors, and the establishment of robust inflammation. It is not yet known whether leukotrienes diffuse across the endothelium to effect neutrophil recruitment out of the blood, or function primarily to guide neutrophils in tissues. Nonetheless, these studies provide a clear example of LTB<sub>4</sub>-mediated communication between neutrophils present at a focus of inflammation and neutrophils undergoing recruitment.

In the following chapter, I describe a novel experimental system that allows investigation of leukotriene-dependent communication in eosinophils and neutrophils in the context of parasitic worm infection.

Figure 16

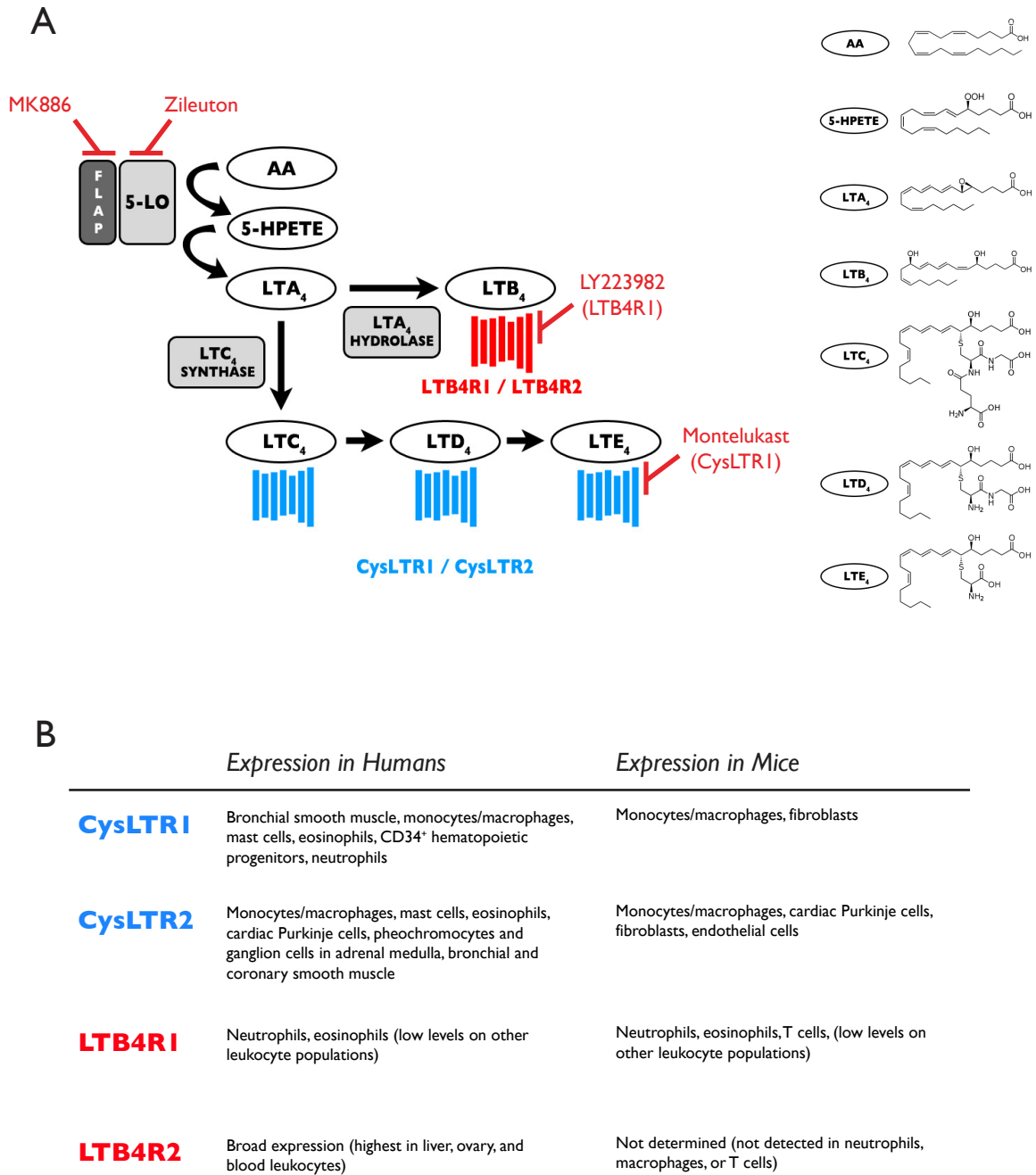


Figure 16. Leukotriene synthesis and leukotriene receptor expression

(A) Leukotriene synthesis pathway with enzymes represented as grey boxes. Lipid products are represented as white ovals, and their structures are depicted on the right. Leukotriene receptors are represented as seven colored bars. Notable inhibitors and the points at which they act in this pathway are shown in dark red. (B) Expression patterns of the four leukotriene receptors. Both human and mouse expression is shown, with emphasis on hematopoietic populations.

## **CHAPTER 6**

### **Leukotriene-Driven Amplification of Eosinophil Accumulation in Response to Diverse Nematode Species**

## SUMMARY

Here, we show that mouse eosinophils migrate toward diverse nematode species in three-dimensional culture. These include the mammalian parasite *Nippostrongylus brasiliensis*, the insect parasite *Heterorhabditis bacteriophora*, and the free-living nematode *Caenorhabditis elegans*. Using an axenic culture system for *C. elegans*, we establish that this migration takes place in the absence of bacterial products. Furthermore, the response requires leukotriene synthesis in eosinophils, as well as expression of the leukotriene receptor LTB4R1. Mouse and human neutrophils also migrate toward nematodes in a leukotriene-dependent manner. Eosinophils also accumulate around *C. elegans* larvae deposited in mouse lung via intravenous injection. This response is independent of bacterial products, TLR4, MyD88, CCR3, and complement component 3. In contrast, mice deficient in leukotriene synthesis or LTB4R1 have dramatic reductions in the number of eosinophils in lung tissue after injection of *C. elegans*. Leukotriene synthesis is also required for normal eosinophil accumulation during infection with *N. brasiliensis*. These results establish that conserved nematode signals induce leukotriene production in eosinophils, and this mediator is then required for further eosinophil accumulation.

## RESULTS

### **Eosinophils Migrate en Mass toward Diverse Nematode Species in Vitro**

To determine whether live nematodes directly attract eosinophils, we mixed *C. elegans* dauer larvae, *H. bacteriophora* infective juvenile larvae, or *N. brasiliensis* L3 larvae with eosinophils in a three-dimensional (3D) Matrigel matrix. This assay differs from typical under-agarose migrations assays (Nelson et al., 1975), since worms and eosinophils are

distributed randomly throughout the gel at the start of the culture. Eosinophils were obtained by culturing mouse bone marrow progenitors in IL-5 for two weeks as previously described (Dyer et al., 2008). This method allowed for the generation of  $\sim 25 \times 10^6$  eosinophils per mouse from wild type or genetically targeted mouse strains. We verified by flow cytometry that eosinophils obtained in this fashion were  $> 98\%$  Siglec-F<sup>+</sup>/Ly-6G<sup>+</sup> (Fig. 17A). Additionally,  $> 90\%$  these cells possessed the multi-lobed nuclei and acidophilic granules characteristic of eosinophils, with the remainder comprised of large mononuclear cells. Within one hour of mixing eosinophils and nematodes, eosinophils had accumulated in large numbers around all three species (Fig. 17B). We also verified that eosinophils isolated from the blood of IL-5<sup>Tg</sup> mice (Lee et al., 1997) accumulated around worms. Eosinophils failed to accumulate around agarose (Fig. 17B), chitin, or Teflon beads, indicating that a general response to foreign surfaces did not account for this effect. In addition to providing novel evidence that worm recognition can involve factors that are conserved across nematode species, *C. elegans* presented a number of distinct technical advantages in this assay. These included the availability of fluorescent strains, methods for growth in the absence of bacterial products, and a low likelihood of evolved mechanisms for immune evasion. Therefore, we proceeded to use this free-living nematode as a model for parasitic nematodes, verifying our most important results using *N. brasiliensis*, a bonafide mammalian parasite.

Eosinophil accumulation could be the result of either directed migration towards nematodes, or random migration accompanied by retention on or near the nematode surface. To distinguish these possibilities, we performed time-lapse imaging of eosinophils mixed with *C. elegans* dauer larvae over the course of two hours (Fig. 17C).



Eosinophils migrated en mass over distances of up to 300  $\mu\text{m}$  toward *C. elegans*. This migration was directed toward specific points along the length of the nematode (Fig. 17C), but these points differed between individual worms. Therefore, it did not appear that a single anatomical structure was responsible for inducing migration.

To quantitatively measure eosinophil migration, we performed co-cultures with yellow fluorescent *C. elegans* dauer larvae and red fluorescent eosinophils. We then used confocal microscopy to collect 3D images, and used image analysis software to calculate the volume of red fluorescence signal that was in contact with each nematode after one hour (Fig 18A,B). Many nematodes, including the three species we examined, feed on bacteria at some point in their life cycle. We performed our migration assays using the non-feeding dauer larval stage, and we washed the worms extensively until LPS was undetectable by *Limulus* amoebocyte lysate testing in worm supernatants. Since free, soluble bacterial contaminants would be distributed evenly at the start of 3D culture, it is unlikely that these would be responsible for the directed migration we observed.

However, the possibility existed that bacterial products bound to worms or released from worms could be responsible. To conclusively determine whether bacterial products were required for eosinophil migration, we grew *C. elegans* for several generations in axenic liquid culture, which has been demonstrated to eliminate detectable bacterial products (Rao et al., 2005). There was no difference in eosinophil accumulation around *C. elegans* grown in non-axenic or axenic culture (Fig 18C).

The secretion of a worm-derived chemoattractant would be predicted to attract eosinophils to a source of secretion, such as the mouth or anus of a worm. The observation that eosinophils accumulated at a seemingly random point on the surface of

each nematode suggested, instead, that eosinophils themselves might be the source of chemoattractants that attracted neighboring cells. To test this possibility, we incubated *C. elegans* with decreasing densities of eosinophils, and measured the accumulation after one hour. At high densities, as expected, the volume of eosinophils that accumulated correlated with the number of eosinophils present (Fig 18D). However, at low densities ( $< 3 \times 10^6$  cells/mL) there was no evident eosinophil migration toward worms (Fig 18E). An eosinophil-independent chemoattractant produced by a worm would be expected to attract the eosinophils within the vicinity, irrespective of cell density. These data establish that a threshold density is required for accumulation around nematodes, and suggest that signaling between eosinophils is involved.

### **Mass Migration Requires Amplification via Dual Sensing and Synthesis of Leukotrienes**

We suspected that eosinophils migration toward nematodes was mediated by soluble, eosinophil-derived chemotactic factors. Since such factors would be likely to signal through GPRCs, we first tested whether  $G\alpha_{i/0}$  proteins were important in eosinophil migration towards *C. elegans*. We incubated eosinophils with pertussis toxin to block  $G\alpha_{i/0}$  signaling and found that this treatment completely abolished eosinophil accumulation (Fig 18F). Next, we mixed differentially labeled pertussis toxin-treated and control eosinophils together, and observed their migration using time-lapse imaging. While control cells migrated robustly toward *C. elegans*, pertussis toxin-treated eosinophils failed to migrate toward the same larvae, demonstrating that the effect of pertussis toxin treatment was eosinophil-intrinsic (Fig 18G).

Neutrophils have been shown to attract other neutrophils in cell culture (Afonso et al., 2012) and in mouse models of arthritis (Sadik et al., 2011). In these systems, migration is mediated by neutrophil-derived LTB<sub>4</sub> (see chapter 5). We tested whether leukotriene synthesis was required for eosinophil migration in response to *C. elegans* by performing our migration assay in the presence of MK886, which inhibits FLAP and the production of leukotrienes (See Chapter 5). There was a dose-dependent reduction in the accumulation of eosinophils around *C. elegans* in the presence of MK886 (Fig. 19A), with an IC<sub>50</sub> (~0.5 μM) comparable to that observed for inhibition of neutrophil leukotriene production (~0.1 μM) (Rouzer et al., 1990). We also tested whether genetic deficiency in *Alox5*, the gene encoding 5-LO (see Chapter 5), altered migration. Bone marrow-derived eosinophils from *Alox5*<sup>-/-</sup> mice were impaired by > 10-fold in their ability to accumulate around *C. elegans* after 2 hours (Fig. 19B). To determine whether paracrine leukotriene signaling accounts for the migration of eosinophils toward nematodes, we incubated fluorescently-labeled wild type (15%), fluorescently-labeled *Alox5*<sup>-/-</sup> (15%), and unlabeled wild type (70%) eosinophils. Importantly, the migration of *Alox5*<sup>-/-</sup> eosinophils was rescued in the presence of wild type eosinophils (Fig. 19C). This experiment ruled out the possibility that *Alox5*<sup>-/-</sup> eosinophils have general defects in cell migration. Additionally, eosinophil accumulation in response to the rodent parasite *N. brasiliensis* was reduced >10-fold in the absence of leukotrienes (Fig. 19D). Since perturbations of 5-LO function affect both LTB<sub>4</sub> and CysLT pathways (see chapter 5), we wanted to determine which leukotrienes were involved in the response to nematodes. Although eosinophils are known to produce CysLTs upon activation (Kanaoka and Boyce, 2004), we found that the CysLTR1 antagonist montelukast failed to alter

eosinophil behavior (Fig. 19E). We next assessed the migratory capacity of bone marrow-derived eosinophils lacking *Ltb4r1*, a receptor that has been implicated in eosinophil migration (Reese et al., 2007; Tager et al., 2000). There was a > 10 fold reduction in eosinophil accumulation in eosinophils from *Ltb4r1*<sup>-/-</sup> mice (Fig. 19F). Taking together, these findings indicate that eosinophil migration toward nematodes in this system requires both the synthesis and sensing of LTB<sub>4</sub>.

Neutrophils often accumulate in tissues during early stages of parasite infection (Makepeace et al., 2012). The known involvement of LTB<sub>4</sub> in PMN migration in vitro and in vivo (see Chapter 5) prompted us to test whether neutrophils would respond to nematodes in this system. We neutrophils from human peripheral blood and found that they migrated toward *C. elegans* in 3D culture (Fig. 20A), as did human eosinophils (Fig. 20B). The migration of human neutrophils was completely inhibited by the addition of MK886. Neutrophils have been shown to produce LTB<sub>4</sub> in response to Fc receptor engagement (Sadik et al., 2012). Therefore, we predicted that IgG-coated beads would induce migration phenomena similar to that observed with nematodes. Mouse neutrophils accumulated around IgG-coated beads but not IgM coated beads, whereas eosinophils did not accumulate around antibody-coated beads at all (Fig. 20C). This may be due to the expression of FcγRI and FcγRIII on neutrophils but not eosinophils (Hogan et al., 2008). It is not yet clear whether this response involves the release of leukotrienes. Furthermore, it will be important to identify stimuli that induce leukotriene production by eosinophils but not neutrophils. Nonetheless, these results are consistent with the notion that leukotriene production and mass migration of granulocytes can be triggered by diverse primary stimuli.

## **Leukotrienes Are Important for Eosinophil Accumulation in the Lung in Response to Nematodes**

Leukotrienes are known to be important for eosinophil accumulation in a number of settings (reviewed in Chapter 5). However, we wanted to specifically address whether eosinophil-derived leukotrienes were involved in eosinophil accumulation in response to nematodes. First, we generated a model of eosinophil accumulation in response to *C. elegans*. We found that live *C. elegans* dauer larvae became trapped in the capillaries of the lung after intravenous injection. The worms ruptured these vessels, causing focal hemorrhage, as well as eosinophil and neutrophil accumulation (Fig. 21A). This effect was apparent in both C57BL/6 (Fig. 21B) and BALB/c mice (Fig. 21G). To quantify eosinophils after nematode injection, we digested perfused lungs with collagenase and analyzed cells expressing Siglec-F by FACS. Eosinophils were rare ( $< 20 \times 10^3$  cells) before and even 12 hours after nematode injection (Fig. 21B). By 24 hours, the number of eosinophils in the lung increased 10-fold, after which the number slowly returned to baseline over the course of 2 weeks (Fig. 21C). Helminth infections typically induce alternative macrophage activation, characterized by the increased expression of several macrophage gene products, including arginase-1 (Arg1). Using arginase-1-YFP reporter mice (Reese et al., 2007), we found significantly increased alternative activation of macrophages 24 hours after *C. elegans* injection (Fig. 21D). Live *C. elegans* L3 larvae grown in axenic culture induced similar levels of eosinophil recruitment, indicating that this response was independent of bacterial products (Fig. 21E). MyD88 is required for detection of bacterial products by all toll-like receptors, with the exception of TLR4, which can signal through the adaptor TRIF (Song and Lee, 2012). To determine whether

these receptors were involved in the response to nematodes, we used *Myd88*<sup>-/-</sup> mice and mice with an inactivating mutation in the TLR4 (*Tlr4*<sup>P712H</sup> mice) (Fig. 21F). After *C. elegans* injection, eosinophil accumulation was indistinguishable in these two mutant strains compared to wild-type mice. CCR3 and the eotaxins function to recruit eosinophils to tissues in several settings (reviewed in Chapter 5). Additionally, C3-dependent complement deposition can mediate interactions between eosinophils and helminths (Ramalho-Pinto et al., 1978). Eosinophil accumulation in *Ccr3*<sup>-/-</sup> and *C3*<sup>-/-</sup> mice did not differ from that in wild-type mice (Fig. 21G). In contrast, the number of eosinophils that accumulated in the lung 24 hours after *C. elegans* injection was decreased by 70% in *Alox5*<sup>-/-</sup> mice (Fig. 22A). This decrease was not due to systemic effects on eosinophils, since *Alox5*<sup>-/-</sup> mice had normal numbers of eosinophils in peripheral blood at the same time point (Fig. 22B). Interestingly, the number of neutrophils in the lung was not affected (Fig. 22C). In *Ltb4r1*<sup>-/-</sup> mice, eosinophil accumulation in the lung was 55% reduced (Fig. 22D), and the number of neutrophils was also modestly but significantly reduced (Fig. 22E). This discrepancy with the *Alox5*<sup>-/-</sup> phenotype may indicate that there is a variable window during which neutrophil accumulation is affected by LTB<sub>4</sub>. To determine whether leukotrienes were also important for eosinophil accumulation in response to a parasitic nematode species, we infected *Alox5*<sup>-/-</sup> mice with the *N. brasiliensis* (as described in Chapter 4). Leukotriene deficiency resulted in an 80% reduction in the number of eosinophils in the lung 9 days after *N. brasiliensis* infection (Fig. 22F). There was no significant difference between the number of peripheral blood eosinophils in wild type and *Alox5*<sup>-/-</sup> mice at this time point (Fig. 22G).

Figure 17

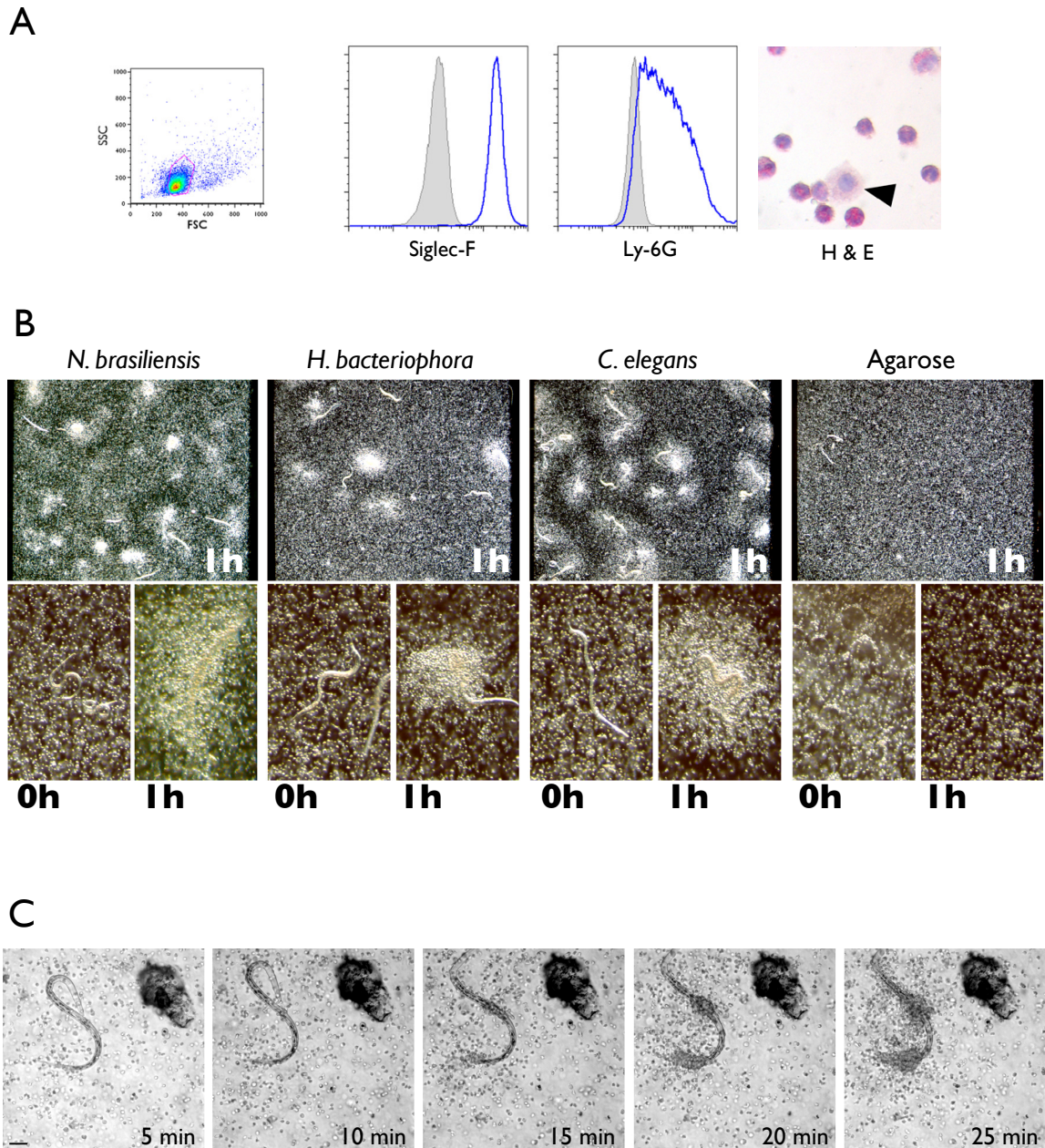


Figure 17. Eosinophil migration in response to nematodes

(A) Flow cytometry and cytopsin analysis of bone marrow-derived eosinophils. Staining with antibodies against Siglec-F and Ly-6G (blue histograms), and hematoxylin/eosin (far right) is shown. Grey histograms show isotype control staining. The arrowhead marks a contaminating non-eosinophil. (B) Dark field dissection scope images of eosinophils (white dots) cultured with nematodes (white ribbons). Low power images (top) show eosinophil accumulation after 1 hour. High power images (bottom) show nematodes before and after eosinophil accumulation. Agarose beads are not visible. (C) Images taken from a DIC time-lapse movie of eosinophils migrating toward a *C. elegans* dauer larva. Eosinophils did not migrate toward the particulate material in the top right. Scale bar represents 50  $\mu$ m.

Figure 18

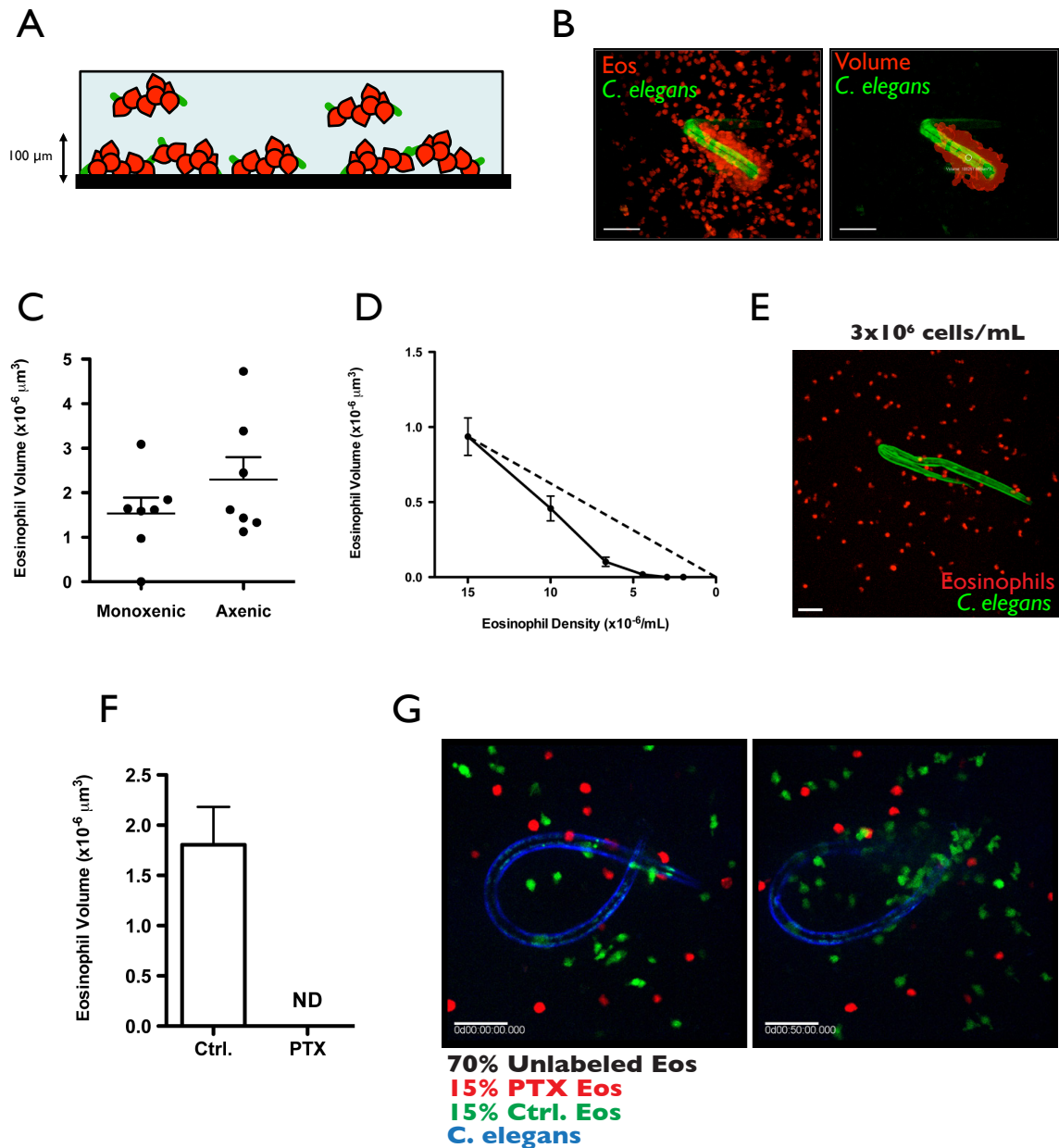


Figure 18. Evidence for paracrine signaling in eosinophil migration towards nematodes (A) Strategy for quantifying eosinophil accumulation around fluorescent nematodes. 3D matrix is depicted in a side-view. Green and red symbols represent nematodes and eosinophils, respectively. Only worms within 100  $\mu\text{m}$  of the coverslip were imaged. (B) An example of a 3D eosinophil volume calculation using Imaris software. The raw image (left) and artificial volume (right) are shown. Scale bar represents 50  $\mu\text{m}$ . (C) Eosinophil volumes surrounding individual *C. elegans* dauer larvae. Monoxenic worms grown on *E. coli* and compared worms grown in axenic culture. (D) Eosinophil accumulation after 2 hours as a function of eosinophil density. The dotted line represents linear proportionality with an x intercept at the origin. (E) Image demonstrating a lack of accumulation when eosinophils are cultured at a density of  $3 \times 10^6$  cells/mL. (F) Control and pertussis toxin-treated eosinophil accumulation around *C. elegans* dauer larvae after 2 hrs of culture. (G) Images taken from a fluorescent time-lapse movie of control (green) and pertussis toxin-treated (red) eosinophils migrating toward a *C. elegans* dauer larva (blue). The worm is shown at 0 min (left) and after 50 min (right) of the culture. The abundant unlabeled wild-type eosinophils are invisible.



## Figure 19

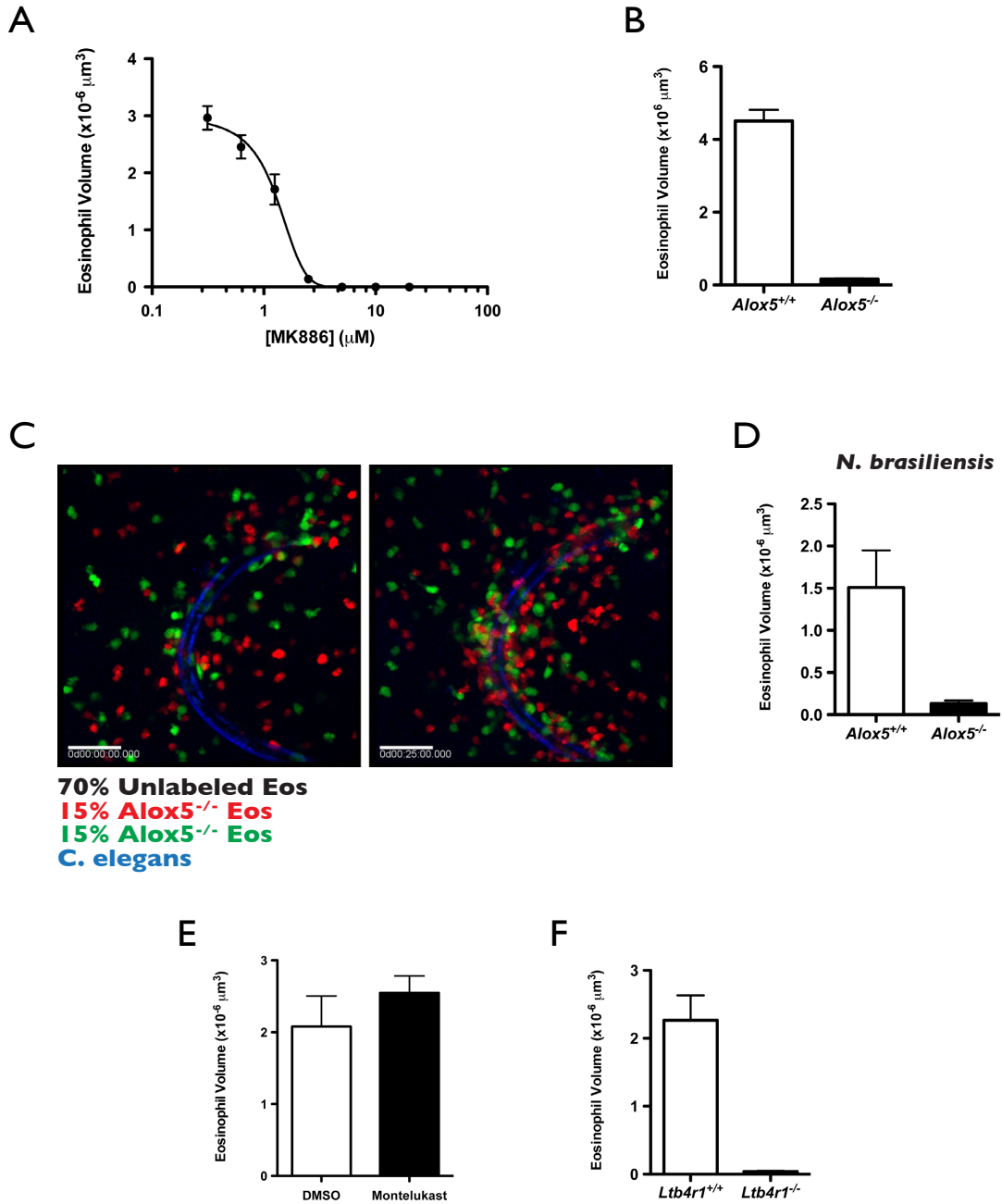


Figure 19. Involvement of leukotrienes in eosinophil migration towards nematodes (A) Eosinophil accumulation in response to *C. elegans* dauer larvae in the presence of MK886 at the indicated final concentrations. The  $IC_{50}$  for this experiment was  $\sim 0.5 \mu\text{M}$ . (B) Accumulation of wild type and *Alox5*<sup>-/-</sup> eosinophils in response to *C. elegans* dauer larvae. (C) Images taken from a fluorescent time-lapse movie of wild type (green) and *Alox5*<sup>-/-</sup> (red) eosinophils migrating toward a *C. elegans* dauer larva (blue). The worm is shown at 0 min (left) and after 25 min (right) of the culture. The abundant unlabeled wild type eosinophils are invisible. (D) Accumulation of wild type and *Alox5*<sup>-/-</sup> eosinophils in response to *N. brasiliensis* L3 larvae. All scale bars represent 50  $\mu\text{m}$ . (E) Eosinophil accumulation in response to *C. elegans* dauer larvae in the presence of 10  $\mu\text{M}$  Montelukast, a CysLTR1 antagonist. (F) Accumulation of wild type and *Ltb4r1*<sup>-/-</sup> eosinophils in response to *C. elegans* dauer larvae.

Figure 20

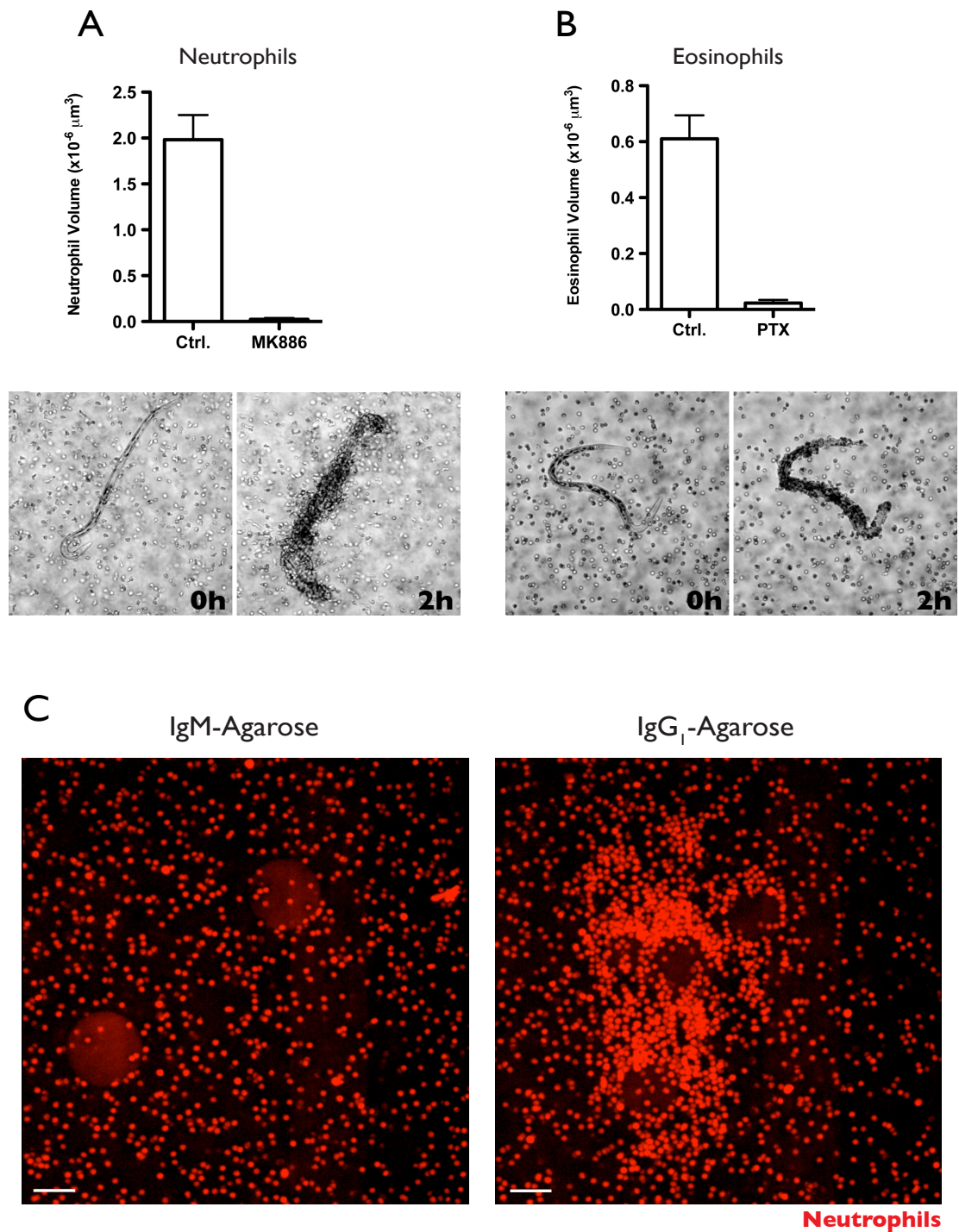


Figure 20. Human leukocyte migration toward nematodes  
(A) Human neutrophil accumulation in response to *C. elegans* dauer larvae in the presence of MK886. (B) Control and pertussis toxin-treated human eosinophil accumulation around *C. elegans* dauer larvae. (C) Images showing mouse neutrophil accumulation around IgG<sub>1</sub>-coated but not IgM-coated agarose beads after 2 hours. Beads are visible as faint red circles. Scale bar represents 50 μm.

# Figure 2I

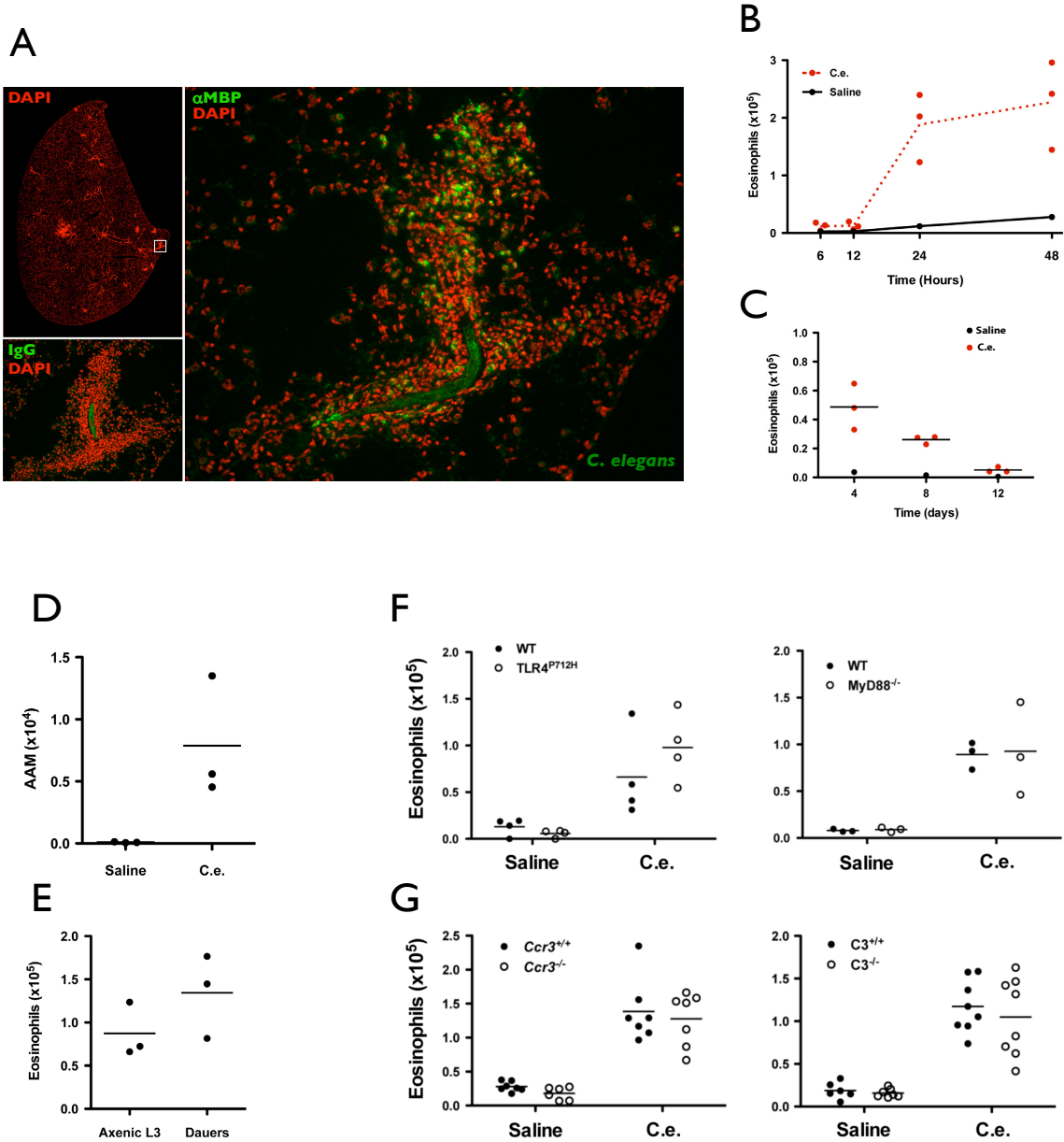


Figure 2I. Eosinophil accumulation in the lung in response to nematodes  
 (A) Micrographs of the entire left lung lobe (top, left) 24 hours after intravenous injection of 500 *C. elegans* dauer larvae. DAPI staining reveals multiple inflammatory foci. The high power view (right) of the boxed region shows a larva surrounded by inflammatory cells, including EMP<sup>+</sup> eosinophils. Non-specific fluorescence of the larva is demonstrated in the IgG control stain (left, bottom). (B,C) Flow cytometry analysis of eosinophil accumulation in the lung at various time points after injection of *C. elegans* dauer larvae or saline. (D) Flow cytometry analysis of alternatively activated macrophages in the lung 24 hours after injection of *C. elegans* dauer larvae or saline. (E) Flow cytometry analysis of eosinophils in the lung 24 hours after injection of axenic *C. elegans* L3 larvae or conventionally cultured dauer larvae. (F,G) Flow cytometry analysis of eosinophil accumulation in the lungs of *Tlr4<sup>P712H</sup>*, *Myd88<sup>-/-</sup>*, *Ccr3<sup>-/-</sup>*, and *C3<sup>-/-</sup>* mice after injection of *C. elegans* dauer larvae or saline. In all experiments, differences between saline and *C. elegans* groups are significant except 6 hours, 12 hours, and 12 days after injection. Differences between wild type and knock out or mutant mice are not significant.

Figure 22

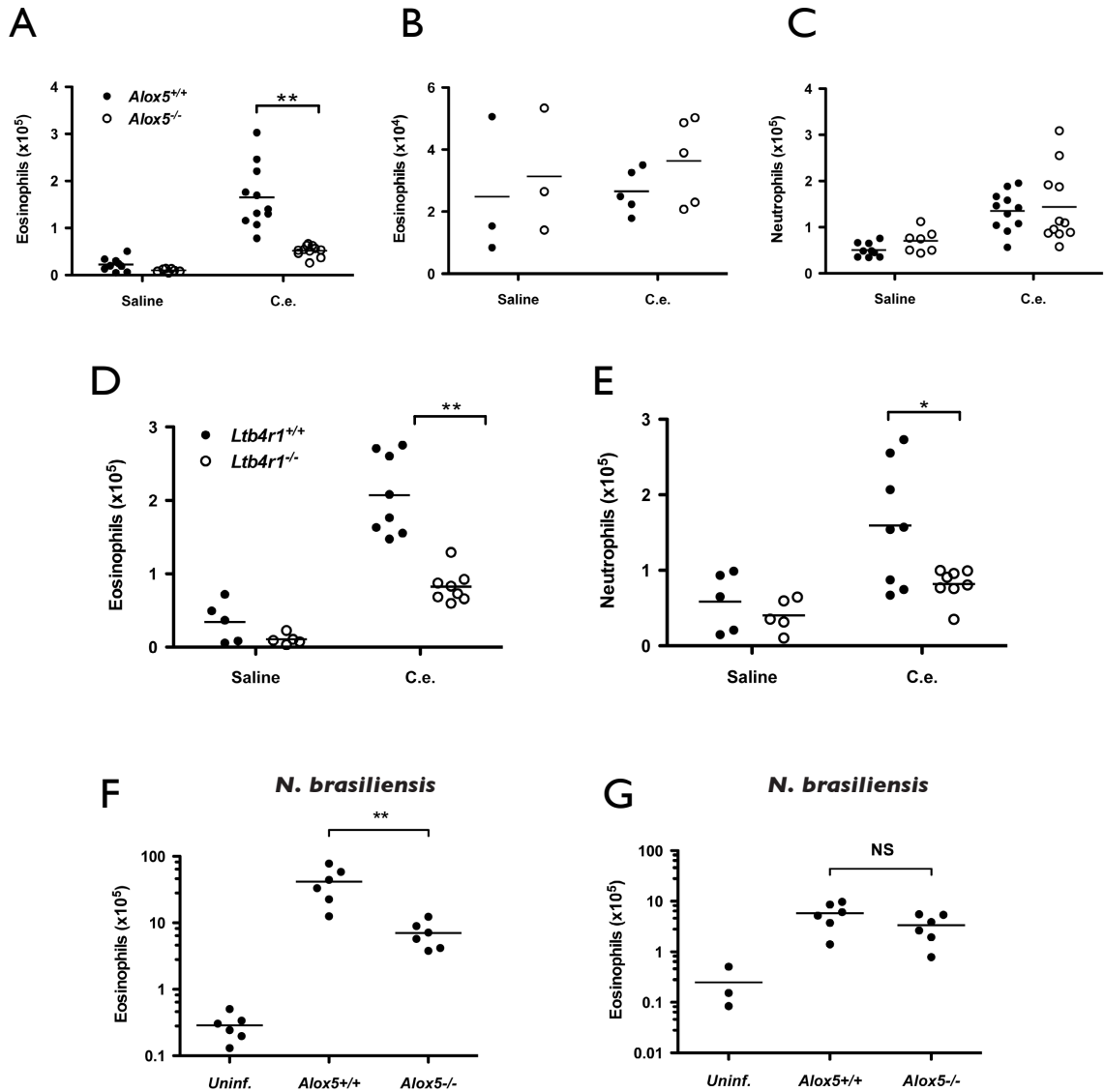


Figure 22. Involvement of leukotrienes in eosinophil accumulation in the lung

(A) Flow cytometry analysis of eosinophil accumulation in the lungs of *Alox5*<sup>-/-</sup> and wild-type mice 24 hours after injection of *C. elegans* dauer larvae or saline. (B) Flow cytometry analysis of eosinophil numbers in the blood of *Alox5*<sup>-/-</sup> and wild-type mice 24 hours after injection of *C. elegans* dauer larvae or saline. (C) Flow cytometry analysis of neutrophil accumulation in the lungs of *Alox5*<sup>-/-</sup> and wild-type mice 24 hours after injection of *C. elegans* dauer larvae or saline. (D) Flow cytometry analysis of eosinophil accumulation in the lungs of *Ltb4r1*<sup>-/-</sup> and wild-type mice 24 hours after injection of *C. elegans* dauer larvae or saline. (E) Flow cytometry analysis of neutrophil accumulation in the lungs of *Ltb4r1*<sup>-/-</sup> and wild-type mice 24 hours after injection of *C. elegans* dauer larvae or saline. (F) Flow cytometry analysis of eosinophil accumulation in the lungs of *Alox5*<sup>-/-</sup> and wild-type mice 9 days after infection *N. brasiliensis* L3 larvae. Numbers of eosinophils in uninfected mouse lung are shown for comparison, but are from a different experiment. (G) Flow cytometry analysis of eosinophil accumulation in the blood of *Alox5*<sup>-/-</sup> and wild-type mice 9 days after infection *N. brasiliensis* L3 larvae. Numbers of eosinophils in uninfected mouse blood are shown for comparison, but are from a different experiment (B). Differences between groups are not significant unless otherwise noted. Differences between saline and *C. elegans* groups are significant in wild type mice. \*, p < 0.05; \*\*, p < 0.005.

Figure 23

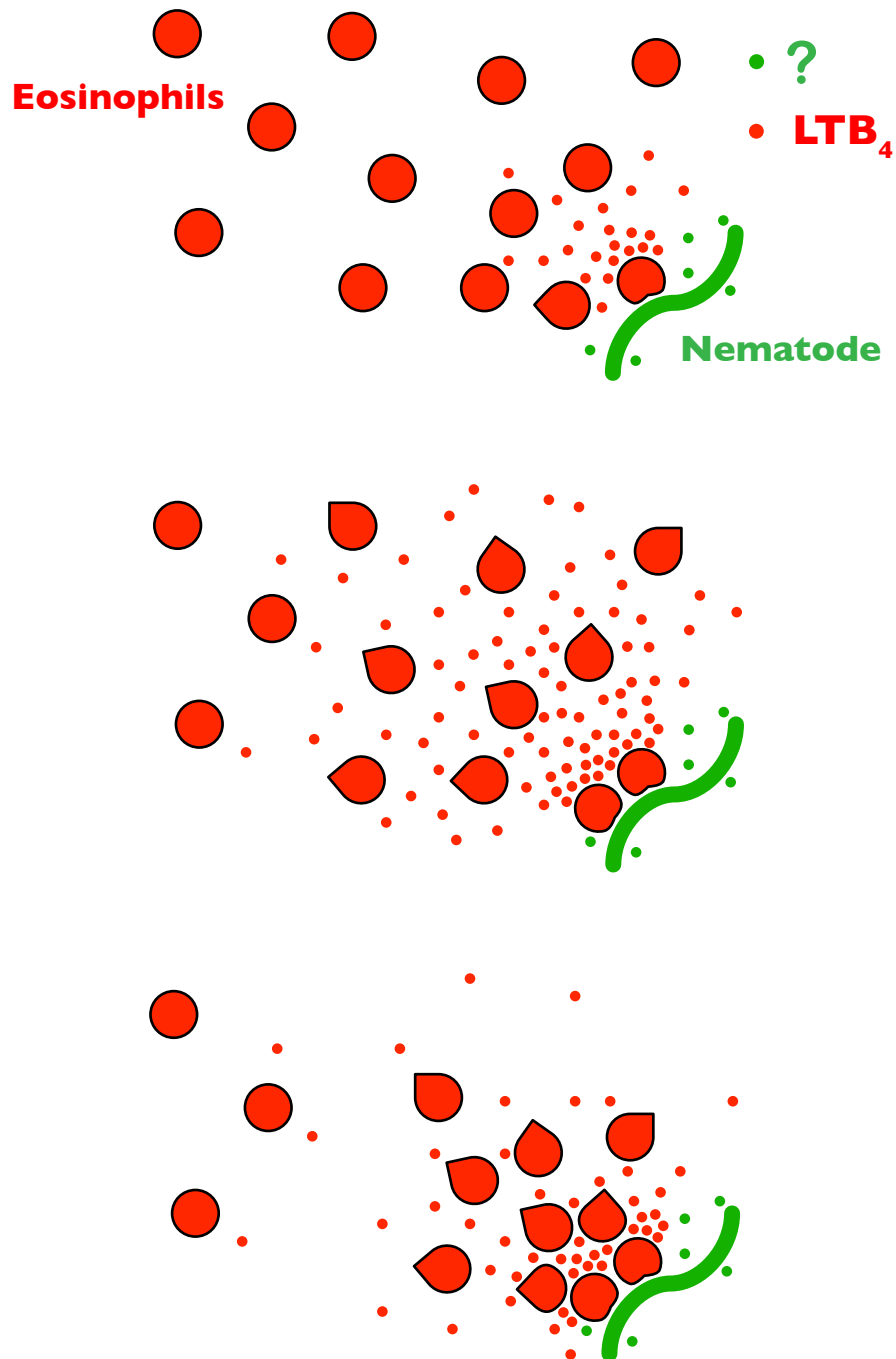


Figure 23. A model for leukotriene-driven migration in response to nematodes  
Chance interactions between eosinophils and nematodes, requiring contact or close proximity, are followed by eosinophil adhesion and spreading on the surface of the worm. Unknown worm-derived signals (green circles) activate eosinophils, resulting in the release of  $LTB_4$  (red circles) that attract neighboring eosinophils. As more eosinophils are drawn into contact or close proximity with the worm surface,  $LTB_4$  production accelerates and the worm is eventually encapsulated by eosinophils.

## DISCUSSION

Here we report that the migration of mouse eosinophils toward nematodes in a 3D matrix requires eosinophil-derived leukotrienes and LTB<sub>4</sub>R1. Although eosinophils have been shown to produce LTB<sub>4</sub>, this property differs across animal species, and human eosinophils produce considerably more cysLTs than LTB<sub>4</sub> when stimulated with calcium ionophores (Sun et al., 1991). Thus, while it is widely appreciated that eosinophils are a major source of cysLTs during inflammation, the possibility that they are a source of LTB<sub>4</sub> during helminth infection has not been investigated (Tager and Luster, 2003). Eosinophils migrate toward cysLTs *in vitro* in transwell assays (Spada et al., 1994). However, thus far there is no experimental support that cysLT receptors on eosinophils mediate chemotaxis *in vivo*, since mice deficient in cysLTs do not have defects in eosinophil recruitment to the skin in a model of atopic dermatitis (Oyoshi et al., 2012a). Instead, this study suggests that eosinophil-derived cysLTs contribute to tissue remodeling by stimulating fibroblasts to secrete collagen and by promoting keratinocyte proliferation. We have demonstrated the CysLTR1 antagonist, montelukast, failed to alter eosinophil migration towards worms, arguing against the involvement of cysLTs. Given the evidence that LTB<sub>4</sub> is sufficient to promote eosinophil and neutrophil recruitment in transwell assays (Spada et al., 1994; Tager et al., 2000), the simplest explanation for our results is that secretion of LTB<sub>4</sub> is responsible for amplification of eosinophil migration toward nematodes *in vitro* (see Fig 23 for a diagram of this model).

Neutrophils can stimulate the migration of neighboring neutrophils through a migration-dependent multi-signal relay, wherein the detection of the chemoattractant peptide fMLF induces leukotriene LTB<sub>4</sub> secretion (Afonso et al., 2012). Migration

towards LTB<sub>4</sub>, in turn, draws cells into regions of higher fMLF concentration, resulting in amplified LTB<sub>4</sub> production. This behavior is distinct from the single-signal relay that takes place in the slime mold *Dictyostelium discoideum* (McCann et al., 2012). In *D. discoideum* cells, detection of cAMP at the leading edge induces secretion of cAMP at the rear, such that the signal can be propagated for millimeters. Since this propagation is independent of the initiating stimulus, migration toward the source is not required. Although we have not directly addressed whether signal relay takes place in granulocytes in response to nematodes, we favor a model that is distinct from previous models, for the following reasons.

First, the recruitment range of the migration we observed is far shorter (~300 μm) than that observed for *D. discoideum* cells, suggesting that single-signal relay is not operating efficiently, if it occurs at all in this setting. Second, even leukocytes that are very close to worms fail to migrate in the absence of leukotrienes. This suggests that the factor that initiates leukotriene synthesis is not chemotactic, in contrast to fMLF (Afonso et al., 2012). Third, we observed that mass migration dissipates when nematodes abruptly crawl away from the focus of leukocyte accumulation. This suggests that the presence of the nematode is required, not just to initiate the response, but also to sustain the generation of leukotrienes by leukocytes. If the factors that initiate leukotriene synthesis were secreted, they must be extremely short lived to be consistent with these observations. Lastly, we observed leukocyte spreading on the nematode surface, which resulted in adhesion sufficient to allow crawling worms to carry attached leukocytes for hundreds of micrometers. Future studies could be aimed at testing medium that is conditioned by parasitic worms to look for evidence of secreted factors that can induce

leukotriene secretion. An alternative possibility consistent with our findings is that an adhesive interaction triggers LTB<sub>4</sub> synthesis and secretion by the adherent eosinophils. If contact is required, the implications are intriguing. The surface area of a worm is necessarily proportional to its size, whereas secreted factors could vary with respect to a number of parameters. Thus, surface-dependent activation of eosinophils could represent a means for ensuring that enough leukocytes are recruited to encapsulate the entire worm, and for suspending additional leukocyte recruitment only once this is achieved.

Additionally, given the rapid speed of worm migration (~500 μm/sec) relative to leukocyte migration (~10 μm/min), a contact dependent signal would be the most reliable reporter of the worm's immediate presence. Conclusive evidence for either contact-dependent or proximity-dependent initiation awaits identification of the factor that is recognized by leukocytes.

One aspect that differentiates our studies of granulocyte-nematode interactions from those carried out previously is the use of 3D Matrigel and collagen gels. Although we observed adhesion and spreading of eosinophils on nematode surfaces in agarose gels, we did not observe mass migration in this matrix. While it is true that optimal stiffness of the 3D matrix was critical for leukocyte migration, no concentration of agarose (over a range from 20 to 100%) was successful. This may reflect differences in the ability adhesion receptors on eosinophils to bind to these substrates. Consistent with this interpretation, eosinophils derived from bone marrow from β2 integrin-deficient mice failed to migrate towards worms in Matrigel. Alternatively, it is possible that the properties of Matrigel and collagen stabilize an LTB<sub>4</sub> gradient to promote optimal migration. Such a gradient could potentially be detected by staining with an antibody against LTB<sub>4</sub>. There could also



be additional factors present in these matrices that contribute to eosinophil activation, or factors in agarose that interfere with worm recognition. This issue will need to be addressed using pure preparations of other extracellular matrices.

Our data highlight the ability of both eosinophils and neutrophils to produce and respond to LTB<sub>4</sub>. This raises questions about the mechanisms that account for their apparent autonomy in response to different stimuli. Eosinophils are rare during most bacterial infections where neutrophils are abundant (Makepeace et al., 2012). Conversely, huge numbers of eosinophils are present during later stages of parasite infection and allergic responses, while neutrophils are scarce. Furthermore, we found that leukotrienes were dispensable for the 2-fold increase in neutrophils that occurs after injection of *C. elegans*. It is likely that cell survival represents an important control point for modulating the numbers of these granulocytes in tissues, since separate cytokines appear to promote these lineages (IL5 for eosinophils, G-CSF for neutrophils) (Borregaard, 2010). It is also possible that cell-type specific recruitment factors operate in situations where one cell type is dominant. Both eosinophils and neutrophils accumulate during the early stages of some fungal infections, and many helminth infections (Makepeace et al., 2012). Thus, these granulocytes may have complementary functions of during acute inflammation that make common recruitment factors advantageous.

Our experiments in the lung have not directly demonstrated that there is impaired migration in the absence of leukotrienes. The effects of leukotrienes on survival or activation of leukocytes, rather than migration, could be contributing to eosinophil accumulation. There do not appear to be systemic effects on eosinophils, since normal numbers of eosinophils are present in blood from *Alox5<sup>-/-</sup>* mice. However, it is possible

that leukotrienes promote eosinophil survival in peripheral tissues. Antigen specific T cells were shown to traffic to the skin in a leukotriene-dependent fashion during atopic dermatitis (Oyoshi et al., 2012b). Thus, Th2 cells expressing IL-5 could be defective in trafficking to the lung in the absence of leukotrienes. It will be important to measure T cell recruitment and IL-5 production in *Alox5<sup>-/-</sup>* mice during *N. brasiliensis* infection. Experiments using two-photon microscopy are in progress to test whether leukotrienes affect recruitment out of the blood or localization within lung tissue in response to worms.

We show that leukotrienes are important for eosinophil accumulation in the lung in response to nematodes, but the cellular source of these mediators remains to be identified. Macrophages isolated from mouse lung release LTB<sub>4</sub> and attract eosinophils across transwell membranes in a leukotriene-dependent fashion (Reese et al., 2007). In addition, we have shown that neutrophils produce leukotrienes in response to nematodes *in vitro*. Nevertheless, based on our experiments *in vitro*, we favor the hypothesis that eosinophils encountering nematodes in the lung secrete LTB<sub>4</sub> in sufficient quantities to attract other eosinophils to the site of accumulation (Fig 6). There are currently no reported conditional alleles of *Alox5* that would allow for cell-type specific deletion of this gene. Furthermore, there are no reported eosinophil-specific recombinase alleles, for manipulating genes in eosinophils only. In order to determine whether eosinophil-derived leukotrienes contribute to eosinophil accumulation in the lung in response to worms, we are performing experiments with chimeric mice. These mice have been lethally irradiated and reconstituted with bone-marrow that will give rise to only wild type eosinophils or only *Alox5<sup>-/-</sup>* eosinophils, whereas wild type representatives of other leukocytes will be

present. Eosinophil accumulation will then be measured in these mice after injection with *C. elegans* or infection with *N. brasiliensis*. An important caveat to this approach is that half of all other leukocyte populations in both sets of mice are deficient in leukotrienes as well. Nonetheless, these mice provide a tool to address the contributions of eosinophil *Alox5* to their recruitment to lung. Additionally, wild type and *Alox5*<sup>-/-</sup> eosinophils will be transferred into *Alox5*<sup>-/-</sup> recipients to determine whether eosinophil-derived leukotrienes are sufficient to induce eosinophil recruitment.

This study establishes that eosinophils respond to diverse nematode species, which may indicate the recognition of conserved features of nematodes. Eosinophils also migrated towards Sephadex beads, which suggests that there are carbohydrate-binding receptors on these cells that can also induce leukotriene production. Sign-R1, Sign-R3, and Langerin are candidates for the recognition of Sephadex, since they have all been shown to mediate uptake of FITC-dextran (Takahara et al., 2004). Glycans differ significantly between nematodes and mammals (Paschinger et al., 2008), thus glycans could represent a molecular target for identification of foreign animal tissues by the immune system. Furthermore, the interactions between the *C. elegans* cuticle and several species of bacteria are highly dependent on nematode glycosylation. Our *in vitro* assay is amenable to genetic screens in *C. elegans*, aimed at characterizing the genes in nematodes required for triggering eosinophil accumulation. Since collagenase digestion effectively releases individual eosinophil-coated worms from the 3D matrix, large numbers of worms can be simultaneously screened in the same gel volume. Uncoated (mutant) worms can then be isolated by differential centrifugation, and retested before being expanded and frozen. When coupled with the ability of *C. elegans* to induce

immune responses in mice, this model provides a powerful methodology for generating and testing candidate nematode factors that could contribute to eosinophil accumulation in the lung.

## **MATERIALS AND METHODS**

### **Mice**

YARG(*Arg1*<sup>YFP</sup>) (Reese et al., 2007), *Tlr4*<sup>P712H</sup> (Dumont and Barrois, 1976), *Myd88*<sup>-/-</sup> (Adachi et al., 1998), *Ccr3*<sup>-/-</sup> (Humbles et al., 2002), *C3*<sup>-/-</sup> (Wessels et al., 1995), *Alox5*<sup>-/-</sup> (Chen et al., 1994), *Ltb4r1*<sup>-/-</sup> (Tager et al., 2000), and *Il5*<sup>Tg</sup> (Lee et al., 1997) mice have been described previously. All strains were used on the C57BL/6J background except *Ccr3*<sup>-/-</sup>, which was maintained on the BALB/c background. Wild type C57BL/6J and BALB/cJ mice were obtained from the Jackson Laboratory. All procedures involving animals were approved by the University California San Francisco Institutional Animal Care and Use Committee, and carried out in accordance with the guidelines established by the National Institutes of Health.

### **Nematodes**

*C. elegans* carrying the *daf-2(e1370)*, *rmIs126[unc-54p::Q0::YFP]* alleles were obtained from the CGC, and crossed to generate a *daf-2(e1370); rmIs126[unc-54p::Q0::YFP]* strain. *C. elegans* dauer larvae were generated by culturing synchronized L1 *daf-2(e1370)* mutants at 27° C for 4 days in sealed petri dishes, then collecting larvae from the sides and lids of the dishes. Dauer larvae were > 99% pure based on body morphology and an absence of pharyngeal pumping (Golden and Riddle, 1984). For axenic culture, mCeHR

medium was prepared as described previously (Rao et al., 2005). Axenic cultures were routinely tested for sterility by culture on brain heart infusion agar plates (BD Bioscience) at 30° C and 37° C. Additionally, LPS was not detectable by *Limulus* amoebocyte lysate testing (Pyrotell) in axenic cultures or in supernatants of *C. elegans* dauer larvae after washing (as described below). *H. bacteriophora* infective juveniles were generated from RET16 *Photobacterium luminescens* cultures, as described previously (Hallem et al., 2007). *N. brasiliensis* infection was performed as described previously (Camberis et al., 2003). Briefly, mice were anesthetized using isoflurane and injected subcutaneously at the base of the tail with 500 *N. brasiliensis* L3 larvae. Mice were maintained on water containing 2 g/L neomycin sulfate, 100 mg/L polymixin B for 5 days, and sacrificed after 9 days. For administration of *C. elegans*, 500 live dauer larvae were injected into the caudal tail vein in 150 µL 0.01% BSA in saline.

### **Three-Dimensional culture of leukocytes and nematodes**

Nematodes were washed by six rounds of suspension in 1.5 mL wash buffer (0.01% BSA in 0.9% NaCl), 5 seconds centrifugation at ~1000 x g, and aspiration of supernatant. Nematodes were suspended at a concentration of 600/mL in Matrigel w/o phenol red (BD Biosciences) or 1 mg/mL collagen (Invitrogen) and kept on ice. Eosinophils were cultured from bone marrow of wild type, *Alox5<sup>-/-</sup>*, or *Ltb4r1<sup>-/-</sup>* mice and incubated in 1 µM CMTMR or CFSE in RPMI containing 2% FBS for 25 min at 37° C. Cells were washed and some samples were treated with 250 ng/mL *B. pertussis* toxin for 1 hour, then washed with RPMI-1640. Other samples were treated with various concentrations of MK886 for 10 minutes before being mixed with worms without washing. Eosinophils

were bone marrow cultures, as described previously (Dyer et al., 2008). Briefly, bone marrow from femurs and tibiae from two mice per group were flushed with RPMI and treated with water to lyse erythrocytes. Cells were then cultured in the presence of recombinant SCF and Flt3L for 4 days, and subsequently cultured in the presence of recombinant IL-5 and collected after 10 additional days. Eosinophils were washed and resuspended at various cell densities in 0.1% BSA in RPMI-1640 (RPMI) w/o phenol red. Eosinophils and nematodes were mixed in 1:1 ratio, and loaded into 6-lane or 18-well chamber imaging slides (Ibidi), and cultured at 37° C.

#### **Time-lapse imaging and quantification of leukocyte migration**

All images were acquired using a microscope setup that has been described previously (Gilden et al., 2012). Briefly, three lasers (Argon 488 nm, Krypton 568 nm, Indium gallium nitride 406 nm) were connected to a spinning disk confocal scan-head (CSU-10b, Yokogawa Corporation, Kanazawa, Japan; modified by Solamere Technology Group, Salt Lake City, UT), which was connected directly to a motorized, inverted microscope (Zeiss Axiovert 200M inverted fluorescence microscope, Carl Zeiss Inc., Thornwood, NJ). Emission light was passed through an automated filter wheel (FW-1000, Applied Scientific Instruments, Eugene, OR) and detected by an intensified charge-coupled device (ICCD) camera (XR-Mega-10EX S-30, Stanford Photonics, Palo Alto, CA). Images were collected through a 10x fluor 0,5 NA and 20x fluor air objectives. For time-lapse imaging, cultures were maintained at 37° C on a heated stage and imaged starting roughly thirty minutes after the start of the culture. For endpoint leukocyte accumulation assays, we acquired image volumes for all nematodes within 100 µm from the bottom of the

imaging slide from three wells (4-7 worms per well) per condition. Images were analyzed using Imaris (BitPlane) software. Volumes representing the accumulated leukocytes were generated in parallel by applying a single, manually set intensity and volume threshold to all worms from all wells. Accumulations of cells that were not in contact with the surface of the worm were rare and not included in the volume measurement.

### **Flow cytometry assays for leukocyte recruitment**

Mice were sacrificed and all right lobes of lungs were collected. Lungs were injected with digestion buffer consisting of 0.2 mU/mL Liberase DL (Roche Applied Sciences) and 10 µg/mL DNase (Sigma) in HBSS (without Ca<sup>2+</sup>/Mg<sup>2+</sup>). Lungs were minced using razor blades and incubated with digestion buffer for 25 min at 37° C. Digestion was stopped by adding EDTA to 10 mM and 2% FBS in RPMI, and tissue was crushed onto 70 µm cell strainers (BD Biosciences). Cells were treated with ammonium chloride buffer (150 mM NH<sub>4</sub>Cl, 10 mM KHCO<sub>3</sub>, 100 µM EDTA) to lyse erythrocytes. Cells were incubated with 10 µg/mL anti-mouse CD16/32 (clone 93, eBioscience) to block Fc receptors, before staining with PE anti-Siglec-F (E50, BD Pharmingen) and APC anti-Ly-6G (1A8, Biolegend). Viability was determined by adding 50 µL/mL 7AAD solution (BD Pharmingen) or 0.5 µg/mL DAPI. Cells were analyzed using a FACSsort cytometer (BD) equipped with CellQuest software (BD). Further analysis was carried out using FlowJo software (Treestar Inc.).

### **Statistical analysis**

All graphical data were plotted as means plus the standard error mean using Prism 5 software (GraphPad Software, La Jolla, CA). Student's *t*-test was used to evaluate the statistical significance of differences between groups.

### **Acknowledgments**

We thank C. Darby for helpful discussion, M.F. Krummel for helpful discussions and access to imaging equipment, J.J. Lee for IL-5 transgenic mice, C. Kenyon for *E. coli* expressing *him-5* and *daf-12* RNAi, T.A. Ciche for *H. bacteriophora*, and I. Hamza for initial stocks of axenic *C. elegans*.



## CONCLUSION

The studies outlined in this dissertation have established that the galactose-6-*O*-sulfotransferase, KSGal6ST is expressed in several interesting anatomical locations in mice, including the brain, kidney glomeruli, lung, and germinal centers in lymph nodes and Peyer's patches. My characterization of the KSGal6ST KO mouse provides a tool for investigating the functions of this enzyme at these sites. I have also demonstrated that KSGal6ST is expressed in HEVs, where it is required for the generation of several Gal6S-containing glycans. These glycans do not contribute to short-term L-selectin-dependent homing to lymph nodes. However, it remains to be investigated whether they serve as ligands for L-selectin in lymphoid organs during immune responses, or in tertiary lymphoid structures that develop at sites of chronic inflammation.

I have also characterized the expression pattern of ligands for Siglec-F. In leukocytes, these ligands are largely restricted to the cell types that express Siglec-F, suggesting that they carry out important functions as cis-ligands. These ligands may also participate in interactions between these cell types as trans-ligands. Siglec-F ligands are present in airway epithelial cells and in mucin-containing fractions of BAL fluid. Since mucins are highly sialylated glycoproteins, it is possible that they are recognized by Siglec-F-expressing leukocytes that enter the airways during lung inflammation. The outcome of Siglec-F signaling upon recognition of leukocyte or mucin ligands represents an attractive area for future studies. None of the Siglec-F ligands I describe are dependent on the two known galactose-6-*O*-sulfotransferases KSGal6ST and C6ST-1. Additionally, eosinophils express very few sulfated O-glycans, with the predominant structures containing sulfo-sialic acids, which are not likely to constitute Siglec ligands. However,

the restricted expression pattern of Siglec-F ligands raises the possibility that a unique sialylated glycan structure exists on these cell types. The identification of such a structure awaits further research.

Lastly, I have uncovered a novel mechanism of eosinophil accumulation in response to nematodes. Recognition of a factor that appears to be conserved across nematode species results in leukotriene B<sub>4</sub> production by eosinophils and neutrophils. The release of this lipid mediator causes rapid migration of surrounding leukocytes, which accumulate on the surface of the worm. This may represent a strategy for encapsulating invading parasitic organisms. The selection of *C. elegans* as a model nematode parasite has facilitated biological imaging and allowed me to separate out the effects of bacteria- and nematode-derived factors on leukocyte behavior. This system also opens the door to genetic dissection of the immunogenic properties of nematodes.

## REFERENCES

- Adachi, O., Kawai, T., Takeda, K., Matsumoto, M., Tsutsui, H., Sakagami, M., Nakanishi, K., and Akira, S. (1998). Targeted disruption of the MyD88 gene results in loss of IL-1- and IL-18-mediated function. *Immunity* 9, 143-150.
- Afonso, P.V., Janka-Junttila, M., Lee, Y.J., McCann, C.P., Oliver, C.M., Aamer, K.A., Losert, W., Cicerone, M.T., and Parent, C.A. (2012). LTB4 is a signal-relay molecule during neutrophil chemotaxis. *Developmental cell* 22, 1079-1091.
- Akama, T.O., Nishida, K., Nakayama, J., Watanabe, H., Ozaki, K., Nakamura, T., Dota, A., Kawasaki, S., Inoue, Y., Maeda, N., *et al.* (2000). Macular corneal dystrophy type I and type II are caused by distinct mutations in a new sulphotransferase gene. *Nature genetics* 26, 237-241.
- Allen, J.E., and Maizels, R.M. (2011). Diversity and dialogue in immunity to helminths. *Nature reviews* 11, 375-388.
- Angata, T., Hingorani, R., Varki, N.M., and Varki, A. (2001). Cloning and characterization of a novel mouse Siglec, mSiglec-F: differential evolution of the mouse and human (CD33) Siglec-3-related gene clusters. *The Journal of biological chemistry* 276, 45128-45136.
- Arata-Kawai, H., Singer, M.S., Bistrup, A., Zante, A., Wang, Y.Q., Ito, Y., Bao, X., Hemmerich, S., Fukuda, M., and Rosen, S.D. (2011). Functional contributions of N- and O-glycans to L-selectin ligands in murine and human lymphoid organs. *The American journal of pathology* 178, 423-433.
- Arbones, M.L., Ord, D.C., Ley, K., Ratech, H., Maynard-Curry, C., Otten, G., Capon, D.J., and Tedder, T.F. (1994). Lymphocyte homing and leukocyte rolling and migration are impaired in L-selectin-deficient mice. *Immunity* 1, 247-260.
- Avril, T., Floyd, H., Lopez, F., Vivier, E., and Crocker, P.R. (2004). The membrane-proximal immunoreceptor tyrosine-based inhibitory motif is critical for the inhibitory signaling mediated by Siglecs-7 and -9, CD33-related Siglecs expressed on human monocytes and NK cells. *J Immunol* 173, 6841-6849.
- Baenziger, J.U. (2003). Glycoprotein hormone GalNAc-4-sulphotransferase. *Biochemical Society transactions* 31, 326-330.

- Bajenoff, M., Egen, J.G., Koo, L.Y., Laugier, J.P., Brau, F., Glaichenhaus, N., and Germain, R.N. (2006). Stromal cell networks regulate lymphocyte entry, migration, and territoriality in lymph nodes. *Immunity* 25, 989-1001.
- Barretto, N., Hallak, L.K., and Peebles, M.E. (2003). Neuraminidase treatment of respiratory syncytial virus-infected cells or virions, but not target cells, enhances cell-cell fusion and infection. *Virology* 313, 33-43.
- Belisle, J.A., Horibata, S., Jennifer, G.A., Petrie, S., Kapur, A., Andre, S., Gabius, H.J., Rancourt, C., Connor, J., Paulson, J.C., *et al.* (2010). Identification of Siglec-9 as the receptor for MUC16 on human NK cells, B cells, and monocytes. *Molecular cancer* 9, 118.
- Bell, R.L., Young, P.R., Albert, D., Lanni, C., Summers, J.B., Brooks, D.W., Rubin, P., and Carter, G.W. (1992). The discovery and development of zileuton: an orally active 5-lipoxygenase inhibitor. *International journal of immunopharmacology* 14, 505-510.
- Bertozzi, C.R., Fukuda, S., and Rosen, S.D. (1995). Sulfated disaccharide inhibitors of L-selectin: deriving structural leads from a physiological selectin ligand. *Biochemistry* 34, 14271-14278.
- Bhattacharya, J., and Matthay, M.A. (2013). Regulation and repair of the alveolar-capillary barrier in acute lung injury. *Annual review of physiology* 75, 593-615.
- Bhavanandan, V.P., and Meyer, K. (1967). Studies on keratosulfates. Methylation and partial acid hydrolysis of bovine corneal keratosulfate. *The Journal of biological chemistry* 242, 4352-4359.
- Bishop, J.R., Schuksz, M., and Esko, J.D. (2007). Heparan sulphate proteoglycans fine-tune mammalian physiology. *Nature* 446, 1030-1037.
- Bistrup, A., Bhakta, S., Lee, J.K., Belov, Y.Y., Gunn, M.D., Zuo, F.R., Huang, C.C., Kannagi, R., Rosen, S.D., and Hemmerich, S. (1999). Sulfotransferases of two specificities function in the reconstitution of high endothelial cell ligands for L-selectin. *The Journal of cell biology* 145, 899-910.
- Blasius, A.L., Cella, M., Maldonado, J., Takai, T., and Colonna, M. (2006). Siglec-H is an IPC-specific receptor that modulates type I IFN secretion through DAP12. *Blood* 107, 2474-2476.
- Blixt, O., Head, S., Mondala, T., Scanlan, C., Huflejt, M.E., Alvarez, R., Bryan, M.C., Fazio, F., Calarese, D., Stevens, J., *et al.* (2004). Printed covalent glycan array for ligand profiling of diverse glycan

- binding proteins. *Proceedings of the National Academy of Sciences of the United States of America* *101*, 17033-17038.
- Bochner, B.S. (2009). Siglec-8 on human eosinophils and mast cells, and Siglec-F on murine eosinophils, are functionally related inhibitory receptors. *Clin Exp Allergy* *39*, 317-324.
- Bochner, B.S., Alvarez, R.A., Mehta, P., Bovin, N.V., Blixt, O., White, J.R., and Schnaar, R.L. (2005). Glycan array screening reveals a candidate ligand for Siglec-8. *The Journal of biological chemistry* *280*, 4307-4312.
- Borghesi, A., Ouyang, Y.B., Westmuckett, A.D., Marcello, M.R., Landel, C.P., Evans, J.P., and Moore, K.L. (2006). Targeted disruption of tyrosylprotein sulfotransferase-2, an enzyme that catalyzes post-translational protein tyrosine O-sulfation, causes male infertility. *The Journal of biological chemistry* *281*, 9423-9431.
- Borregaard, N. (2010). Neutrophils, from marrow to microbes. *Immunity* *33*, 657-670.
- Broughton, S.E., Dhagat, U., Hercus, T.R., Nero, T.L., Grimbaldeston, M.A., Bonder, C.S., Lopez, A.F., and Parker, M.W. (2012). The GM-CSF/IL-3/IL-5 cytokine receptor family: from ligand recognition to initiation of signaling. *Immunological reviews* *250*, 277-302.
- Bruehl, R.E., Bertozzi, C.R., and Rosen, S.D. (2000). Minimal sulfated carbohydrates for recognition by L-selectin and the MECA-79 antibody. *The Journal of biological chemistry* *275*, 32642-32648.
- Bulai, T., Bratosin, D., Pons, A., Montreuil, J., and Zanetta, J.P. (2003). Diversity of the human erythrocyte membrane sialic acids in relation with blood groups. *FEBS letters* *534*, 185-189.
- Bulow, H.E., and Hobert, O. (2006). The molecular diversity of glycosaminoglycans shapes animal development. *Annu Rev Cell Dev Biol* *22*, 375-407.
- Butcher, E.C., and Picker, L.J. (1996). Lymphocyte homing and homeostasis. *Science (New York, NY)* *272*, 60-66.
- Butterworth, A.E., Sturrock, R.F., Houba, V., Mahmoud, A.A., Sher, A., and Rees, P.H. (1975). Eosinophils as mediators of antibody-dependent damage to schistosomula. *Nature* *256*, 727-729.
- Butterworth, A.E., Wassom, D.L., Gleich, G.J., Loegering, D.A., and David, J.R. (1979). Damage to schistosomula of *Schistosoma mansoni* induced directly by eosinophil major basic protein. *J Immunol* *122*, 221-229.

- Camberis, M., Le Gros, G., and Urban, J., Jr. (2003). Animal model of *Nippostrongylus brasiliensis* and *Heligmosomoides polygyrus*. *Current protocols in immunology* / edited by John E Coligan [et al] *Chapter 19*, Unit 19 12.
- Campanero-Rhodes, M.A., Childs, R.A., Kiso, M., Komba, S., Le Narvor, C., Warren, J., Otto, D., Crocker, P.R., and Feizi, T. (2006). Carbohydrate microarrays reveal sulphation as a modulator of siglec binding. *Biochem Biophys Res Commun* *344*, 1141-1146.
- Carlin, A.F., Uchiyama, S., Chang, Y.C., Lewis, A.L., Nizet, V., and Varki, A. (2009). Molecular mimicry of host sialylated glycans allows a bacterial pathogen to engage neutrophil Siglec-9 and dampen the innate immune response. *Blood* *113*, 3333-3336.
- Carvalho, E.M., Bastos, L.S., and Araujo, M.I. (2006). Worms and allergy. *Parasite immunology* *28*, 525-534.
- Chen, G.Y., Tang, J., Zheng, P., and Liu, Y. (2009). CD24 and Siglec-10 selectively repress tissue damage-induced immune responses. *Science (New York, NY)* *323*, 1722-1725.
- Chen, M., Lam, B.K., Kanaoka, Y., Nigrovic, P.A., Audoly, L.P., Austen, K.F., and Lee, D.M. (2006). Neutrophil-derived leukotriene B4 is required for inflammatory arthritis. *The Journal of experimental medicine* *203*, 837-842.
- Chen, W., Han, C., Xie, B., Hu, X., Yu, Q., Shi, L., Wang, Q., Li, D., Wang, J., Zheng, P., *et al.* (2013). Induction of Siglec-G by RNA Viruses Inhibits the Innate Immune Response by Promoting RIG-I Degradation. *Cell* *152*, 467-478.
- Chen, X.S., Sheller, J.R., Johnson, E.N., and Funk, C.D. (1994). Role of leukotrienes revealed by targeted disruption of the 5-lipoxygenase gene. *Nature* *372*, 179-182.
- Cho, J.Y., Song, D.J., Pham, A., Rosenthal, P., Miller, M., Dayan, S., Doherty, T.A., Varki, A., and Broide, D.H. (2010). Chronic OVA allergen challenged Siglec-F deficient mice have increased mucus, remodeling, and epithelial Siglec-F ligands which are up-regulated by IL-4 and IL-13. *Respiratory research* *11*, 154.
- Chtanova, T., Schaeffer, M., Han, S.J., van Dooren, G.G., Nollmann, M., Herzmark, P., Chan, S.W., Satija, H., Camfield, K., Aaron, H., *et al.* (2008). Dynamics of neutrophil migration in lymph nodes during infection. *Immunity* *29*, 487-496.

- Chu, V.T., Frohlich, A., Steinhauser, G., Scheel, T., Roch, T., Fillatreau, S., Lee, J.J., Lohning, M., and Berek, C. (2011). Eosinophils are required for the maintenance of plasma cells in the bone marrow. *Nature immunology* *12*, 151-159.
- Coffman, R.L., Seymour, B.W., Hudak, S., Jackson, J., and Rennick, D. (1989). Antibody to interleukin-5 inhibits helminth-induced eosinophilia in mice. *Science (New York, NY)* *245*, 308-310.
- Cohen, M., and Varki, A. (2010). The sialome--far more than the sum of its parts. *Omics* *14*, 455-464.
- Collins, B.E., Blixt, O., DeSieno, A.R., Bovin, N., Marth, J.D., and Paulson, J.C. (2004). Masking of CD22 by cis ligands does not prevent redistribution of CD22 to sites of cell contact. *Proceedings of the National Academy of Sciences of the United States of America* *101*, 6104-6109.
- Condliffe, A.M., Kitchen, E., and Chilvers, E.R. (1998). Neutrophil priming: pathophysiological consequences and underlying mechanisms. *Clin Sci (Lond)* *94*, 461-471.
- Corfield, A.P., Wagner, S.A., Clamp, J.R., Kriaris, M.S., and Hoskins, L.C. (1992). Mucin degradation in the human colon: production of sialidase, sialate O-acetyltransferase, N-acetylneuraminidase, arylesterase, and glycosulfatase activities by strains of fecal bacteria. *Infection and immunity* *60*, 3971-3978.
- Courtney, A.H., Puffer, E.B., Pontrello, J.K., Yang, Z.Q., and Kiessling, L.L. (2009). Sialylated multivalent antigens engage CD22 in trans and inhibit B cell activation. *Proceedings of the National Academy of Sciences of the United States of America* *106*, 2500-2505.
- Crocker, P.R., Paulson, J.C., and Varki, A. (2007). Siglecs and their roles in the immune system. *Nat Rev Immunol* *7*, 255-266.
- Cummings, R.D. (2009). The repertoire of glycan determinants in the human glycome. *Molecular bioSystems* *5*, 1087-1104.
- Cyster, J.G. (2003). Lymphoid organ development and cell migration. *Immunological reviews* *195*, 5-14.
- Daeron, M., Jaeger, S., Du Pasquier, L., and Vivier, E. (2008). Immunoreceptor tyrosine-based inhibition motifs: a quest in the past and future. *Immunological reviews* *224*, 11-43.
- Daneman, R. (2012). The blood-brain barrier in health and disease. *Annals of neurology* *72*, 648-672.

- David, J.R., Butterworth, A.E., and Vadas, M.A. (1980). Mechanism of the interaction mediating killing of *Schistosoma mansoni* by human eosinophils. *The American journal of tropical medicine and hygiene* 29, 842-848.
- Dean, D.A., Wistar, R., and Murrell, K.D. (1974). Combined in vitro effects of rat antibody and neutrophilic leukocytes on schistosomula of *Schistosoma mansoni*. *The American journal of tropical medicine and hygiene* 23, 420-428.
- Dekan, G., Gabel, C., and Farquhar, M.G. (1991). Sulfate contributes to the negative charge of podocalyxin, the major sialoglycoprotein of the glomerular filtration slits. *Proceedings of the National Academy of Sciences of the United States of America* 88, 5398-5402.
- Denzler, K.L., Farmer, S.C., Crosby, J.R., Borchers, M., Cieslewicz, G., Larson, K.A., Cormier-Regard, S., Lee, N.A., and Lee, J.J. (2000). Eosinophil major basic protein-1 does not contribute to allergen-induced airway pathologies in mouse models of asthma. *J Immunol* 165, 5509-5517.
- Dixon, H., Blanchard, C., Deschoolmeester, M.L., Yuill, N.C., Christie, J.W., Rothenberg, M.E., and Else, K.J. (2006). The role of Th2 cytokines, chemokines and parasite products in eosinophil recruitment to the gastrointestinal mucosa during helminth infection. *European journal of immunology* 36, 1753-1763.
- Drayton, D.L., Liao, S., Mounzer, R.H., and Ruddle, N.H. (2006). Lymphoid organ development: from ontogeny to neogenesis. *Nature immunology* 7, 344-353.
- Ducreux, J., Crocker, P.R., and Vanbever, R. (2009). Analysis of sialoadhesin expression on mouse alveolar macrophages. *Immunology letters* 124, 77-80.
- Dumont, F., and Barrois, R. (1976). Electrokinetic properties of splenic lymphocytes from the low-lipopolysaccharide responder C3H/HeJ mice. *Folia biologica* 12, 145-150.
- Duong, B.H., Tian, H., Ota, T., Completo, G., Han, S., Vela, J.L., Ota, M., Kubitz, M., Bovin, N., Paulson, J.C., *et al.* (2010). Decoration of T-independent antigen with ligands for CD22 and Siglec-G can suppress immunity and induce B cell tolerance in vivo. *The Journal of experimental medicine* 207, 173-187.



- Dyer, K.D., Garcia-Crespo, K.E., Killoran, K.E., and Rosenberg, H.F. (2011). Antigen profiles for the quantitative assessment of eosinophils in mouse tissues by flow cytometry. *Journal of immunological methods* 369, 91-97.
- Dyer, K.D., Moser, J.M., Czapiga, M., Siegel, S.J., Percopo, C.M., and Rosenberg, H.F. (2008). Functionally competent eosinophils differentiated ex vivo in high purity from normal mouse bone marrow. *J Immunol* 181, 4004-4009.
- Fabre, V., Beiting, D.P., Bliss, S.K., Gebreselassie, N.G., Gagliardo, L.F., Lee, N.A., Lee, J.J., and Appleton, J.A. (2009). Eosinophil deficiency compromises parasite survival in chronic nematode infection. *J Immunol* 182, 1577-1583.
- Fagarasan, S., and Honjo, T. (2000). T-Independent immune response: new aspects of B cell biology. *Science (New York, NY)* 290, 89-92.
- Foxall, C., Watson, S.R., Dowbenko, D., Fennie, C., Lasky, L.A., Kiso, M., Hasegawa, A., Asa, D., and Brandley, B.K. (1992). The three members of the selectin receptor family recognize a common carbohydrate epitope, the sialyl Lewis(x) oligosaccharide. *The Journal of cell biology* 117, 895-902.
- Friden, V., Oveland, E., Tenstad, O., Ebefors, K., Nystrom, J., Nilsson, U.A., and Haraldsson, B. (2011). The glomerular endothelial cell coat is essential for glomerular filtration. *Kidney international* 79, 1322-1330.
- Fujiwara, Y., Browne, C.P., Cunniff, K., Goff, S.C., and Orkin, S.H. (1996). Arrested development of embryonic red cell precursors in mouse embryos lacking transcription factor GATA-1. *Proceedings of the National Academy of Sciences of the United States of America* 93, 12355-12358.
- Fujikuyama, Y., Tokuhara, D., Kataoka, K., Gilbert, R.S., McGhee, J.R., Yuki, Y., Kiyono, H., and Fujihashi, K. (2012). Novel vaccine development strategies for inducing mucosal immunity. *Expert review of vaccines* 11, 367-379.
- Fukuda, M., Hiraoka, N., Akama, T.O., and Fukuda, M.N. (2001). Carbohydrate-modifying sulfotransferases: structure, function, and pathophysiology. *The Journal of biological chemistry* 276, 47747-47750.

- Fukuta, M., Inazawa, J., Torii, T., Tsuzuki, K., Shimada, E., and Habuchi, O. (1997). Molecular cloning and characterization of human keratan sulfate Gal-6-sulfotransferase. *The Journal of biological chemistry* *272*, 32321-32328.
- Fulkerson, P.C., Fischetti, C.A., McBride, M.L., Hassman, L.M., Hogan, S.P., and Rothenberg, M.E. (2006). A central regulatory role for eosinophils and the eotaxin/CCR3 axis in chronic experimental allergic airway inflammation. *Proceedings of the National Academy of Sciences of the United States of America* *103*, 16418-16423.
- Galeano, B., Klootwijk, R., Manoli, I., Sun, M., Ciccone, C., Darvish, D., Starost, M.F., Zervas, P.M., Hoffmann, V.J., Hoogstraten-Miller, S., *et al.* (2007). Mutation in the key enzyme of sialic acid biosynthesis causes severe glomerular proteinuria and is rescued by N-acetylmannosamine. *The Journal of clinical investigation* *117*, 1585-1594.
- Galustian, C., Lawson, A.M., Komba, S., Ishida, H., Kiso, M., and Feizi, T. (1997). Sialyl-Lewis(x) sequence 6-O-sulfated at N-acetylglucosamine rather than at galactose is the preferred ligand for L-selectin and de-N-acetylation of the sialic acid enhances the binding strength. *Biochemical and biophysical research communications* *240*, 748-751.
- Gebreselassie, N.G., Moorhead, A.R., Fabre, V., Gagliardo, L.F., Lee, N.A., Lee, J.J., and Appleton, J.A. (2012). Eosinophils preserve parasitic nematode larvae by regulating local immunity. *J Immunol* *188*, 417-425.
- Genbacev, O.D., Prakobphol, A., Foulk, R.A., Krtolica, A.R., Ilic, D., Singer, M.S., Yang, Z.Q., Kiessling, L.L., Rosen, S.D., and Fisher, S.J. (2003). Trophoblast L-selectin-mediated adhesion at the maternal-fetal interface. *Science (New York, NY)* *299*, 405-408.
- Gilden, J.K., Peck, S., Chen, Y.C., and Krummel, M.F. (2012). The septin cytoskeleton facilitates membrane retraction during motility and blebbing. *The Journal of cell biology* *196*, 103-114.
- Girard, J.P., Moussion, C., and Forster, R. (2012). HEVs, lymphatics and homeostatic immune cell trafficking in lymph nodes. *Nature reviews* *12*, 762-773.
- Girard, J.P., and Springer, T.A. (1995). High endothelial venules (HEVs): specialized endothelium for lymphocyte migration. *Immunology today* *16*, 449-457.

- Glauert, A.M., Butterworth, A.E., Sturrock, R.F., and Houba, V. (1978). The mechanism of antibody-dependent, eosinophil-mediated damage to schistosomula of *Schistosoma mansoni* in vitro: a study by phase-contrast and electron microscopy. *Journal of cell science* 34, 173-192.
- Golden, J.W., and Riddle, D.L. (1984). The *Caenorhabditis elegans* dauer larva: developmental effects of pheromone, food, and temperature. *Developmental biology* 102, 368-378.
- Gorfu, G., Rivera-Nieves, J., and Ley, K. (2009). Role of beta7 integrins in intestinal lymphocyte homing and retention. *Current molecular medicine* 9, 836-850.
- Gowans, J.L., and Knight, E.J. (1964). The Route of Re-Circulation of Lymphocytes in the Rat. *Proceedings of the Royal Society of London Series B, Containing papers of a Biological character* 159, 257-282.
- Grunwell, J.R., and Bertozzi, C.R. (2002). Carbohydrate sulfotransferases of the GalNAc/Gal/GlcNAc6ST family. *Biochemistry* 41, 13117-13126.
- Gunnarsson, P., Levander, L., Pahlsson, P., and Grenegard, M. (2007). The acute-phase protein alpha 1-acid glycoprotein (AGP) induces rises in cytosolic Ca<sup>2+</sup> in neutrophil granulocytes via sialic acid binding immunoglobulin-like lectins (siglecs). *FASEB J* 21, 4059-4069.
- Guo, J.P., Brummet, M.E., Myers, A.C., Na, H.J., Rowland, E., Schnaar, R.L., Zheng, T., Zhu, Z., and Bochner, B.S. (2011). Characterization of expression of glycan ligands for Siglec-F in normal mouse lungs. *American journal of respiratory cell and molecular biology* 44, 238-243.
- Guzman-Aranguez, A., and Argueso, P. (2010). Structure and biological roles of mucin-type O-glycans at the ocular surface. *The ocular surface* 8, 8-17.
- Habuchi, O., Hirahara, Y., Uchimura, K., and Fukuta, M. (1996). Enzymatic sulfation of galactose residue of keratan sulfate by chondroitin 6-sulfotransferase. *Glycobiology* 6, 51-57.
- Habuchi, O., Suzuki, Y., and Fukuta, M. (1997). Sulfation of sialyl lactosamine oligosaccharides by chondroitin 6-sulfotransferase. *Glycobiology* 7, 405-412.
- Haeggstrom, J.Z., and Wetterholm, A. (2002). Enzymes and receptors in the leukotriene cascade. *Cell Mol Life Sci* 59, 742-753.
- Hallem, E.A., Rengarajan, M., Ciche, T.A., and Sternberg, P.W. (2007). Nematodes, bacteria, and flies: a tripartite model for nematode parasitism. *Curr Biol* 17, 898-904.

- Han, S., Collins, B.E., Bengtson, P., and Paulson, J.C. (2005). Homomultimeric complexes of CD22 in B cells revealed by protein-glycan cross-linking. *Nature chemical biology* *1*, 93-97.
- Hartwell, D.W., and Wagner, D.D. (1999). New discoveries with mice mutant in endothelial and platelet selectins. *Thrombosis and haemostasis* *82*, 850-857.
- Hayashida, Y., Akama, T.O., Beecher, N., Lewis, P., Young, R.D., Meek, K.M., Kerr, B., Hughes, C.E., Caterson, B., Tanigami, A., *et al.* (2006). Matrix morphogenesis in cornea is mediated by the modification of keratan sulfate by GlcNAc 6-O-sulfotransferase. *Proceedings of the National Academy of Sciences of the United States of America* *103*, 13333-13338.
- Hemmerich, S., Bertozzi, C.R., Leffler, H., and Rosen, S.D. (1994). Identification of the sulfated monosaccharides of GlyCAM-1, an endothelial-derived ligand for L-selectin. *Biochemistry* *33*, 4820-4829.
- Hemmerich, S., Leffler, H., and Rosen, S.D. (1995). Structure of the O-glycans in GlyCAM-1, an endothelial-derived ligand for L-selectin. *The Journal of biological chemistry* *270*, 12035-12047.
- Henderson, W.R., Harley, J.B., and Fauci, A.S. (1984). Arachidonic acid metabolism in normal and hypereosinophilic syndrome human eosinophils: generation of leukotrienes B<sub>4</sub>, C<sub>4</sub>, D<sub>4</sub> and 15-lipoxygenase products. *Immunology* *51*, 679-686.
- Hernandez Mir, G., Helin, J., Skarp, K.P., Cummings, R.D., Makitie, A., Renkonen, R., and Leppanen, A. (2009). Glycoforms of human endothelial CD34 that bind L-selectin carry sulfated sialyl Lewis x capped O- and N-glycans. *Blood* *114*, 733-741.
- Hirakawa, J., Tsuboi, K., Sato, K., Kobayashi, M., Watanabe, S., Takakura, A., Imai, Y., Ito, Y., Fukuda, M., and Kawashima, H. (2010). Novel anti-carbohydrate antibodies reveal the cooperative function of sulfated N- and O-glycans in lymphocyte homing. *The Journal of biological chemistry* *285*, 40864-40878.
- Hiraoka, N., Petryniak, B., Kawashima, H., Mitoma, J., Akama, T.O., Fukuda, M.N., Lowe, J.B., and Fukuda, M. (2007). Significant decrease in alpha1,3-linked fucose in association with increase in 6-sulfated N-acetylglucosamine in peripheral lymph node addressin of FucT-VII-deficient mice exhibiting diminished lymphocyte homing. *Glycobiology* *17*, 277-293.

- Hoffmann, A., Kerr, S., Jellusova, J., Zhang, J., Weisel, F., Wellmann, U., Winkler, T.H., Kneitz, B., Crocker, P.R., and Nitschke, L. (2007). Siglec-G is a B1 cell-inhibitory receptor that controls expansion and calcium signaling of the B1 cell population. *Nature immunology* 8, 695-704.
- Hogan, S.P., Rosenberg, H.F., Moqbel, R., Phipps, S., Foster, P.S., Lacy, P., Kay, A.B., and Rothenberg, M.E. (2008). Eosinophils: biological properties and role in health and disease. *Clin Exp Allergy* 38, 709-750.
- Homeister, J.W., Thall, A.D., Petryniak, B., Maly, P., Rogers, C.E., Smith, P.L., Kelly, R.J., Gersten, K.M., Askari, S.W., Cheng, G., *et al.* (2001). The alpha(1,3)fucosyltransferases FucT-IV and FucT-VII exert collaborative control over selectin-dependent leukocyte recruitment and lymphocyte homing. *Immunity* 15, 115-126.
- Honke, K., Zhang, Y., Cheng, X., Kotani, N., and Taniguchi, N. (2004). Biological roles of sulfoglycolipids and pathophysiology of their deficiency. *Glycoconjugate journal* 21, 59-62.
- Horwitz, R.J., McGill, K.A., and Busse, W.W. (1998). The role of leukotriene modifiers in the treatment of asthma. *American journal of respiratory and critical care medicine* 157, 1363-1371.
- Hosono-Fukao, T., Ohtake-Niimi, S., Nishitsuji, K., Hossain, M.M., van Kuppevelt, T.H., Michikawa, M., and Uchimura, K. (2011). RB4CD12 epitope expression and heparan sulfate disaccharide composition in brain vasculature. *Journal of neuroscience research* 89, 1840-1848.
- Hudson, S.A., Bovin, N.V., Schnaar, R.L., Crocker, P.R., and Bochner, B.S. (2009). Eosinophil-selective binding and proapoptotic effect in vitro of a synthetic Siglec-8 ligand, polymeric 6'-sulfated sialyl Lewis x. *The Journal of pharmacology and experimental therapeutics* 330, 608-612.
- Humbles, A.A., Lu, B., Friend, D.S., Okinaga, S., Lora, J., Al-Garawi, A., Martin, T.R., Gerard, N.P., and Gerard, C. (2002). The murine CCR3 receptor regulates both the role of eosinophils and mast cells in allergen-induced airway inflammation and hyperresponsiveness. *Proceedings of the National Academy of Sciences of the United States of America* 99, 1479-1484.
- Humphrey, M.B., Lanier, L.L., and Nakamura, M.C. (2005). Role of ITAM-containing adapter proteins and their receptors in the immune system and bone. *Immunological reviews* 208, 50-65.
- Ikehara, Y., Ikehara, S.K., and Paulson, J.C. (2004). Negative regulation of T cell receptor signaling by Siglec-7 (p70/AIRM) and Siglec-9. *The Journal of biological chemistry* 279, 43117-43125.

- Ishida, A., Ohta, M., Toda, M., Murata, T., Usui, T., Akita, K., Inoue, M., and Nakada, H. (2008). Mucin-induced apoptosis of monocyte-derived dendritic cells during maturation. *Proteomics* 8, 3342-3349.
- Kanaoka, Y., and Boyce, J.A. (2004). Cysteinyl leukotrienes and their receptors: cellular distribution and function in immune and inflammatory responses. *J Immunol* 173, 1503-1510.
- Kanda, H., Newton, R., Klein, R., Morita, Y., Gunn, M.D., and Rosen, S.D. (2008). Autotaxin, an ectoenzyme that produces lysophosphatidic acid, promotes the entry of lymphocytes into secondary lymphoid organs. *Nature immunology* 9, 415-423.
- Kawashima, H., Petryniak, B., Hiraoka, N., Mitoma, J., Huckaby, V., Nakayama, J., Uchimura, K., Kadomatsu, K., Muramatsu, T., Lowe, J.B., *et al.* (2005). N-acetylglucosamine-6-O-sulfotransferases 1 and 2 cooperatively control lymphocyte homing through L-selectin ligand biosynthesis in high endothelial venules. *Nature immunology* 6, 1096-1104.
- Kazura, J.W., and Grove, D.I. (1978). Stage-specific antibody-dependent eosinophil-mediated destruction of *Trichinella spiralis*. *Nature* 274, 588-589.
- Kerrigan, A.M., and Brown, G.D. (2011). Syk-coupled C-type lectins in immunity. *Trends in immunology* 32, 151-156.
- Khoo, K.H., and Yu, S.Y. (2010). Mass spectrometric analysis of sulfated N- and O-glycans. *Methods in enzymology* 478, 3-26.
- Kim, N.D., Chou, R.C., Seung, E., Tager, A.M., and Luster, A.D. (2006). A unique requirement for the leukotriene B4 receptor BLT1 for neutrophil recruitment in inflammatory arthritis. *The Journal of experimental medicine* 203, 829-835.
- Kimura, N., Ohmori, K., Miyazaki, K., Izawa, M., Matsuzaki, Y., Yasuda, Y., Takematsu, H., Kozutsumi, Y., Moriyama, A., and Kannagi, R. (2007). Human B-lymphocytes express alpha2-6-sialylated 6-sulfo-N-acetylglucosamine serving as a preferred ligand for CD22/Siglec-2. *The Journal of biological chemistry* 282, 32200-32207.
- Kirkitadze, M.D., and Barlow, P.N. (2001). Structure and flexibility of the multiple domain proteins that regulate complement activation. *Immunological reviews* 180, 146-161.

- Kitaura, M., Suzuki, N., Imai, T., Takagi, S., Suzuki, R., Nakajima, T., Hirai, K., Nomiya, H., and Yoshie, O. (1999). Molecular cloning of a novel human CC chemokine (Eotaxin-3) that is a functional ligand of CC chemokine receptor 3. *The Journal of biological chemistry* *274*, 27975-27980.
- Kitazume, S., Kitajima, K., Inoue, S., Haslam, S.M., Morris, H.R., Dell, A., Lennarz, W.J., and Inoue, Y. (1996). The occurrence of novel 9-O-sulfated N-glycolylneuraminic acid-capped alpha2-->5-Oglycolyl-linked oligo/polyNeu5Gc chains in sea urchin egg cell surface glycoprotein. Identification of a new chain termination signal for polysialyltransferase. *The Journal of biological chemistry* *271*, 6694-6701.
- Kiwamoto, T., Katoh, T., Tiemeyer, M., and Bochner, B.S. (2013). The role of lung epithelial ligands for Siglec-8 and Siglec-F in eosinophilic inflammation. *Current opinion in allergy and clinical immunology* *13*, 106-111.
- Klaas, M., and Crocker, P.R. (2012). Sialoadhesin in recognition of self and non-self. *Seminars in immunopathology* *34*, 353-364.
- Klion, A.D., and Nutman, T.B. (2004). The role of eosinophils in host defense against helminth parasites. *The Journal of allergy and clinical immunology* *113*, 30-37.
- Knott, M.L., Matthaei, K.I., Foster, P.S., and Dent, L.A. (2009). The roles of eotaxin and the STAT6 signalling pathway in eosinophil recruitment and host resistance to the nematodes *Nippostrongylus brasiliensis* and *Heligmosomoides bakeri*. *Molecular immunology* *46*, 2714-2722.
- Koenig, A., Jain, R., Vig, R., Norgard-Sumnicht, K.E., Matta, K.L., and Varki, A. (1997). Selectin inhibition: synthesis and evaluation of novel sialylated, sulfated and fucosylated oligosaccharides, including the major capping group of GlyCAM-1. *Glycobiology* *7*, 79-93.
- Kogelberg, H., and Feizi, T. (2001). New structural insights into lectin-type proteins of the immune system. *Current opinion in structural biology* *11*, 635-643.
- Kopf, M., Brombacher, F., Hodgkin, P.D., Ramsay, A.J., Milbourne, E.A., Dai, W.J., Ovington, K.S., Behm, C.A., Kohler, G., Young, I.G., *et al.* (1996). IL-5-deficient mice have a developmental defect in CD5+ B-1 cells and lack eosinophilia but have normal antibody and cytotoxic T cell responses. *Immunity* *4*, 15-24.

- Kouro, T., and Takatsu, K. (2009). IL-5- and eosinophil-mediated inflammation: from discovery to therapy. *International immunology* 21, 1303-1309.
- Lee, J.J., and Lee, N.A. (2005). Eosinophil degranulation: an evolutionary vestige or a universally destructive effector function? *Clin Exp Allergy* 35, 986-994.
- Lee, N.A., McGarry, M.P., Larson, K.A., Horton, M.A., Kristensen, A.B., and Lee, J.J. (1997). Expression of IL-5 in thymocytes/T cells leads to the development of a massive eosinophilia, extramedullary eosinophilopoiesis, and unique histopathologies. *J Immunol* 158, 1332-1344.
- Ley, K., Laudanna, C., Cybulsky, M.I., and Nourshargh, S. (2007). Getting to the site of inflammation: the leukocyte adhesion cascade updated. *Nature reviews* 7, 678-689.
- Li, X., Tu, L., Murphy, P.G., Kadono, T., Steeber, D.A., and Tedder, T.F. (2001). CHST1 and CHST2 sulfotransferase expression by vascular endothelial cells regulates shear-resistant leukocyte rolling via L-selectin. *Journal of leukocyte biology* 69, 565-574.
- Liao, S., and Ruddle, N.H. (2006). Synchrony of high endothelial venules and lymphatic vessels revealed by immunization. *J Immunol* 177, 3369-3379.
- Lowenstein, C.J., Morrell, C.N., and Yamakuchi, M. (2005). Regulation of Weibel-Palade body exocytosis. *Trends in cardiovascular medicine* 15, 302-308.
- Ma, W., Bryce, P.J., Humbles, A.A., Laouini, D., Yalcindag, A., Alenius, H., Friend, D.S., Oettgen, H.C., Gerard, C., and Geha, R.S. (2002). CCR3 is essential for skin eosinophilia and airway hyperresponsiveness in a murine model of allergic skin inflammation. *The Journal of clinical investigation* 109, 621-628.
- Machado, E.R., Ueta, M.T., Lourenco, E.V., Anibal, F.F., Sorgi, C.A., Soares, E.G., Roque-Barreira, M.C., Medeiros, A.I., and Faccioli, L.H. (2005). Leukotrienes play a role in the control of parasite burden in murine strongyloidiasis. *J Immunol* 175, 3892-3899.
- Makepeace, B.L., Martin, C., Turner, J.D., and Specht, S. (2012). Granulocytes in helminth infection -- who is calling the shots? *Current medicinal chemistry* 19, 1567-1586.
- Matthews, A.N., Friend, D.S., Zimmermann, N., Sarafi, M.N., Luster, A.D., Pearlman, E., Wert, S.E., and Rothenberg, M.E. (1998). Eotaxin is required for the baseline level of tissue eosinophils. *Proceedings of the National Academy of Sciences of the United States of America* 95, 6273-6278.



- McCann, C.P., Kriebel, P.W., Parent, C.A., and Losert, W. (2012). Cell speed, persistence and information transmission during signal relay and collective migration. *Journal of cell science* *123*, 1724-1731.
- McDonald, B., Pittman, K., Menezes, G.B., Hirota, S.A., Slaba, I., Waterhouse, C.C., Beck, P.L., Muruve, D.A., and Kubers, P. (2010). Intravascular danger signals guide neutrophils to sites of sterile inflammation. *Science (New York, NY)* *330*, 362-366.
- McMillan, S.J., Sharma, R.S., McKenzie, E.J., Richards, H.E., Zhang, J., Prescott, A., and Crocker, P.R. (2013). Siglec-E is a negative regulator of acute pulmonary neutrophil inflammation and suppresses CD11b beta2-integrin-dependent signalling. *Blood*.
- Mehmet, H., Scudder, P., Tang, P.W., Hounsell, E.F., Caterson, B., and Feizi, T. (1986). The antigenic determinants recognized by three monoclonal antibodies to keratan sulphate involve sulphated hepta- or larger oligosaccharides of the poly(N-acetyllactosamine) series. *European journal of biochemistry / FEBS* *157*, 385-391.
- Mitoma, J., Bao, X., Petryanik, B., Schaerli, P., Gauguier, J.M., Yu, S.Y., Kawashima, H., Saito, H., Ohtsubo, K., Marth, J.D., *et al.* (2007). Critical functions of N-glycans in L-selectin-mediated lymphocyte homing and recruitment. *Nature immunology* *8*, 409-418.
- Mitsuoka, C., Sawada-Kasugai, M., Ando-Furui, K., Izawa, M., Nakanishi, H., Nakamura, S., Ishida, H., Kiso, M., and Kannagi, R. (1998). Identification of a major carbohydrate capping group of the L-selectin ligand on high endothelial venules in human lymph nodes as 6-sulfo sialyl Lewis X. *The Journal of biological chemistry* *273*, 11225-11233.
- Miyazaki, K., Sakuma, K., Kawamura, Y.I., Izawa, M., Ohmori, K., Mitsuki, M., Yamaji, T., Hashimoto, Y., Suzuki, A., Saito, Y., *et al.* (2012). Colonic epithelial cells express specific ligands for mucosal macrophage immunosuppressive receptors siglec-7 and -9. *J Immunol* *188*, 4690-4700.
- Mohrs, M., Shinkai, K., Mohrs, K., and Locksley, R.M. (2001). Analysis of type 2 immunity in vivo with a bicistronic IL-4 reporter. *Immunity* *15*, 303-311.
- Morimoto, N., Nakano, M., Kinoshita, M., Kawabata, A., Morita, M., Oda, Y., Kuroda, R., and Kakehi, K. (2001). Specific distribution of sialic acids in animal tissues as examined by LC-ESI-MS after derivatization with 1,2-diamino-4,5-methylenedioxybenzene. *Analytical chemistry* *73*, 5422-5428.

- Munitz, A., Bachelet, I., Eliashar, R., Moretta, A., Moretta, L., and Levi-Schaffer, F. (2006). The inhibitory receptor IRp60 (CD300a) suppresses the effects of IL-5, GM-CSF, and eotaxin on human peripheral blood eosinophils. *Blood* *107*, 1996-2003.
- Munitz, A., McBride, M.L., Bernstein, J.S., and Rothenberg, M.E. (2008). A dual activation and inhibition role for the paired immunoglobulin-like receptor B in eosinophils. *Blood* *111*, 5694-5703.
- Nath, D., Hartnell, A., Happerfield, L., Miles, D.W., Burchell, J., Taylor-Papadimitriou, J., and Crocker, P.R. (1999). Macrophage-tumour cell interactions: identification of MUC1 on breast cancer cells as a potential counter-receptor for the macrophage-restricted receptor, sialoadhesin. *Immunology* *98*, 213-219.
- Nelson, R.D., Quie, P.G., and Simmons, R.L. (1975). Chemotaxis under agarose: a new and simple method for measuring chemotaxis and spontaneous migration of human polymorphonuclear leukocytes and monocytes. *J Immunol* *115*, 1650-1656.
- Ng, T.F., and Streilein, J.W. (2001). Light-induced migration of retinal microglia into the subretinal space. *Investigative ophthalmology & visual science* *42*, 3301-3310.
- Nielsen, J.S., and McNagny, K.M. (2009). The role of podocalyxin in health and disease. *J Am Soc Nephrol* *20*, 1669-1676.
- Norris, H.H., Peterson, M.E., Stebbins, C.C., McConchie, B.W., Bundoc, V.G., Trivedi, S., Hodges, M.G., Anthony, R.M., Urban, J.F., Jr., Long, E.O., *et al.* (2007). Inhibitory receptor gp49B regulates eosinophil infiltration during allergic inflammation. *Journal of leukocyte biology* *82*, 1531-1541.
- Nutku, E., Aizawa, H., Hudson, S.A., and Bochner, B.S. (2003). Ligation of Siglec-8: a selective mechanism for induction of human eosinophil apoptosis. *Blood* *101*, 5014-5020.
- Nutku, E., Hudson, S.A., and Bochner, B.S. (2005). Mechanism of Siglec-8-induced human eosinophil apoptosis: role of caspases and mitochondrial injury. *Biochemical and biophysical research communications* *336*, 918-924.
- Ohta, M., Ishida, A., Toda, M., Akita, K., Inoue, M., Yamashita, K., Watanabe, M., Murata, T., Usui, T., and Nakada, H. (2010). Immunomodulation of monocyte-derived dendritic cells through ligation of tumor-produced mucins to Siglec-9. *Biochemical and biophysical research communications* *402*, 663-669.

- Oyoshi, M.K., He, R., Kanaoka, Y., ElKhal, A., Kawamoto, S., Lewis, C.N., Austen, K.F., and Geha, R.S. (2012a). Eosinophil-derived leukotriene C4 signals via type 2 cysteinyl leukotriene receptor to promote skin fibrosis in a mouse model of atopic dermatitis. *Proceedings of the National Academy of Sciences of the United States of America* *109*, 4992-4997.
- Oyoshi, M.K., He, R., Li, Y., Mondal, S., Yoon, J., Afshar, R., Chen, M., Lee, D.M., Luo, H.R., Luster, A.D., *et al.* (2012b). Leukotriene B4-driven neutrophil recruitment to the skin is essential for allergic skin inflammation. *Immunity* *37*, 747-758.
- Paschinger, K., Gutternigg, M., Rendic, D., and Wilson, I.B. (2008). The N-glycosylation pattern of *Caenorhabditis elegans*. *Carbohydrate research* *343*, 2041-2049.
- Patnode, M.L., Yu, S.Y., Cheng, C.W., Ho, M.Y., Tegesjö, L., Sakuma, K., Uchimura, K., Khoo, K.H., Kannagi, R., and Rosen, S.D. (2013). KSGal6ST generates galactose-6-O-sulfate in high endothelial venules but does not contribute to L-selectin-dependent lymphocyte homing. *Glycobiology* *23*, 381-394.
- Paulson, J.C., Macauley, M.S., and Kawasaki, N. (2012). Siglecs as sensors of self in innate and adaptive immune responses. *Annals of the New York Academy of Sciences* *1253*, 37-48.
- Pease, J.E. (2006). Asthma, allergy and chemokines. *Current drug targets* *7*, 3-12.
- Peters-Golden, M., and Henderson, W.R., Jr. (2007). Leukotrienes. *The New England journal of medicine* *357*, 1841-1854.
- Ramalho-Pinto, F.J., McLaren, D.J., and Smithers, S.R. (1978). Complement-mediated killing of schistosomula of *Schistosoma mansoni* by rat eosinophils in vitro. *The Journal of experimental medicine* *147*, 147-156.
- Rao, A.U., Carta, L.K., Lesuisse, E., and Hamza, I. (2005). Lack of heme synthesis in a free-living eukaryote. *Proceedings of the National Academy of Sciences of the United States of America* *102*, 4270-4275.
- Rapoport, E.M., Pazynina, G.V., Sablina, M.A., Crocker, P.R., and Bovin, N.V. (2006). Probing sialic acid binding Ig-like lectins (siglecs) with sulfated oligosaccharides. *Biochemistry* *71*, 496-504.
- Ravetch, J.V., and Lanier, L.L. (2000). Immune inhibitory receptors. *Science (New York, NY)* *290*, 84-89.

- Redelinghuys, P., Antonopoulos, A., Liu, Y., Campanero-Rhodes, M.A., McKenzie, E., Haslam, S.M., Dell, A., Feizi, T., and Crocker, P.R. (2011). Early murine T-lymphocyte activation is accompanied by a switch from N-Glycolyl- to N-acetyl-neuraminic acid and generation of ligands for siglec-E. *The Journal of biological chemistry* 286, 34522-34532.
- Reese, T.A., Liang, H.E., Tager, A.M., Luster, A.D., Van Rooijen, N., Voehringer, D., and Locksley, R.M. (2007). Chitin induces accumulation in tissue of innate immune cells associated with allergy. *Nature* 447, 92-96.
- Rhodes, J.M., Campbell, B.J., and Yu, L.G. (2008). Lectin-epithelial interactions in the human colon. *Biochemical Society transactions* 36, 1482-1486.
- Rosen, S.D. (2004). Ligands for L-selectin: homing, inflammation, and beyond. *Annu Rev Immunol* 22, 129-156.
- Rosenberg, H.F., Dyer, K.D., and Domachowske, J.B. (2009). Respiratory viruses and eosinophils: exploring the connections. *Antiviral research* 83, 1-9.
- Rouzer, C.A., Ford-Hutchinson, A.W., Morton, H.E., and Gillard, J.W. (1990). MK886, a potent and specific leukotriene biosynthesis inhibitor blocks and reverses the membrane association of 5-lipoxygenase in ionophore-challenged leukocytes. *The Journal of biological chemistry* 265, 1436-1442.
- Roy, M.G., Rahmani, M., Hernandez, J.R., Alexander, S.N., Ehre, C., Ho, S.B., and Evans, C.M. (2011). Mucin production during prenatal and postnatal murine lung development. *American journal of respiratory cell and molecular biology* 44, 755-760.
- Sadik, C.D., Kim, N.D., Iwakura, Y., and Luster, A.D. (2012). Neutrophils orchestrate their own recruitment in murine arthritis through C5aR and FcγR signaling. *Proceedings of the National Academy of Sciences of the United States of America* 109, E3177-3185.
- Sadik, C.D., Kim, N.D., and Luster, A.D. (2011). Neutrophils cascading their way to inflammation. *Trends in immunology* 32, 452-460.
- Sakuishi, K., Jayaraman, P., Behar, S.M., Anderson, A.C., and Kuchroo, V.K. (2011). Emerging Tim-3 functions in antimicrobial and tumor immunity. *Trends in immunology* 32, 345-349.

- Satomaa, T., Renkonen, O., Helin, J., Kirveskari, J., Makitie, A., and Renkonen, R. (2002). O-glycans on human high endothelial CD34 putatively participating in L-selectin recognition. *Blood* 99, 2609-2611.
- Schauer, R. (2009). Sialic acids as regulators of molecular and cellular interactions. *Current opinion in structural biology* 19, 507-514.
- Scheller, J., Chalaris, A., Garbers, C., and Rose-John, S. (2011). ADAM17: a molecular switch to control inflammation and tissue regeneration. *Trends in immunology* 32, 380-387.
- Shamri, R., Xenakis, J.J., and Spencer, L.A. (2011). Eosinophils in innate immunity: an evolving story. *Cell and tissue research* 343, 57-83.
- Shibata, T.K., Matsumura, F., Wang, P., Yu, S., Chou, C.C., Khoo, K.H., Kitayama, K., Akama, T.O., Sugihara, K., Kanayama, N., *et al.* (2012). Identification of mono- and disulfated N-acetyl-lactosaminyl Oligosaccharide structures as epitopes specifically recognized by humanized monoclonal antibody HMOCC-1 raised against ovarian cancer. *The Journal of biological chemistry* 287, 6592-6602.
- Shinkai, A., Yoshisue, H., Koike, M., Shoji, E., Nakagawa, S., Saito, A., Takeda, T., Imabeppu, S., Kato, Y., Hanai, N., *et al.* (1999). A novel human CC chemokine, eotaxin-3, which is expressed in IL-4-stimulated vascular endothelial cells, exhibits potent activity toward eosinophils. *J Immunol* 163, 1602-1610.
- Shiow, L.R., Rosen, D.B., Brdickova, N., Xu, Y., An, J., Lanier, L.L., Cyster, J.G., and Matloubian, M. (2006). CD69 acts downstream of interferon-alpha/beta to inhibit S1P1 and lymphocyte egress from lymphoid organs. *Nature* 440, 540-544.
- Simons, J.E., Rothenberg, M.E., and Lawrence, R.A. (2005). Eotaxin-1-regulated eosinophils have a critical role in innate immunity against experimental *Brugia malayi* infection. *European journal of immunology* 35, 189-197.
- Song, D.H., and Lee, J.O. (2012). Sensing of microbial molecular patterns by Toll-like receptors. *Immunological reviews* 250, 216-229.
- Song, D.J., Cho, J.Y., Lee, S.Y., Miller, M., Rosenthal, P., Soroosh, P., Croft, M., Zhang, M., Varki, A., and Broide, D.H. (2009a). Anti-Siglec-F antibody reduces allergen-induced eosinophilic inflammation and airway remodeling. *J Immunol* 183, 5333-5341.

- Song, D.J., Cho, J.Y., Miller, M., Strangman, W., Zhang, M., Varki, A., and Broide, D.H. (2009b). Anti-Siglec-F antibody inhibits oral egg allergen induced intestinal eosinophilic inflammation in a mouse model. *Clinical immunology (Orlando, Fla)* *131*, 157-169.
- Spada, C.S., Nieves, A.L., Krauss, A.H., and Woodward, D.F. (1994). Comparison of leukotriene B4 and D4 effects on human eosinophil and neutrophil motility in vitro. *Journal of leukocyte biology* *55*, 183-191.
- Stevens, W.W., Kim, T.S., Pujanauski, L.M., Hao, X., and Braciale, T.J. (2007). Detection and quantitation of eosinophils in the murine respiratory tract by flow cytometry. *Journal of immunological methods* *327*, 63-74.
- Su, A.I., Wiltshire, T., Batalov, S., Lapp, H., Ching, K.A., Block, D., Zhang, J., Soden, R., Hayakawa, M., Kreiman, G., *et al.* (2004). A gene atlas of the mouse and human protein-encoding transcriptomes. *Proceedings of the National Academy of Sciences of the United States of America* *101*, 6062-6067.
- Sun, F.F., Crittenden, N.J., Czuk, C.I., Taylor, B.M., Stout, B.K., and Johnson, H.G. (1991). Biochemical and functional differences between eosinophils from animal species and man. *Journal of leukocyte biology* *50*, 140-150.
- Sun, G., Pan, J., Liu, K., Wang, X., and Wang, S. (2010). Molecular Cloning and Expression Analysis of P-Selectin from Zebrafish (*Danio rerio*). *International journal of molecular sciences* *11*, 4618-4630.
- Suzuki-Inoue, K., Inoue, O., and Ozaki, Y. (2011). Novel platelet activation receptor CLEC-2: from discovery to prospects. *J Thromb Haemost* *9 Suppl 1*, 44-55.
- Swanson, B.J., McDermott, K.M., Singh, P.K., Eggers, J.P., Crocker, P.R., and Hollingsworth, M.A. (2007). MUC1 is a counter-receptor for myelin-associated glycoprotein (Siglec-4a) and their interaction contributes to adhesion in pancreatic cancer perineural invasion. *Cancer research* *67*, 10222-10229.
- Tager, A.M., Dufour, J.H., Goodarzi, K., Bercury, S.D., von Andrian, U.H., and Luster, A.D. (2000). BLTR mediates leukotriene B(4)-induced chemotaxis and adhesion and plays a dominant role in eosinophil accumulation in a murine model of peritonitis. *The Journal of experimental medicine* *192*, 439-446.

- Tager, A.M., and Luster, A.D. (2003). BLT1 and BLT2: the leukotriene B(4) receptors. *Prostaglandins, leukotrienes, and essential fatty acids* 69, 123-134.
- Takahara, K., Yashima, Y., Omatsu, Y., Yoshida, H., Kimura, Y., Kang, Y.S., Steinman, R.M., Park, C.G., and Inaba, K. (2004). Functional comparison of the mouse DC-SIGN, SIGNR1, SIGNR3 and Langerin, C-type lectins. *International immunology* 16, 819-829.
- Takashima, S. (2008). Characterization of mouse sialyltransferase genes: their evolution and diversity. *Bioscience, biotechnology, and biochemistry* 72, 1155-1167.
- Tam, A., Wadsworth, S., Dorscheid, D., Man, S.F., and Sin, D.D. (2011). The airway epithelium: more than just a structural barrier. *Therapeutic advances in respiratory disease* 5, 255-273.
- Tangemann, K., Bistrup, A., Hemmerich, S., and Rosen, S.D. (1999). Sulfation of a high endothelial venule-expressed ligand for L-selectin. Effects on tethering and rolling of lymphocytes. *The Journal of experimental medicine* 190, 935-942.
- Tateno, H., Crocker, P.R., and Paulson, J.C. (2005). Mouse Siglec-F and human Siglec-8 are functionally convergent paralogs that are selectively expressed on eosinophils and recognize 6'-sulfo-sialyl Lewis X as a preferred glycan ligand. *Glycobiology* 15, 1125-1135.
- Tateno, H., Li, H., Schur, M.J., Bovin, N., Crocker, P.R., Wakarchuk, W.W., and Paulson, J.C. (2007). Distinct endocytic mechanisms of CD22 (Siglec-2) and Siglec-F reflect roles in cell-signaling and innate immunity. *Mol Cell Biol*.
- Tateno, H., Ohnishi, K., Yabe, R., Hayatsu, N., Sato, T., Takeya, M., Narimatsu, H., and Hirabayashi, J. (2010). Dual specificity of Langerin to sulfated and mannosylated glycans via a single C-type carbohydrate recognition domain. *The Journal of biological chemistry* 285, 6390-6400.
- Thomas, S.N., Schnaar, R.L., and Konstantopoulos, K. (2009). Podocalyxin-like protein is an E-/L-selectin ligand on colon carcinoma cells: comparative biochemical properties of selectin ligands in host and tumor cells. *Am J Physiol Cell Physiol* 296, C505-513.
- Thornton, D.J., Davies, J.R., Kirkham, S., Gautrey, A., Khan, N., Richardson, P.S., and Sheehan, J.K. (2001). Identification of a nonmucin glycoprotein (gp-340) from a purified respiratory mucin preparation: evidence for an association involving the MUC5B mucin. *Glycobiology* 11, 969-977.

- Thornton, D.J., Rousseau, K., and McGuckin, M.A. (2008). Structure and function of the polymeric mucins in airways mucus. *Annual review of physiology* *70*, 459-486.
- Toda, M., Akita, K., Inoue, M., Taketani, S., and Nakada, H. (2008). Down-modulation of B cell signal transduction by ligation of mucins to CD22. *Biochemical and biophysical research communications* *372*, 45-50.
- Tomita, M., Kobayashi, T., Itoh, H., Onitsuka, T., and Nawa, Y. (2000). Goblet cell hyperplasia in the airway of *Nippostrongylus brasiliensis*-infected rats. *Respiration; international review of thoracic diseases* *67*, 565-569.
- Torii, T., Fukuta, M., and Habuchi, O. (2000). Sulfation of sialyl N-acetyllactosamine oligosaccharides and fetuin oligosaccharides by keratan sulfate Gal-6-sulfotransferase. *Glycobiology* *10*, 203-211.
- Torres, R.M., Law, C.L., Santos-Argumedo, L., Kirkham, P.A., Grabstein, K., Parkhouse, R.M., and Clark, E.A. (1992). Identification and characterization of the murine homologue of CD22, a B lymphocyte-restricted adhesion molecule. *J Immunol* *149*, 2641-2649.
- Turner, H., and Kinet, J.P. (1999). Signalling through the high-affinity IgE receptor Fc epsilonRI. *Nature* *402*, B24-30.
- Uchimura, K., Gauguier, J.M., Singer, M.S., Tsay, D., Kannagi, R., Muramatsu, T., von Andrian, U.H., and Rosen, S.D. (2005). A major class of L-selectin ligands is eliminated in mice deficient in two sulfotransferases expressed in high endothelial venules. *Nature immunology* *6*, 1105-1113.
- Uchimura, K., Kadomatsu, K., Nishimura, H., Muramatsu, H., Nakamura, E., Kurosawa, N., Habuchi, O., El-Fasakhany, F.M., Yoshikai, Y., and Muramatsu, T. (2002). Functional analysis of the chondroitin 6-sulfotransferase gene in relation to lymphocyte subpopulations, brain development, and oversulfated chondroitin sulfates. *The Journal of biological chemistry* *277*, 1443-1450.
- Valenzuela, D.M., Murphy, A.J., Friendewey, D., Gale, N.W., Economides, A.N., Auerbach, W., Poueymirou, W.T., Adams, N.C., Rojas, J., Yasenchak, J., *et al.* (2003). High-throughput engineering of the mouse genome coupled with high-resolution expression analysis. *Nature biotechnology* *21*, 652-659.
- Vandivier, R.W., Henson, P.M., and Douglas, I.S. (2006). Burying the dead: the impact of failed apoptotic cell removal (efferocytosis) on chronic inflammatory lung disease. *Chest* *129*, 1673-1682.



- Varki, A. (2009). Natural ligands for CD33-related Siglecs? *Glycobiology* *19*, 810-812.
- Varki, A., and Angata, T. (2006). Siglecs--the major subfamily of I-type lectins. *Glycobiology* *16*, 1R-27R.
- Varki, A., and Gagneux, P. (2012). Multifarious roles of sialic acids in immunity. *Annals of the New York Academy of Sciences* *1253*, 16-36.
- Voehringer, D., Shinkai, K., and Locksley, R.M. (2004). Type 2 immunity reflects orchestrated recruitment of cells committed to IL-4 production. *Immunity* *20*, 267-277.
- Voehringer, D., van Rooijen, N., and Locksley, R.M. (2007). Eosinophils develop in distinct stages and are recruited to peripheral sites by alternatively activated macrophages. *J Leukoc Biol* *81*, 1434-1444.
- von Gunten, S., Yousefi, S., Seitz, M., Jakob, S.M., Schaffner, T., Seger, R., Takala, J., Villiger, P.M., and Simon, H.U. (2005). Siglec-9 transduces apoptotic and nonapoptotic death signals into neutrophils depending on the proinflammatory cytokine environment. *Blood* *106*, 1423-1431.
- Walker, J.A., and Smith, K.G. (2008). CD22: an inhibitory enigma. *Immunology* *123*, 314-325.
- Watson, M.L., Kingsmore, S.F., Johnston, G.I., Siegelman, M.H., Le Beau, M.M., Lemons, R.S., Bora, N.S., Howard, T.A., Weissman, I.L., McEver, R.P., *et al.* (1990). Genomic organization of the selectin family of leukocyte adhesion molecules on human and mouse chromosome 1. *The Journal of experimental medicine* *172*, 263-272.
- Wessels, M.R., Butko, P., Ma, M., Warren, H.B., Lage, A.L., and Carroll, M.C. (1995). Studies of group B streptococcal infection in mice deficient in complement component C3 or C4 demonstrate an essential role for complement in both innate and acquired immunity. *Proceedings of the National Academy of Sciences of the United States of America* *92*, 11490-11494.
- Whitsett, J.A., Wert, S.E., and Weaver, T.E. (2010). Alveolar surfactant homeostasis and the pathogenesis of pulmonary disease. *Annual review of medicine* *61*, 105-119.
- Winn, V.D., Gormley, M., Paquet, A.C., Kjaer-Sorensen, K., Kramer, A., Rumer, K.K., Haimov-Kochman, R., Yeh, R.F., Overgaard, M.T., Varki, A., *et al.* (2009). Severe preeclampsia-related changes in gene expression at the maternal-fetal interface include sialic acid-binding immunoglobulin-like lectin-6 and pappalysin-2. *Endocrinology* *150*, 452-462.

- Wu, D., Molofsky, A.B., Liang, H.E., Ricardo-Gonzalez, R.R., Jouihan, H.A., Bando, J.K., Chawla, A., and Locksley, R.M. (2011). Eosinophils sustain adipose alternatively activated macrophages associated with glucose homeostasis. *Science (New York, NY)* *332*, 243-247.
- Yamaguchi, Y., Hayashi, Y., Sugama, Y., Miura, Y., Kasahara, T., Kitamura, S., Torisu, M., Mita, S., Tominaga, A., and Takatsu, K. (1988). Highly purified murine interleukin 5 (IL-5) stimulates eosinophil function and prolongs in vitro survival. IL-5 as an eosinophil chemotactic factor. *The Journal of experimental medicine* *167*, 1737-1742.
- Yamakawa, N., Sato, C., Miyata, S., Maehashi, E., Toriyama, M., Sato, N., Furuhata, K., and Kitajima, K. (2007). Development of sensitive chemical and immunochemical methods for detecting sulfated sialic acids and their application to glycoconjugates from sea urchin sperm and eggs. *Biochimie* *89*, 1396-1408.
- Yang, M., Hogan, S.P., Mahalingam, S., Pope, S.M., Zimmermann, N., Fulkerson, P., Dent, L.A., Young, I.G., Matthaei, K.I., Rothenberg, M.E., *et al.* (2003). Eotaxin-2 and IL-5 cooperate in the lung to regulate IL-13 production and airway eosinophilia and hyperreactivity. *The Journal of allergy and clinical immunology* *112*, 935-943.
- Yang, W.H., Nussbaum, C., Grewal, P.K., Marth, J.D., and Sperandio, M. (2012). Coordinated roles of ST3Gal-VI and ST3Gal-IV sialyltransferases in the synthesis of selectin ligands. *Blood* *120*, 1015-1026.
- Yang, Y., Loy, J., Ryseck, R.P., Carrasco, D., and Bravo, R. (1998). Antigen-induced eosinophilic lung inflammation develops in mice deficient in chemokine eotaxin. *Blood* *92*, 3912-3923.
- Yeh, J.C., Hiraoka, N., Petryniak, B., Nakayama, J., Ellies, L.G., Rabuka, D., Hindsgaul, O., Marth, J.D., Lowe, J.B., and Fukuda, M. (2001). Novel sulfated lymphocyte homing receptors and their control by a Core1 extension beta 1,3-N-acetylglucosaminyltransferase. *Cell* *105*, 957-969.
- Yokoi, H., Choi, O.H., Hubbard, W., Lee, H.S., Canning, B.J., Lee, H.H., Ryu, S.D., von Gunten, S., Bickel, C.A., Hudson, S.A., *et al.* (2008). Inhibition of FcepsilonRI-dependent mediator release and calcium flux from human mast cells by sialic acid-binding immunoglobulin-like lectin 8 engagement. *The Journal of allergy and clinical immunology* *121*, 499-505 e491.

- Yoshino, K., Ohmoto, H., Kondo, N., Tsujishita, H., Hiramatsu, Y., Inoue, Y., and Kondo, H. (1997). Studies on selectin blockers. 4. Structure-function relationships of sulfated sialyl Lewis X hexasaccharide ceramides toward E-, P-, and L-selectin binding. *Journal of medicinal chemistry* *40*, 455-462.
- Yu, C., Cantor, A.B., Yang, H., Browne, C., Wells, R.A., Fujiwara, Y., and Orkin, S.H. (2002). Targeted deletion of a high-affinity GATA-binding site in the GATA-1 promoter leads to selective loss of the eosinophil lineage in vivo. *The Journal of experimental medicine* *195*, 1387-1395.
- Yu, S.Y., Wu, S.W., Hsiao, H.H., and Khoo, K.H. (2009). Enabling techniques and strategic workflow for sulfoglycomics based on mass spectrometry mapping and sequencing of permethylated sulfated glycans. *Glycobiology* *19*, 1136-1149.
- Zarbock, A., and Ley, K. (2009). Neutrophil adhesion and activation under flow. *Microcirculation* *16*, 31-42.
- Zhang, H., Muramatsu, T., Murase, A., Yuasa, S., Uchimura, K., and Kadomatsu, K. (2006). N-Acetylglucosamine 6-O-sulfotransferase-1 is required for brain keratan sulfate biosynthesis and glial scar formation after brain injury. *Glycobiology* *16*, 702-710.
- Zhang, J.Q., Biedermann, B., Nitschke, L., and Crocker, P.R. (2004). The murine inhibitory receptor mSiglec-E is expressed broadly on cells of the innate immune system whereas mSiglec-F is restricted to eosinophils. *European journal of immunology* *34*, 1175-1184.
- Zhang, M., Angata, T., Cho, J.Y., Miller, M., Broide, D.H., and Varki, A. (2007). Defining the in vivo function of Siglec-F, a CD33-related Siglec expressed on mouse eosinophils. *Blood* *109*, 4280-4287.
- Zhang, Y., Chen, Y.C., Krummel, M.F., and Rosen, S.D. (2012). Autotaxin through lysophosphatidic acid stimulates polarization, motility, and transendothelial migration of naive T cells. *J Immunol* *189*, 3914-3924.
- Zhou, L., Lim, L., Costa, R.H., and Whitsett, J.A. (1996). Thyroid transcription factor-1, hepatocyte nuclear factor-3beta, surfactant protein B, C, and Clara cell secretory protein in developing mouse lung. *J Histochem Cytochem* *44*, 1183-1193.

Zimmermann, N., McBride, M.L., Yamada, Y., Hudson, S.A., Jones, C., Cromie, K.D., Crocker, P.R.,  
Rothenberg, M.E., and Bochner, B.S. (2008). Siglec-F antibody administration to mice selectively  
reduces blood and tissue eosinophils. *Allergy* 63, 1156-1163.

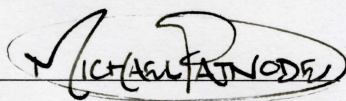
**Publishing Agreement**

*It is the policy of the University to encourage the distribution of all theses, dissertations, and manuscripts. Copies of all UCSF theses, dissertations, and manuscripts will be routed to the library via the Graduate Division. The library will make all theses, dissertations, and manuscripts accessible to the public and will preserve these to the best of their abilities, in perpetuity.*

***Please sign the following statement:***

*I hereby grant permission to the Graduate Division of the University of California, San Francisco to release copies of my thesis, dissertation, or manuscript to the Campus Library to provide access and preservation, in whole or in part, in perpetuity.*

\_\_\_\_\_  
Author Signature

A handwritten signature in black ink, appearing to read "MICHAEL FATNOUDA", is written over a horizontal line. The signature is enclosed in a hand-drawn oval.

\_\_\_\_\_  
Date

24 MAR 2013